The University Of Sheffield.

Department of Automatic Control and Systems Engineering

Wireless Vibration Sensing with Local Signal Processing for Condition Monitoring within a Gas Turbine Engine

A thesis submitted to the University of Sheffield in partial satisfaction of the requirements for the degree of Doctor of Philosophy

by

Aldo Villanueva Marcocchio

Supervisor: Dr. Bryn Ll. Jones

September 2018

Dedicated to my parents Rita and Juan Manuel, and to my siblings Itzel and Juan

Thank you for your love and unconditional support, proud to be your son.

Publications and Presentations

- **A. Villanueva-Marcocchio**, B. Ll. Jones, "A Framework for Wireless Vibration Sensing with Fast Signal Recovery using Enhanced Orthogonal Matching Pursuit", *IEEE Transactions on Industrial Electronics*, (Under Review) 2017.
- **A. Villanueva-Marcocchio**, B. Ll. Jones, "A Low-Power Wireless Vibration Sensing Framework for Machine Health Monitoring using a Packet Loss Tolerant Approach", in *ISCM 1st World Congress on Condition Monitoring*, London UK, 13th – 16th June 2017.
- **A. Villanueva-Marcocchio**, C. Luna, "Towards a Reliable Wireless Vibration Sensing System for Machine Health Monitoring in Industrial Environments using Local Signal Processing", in *Innovation Match 2nd International Forum of Mexican Talent*, Mexico City, 31st May – 2th June 2017.
- **A. Villanueva-Marcocchio**, C. Luna. "Local Signal Processing for Condition Monitoring in an Industrial Plant using Wireless Sensor Networks", in *Innovation Match 1st International Forum of Mexican Talent*, Guadalajara, Mexico, 6th -8th April 2016.

Acknowledgements

My sincerest gratitude to my supervisor Dr. Bryn Jones for his valuable support and guidance throughout my studies. His continuous advice and perspective were fundamental during this long journey. I would also like to thank my second supervisor Dr. Iñaki Esnaola who played an essential role during my PhD. His feedback and expertise helped me a lot during the development of this research work.

I feel privileged to had been a member of the Department of Automatic Control and Systems Engineering UTC. It was a group of incredible people opened to help and exchange ideas, thank you to all the staff and colleagues. I am especially indebted to Dr. Andy Mills who have been supportive and always providing invaluable feedback during my studies. You have been an incredible mentor and a friend. Special thanks to my UTC colleagues Masz, Chris, Ibra, Ariel, Shlomo, Dan, Andrew. I am also grateful to my hermanos Ramón, Gaspar, Pablo and Carlos I learned a lot from all of you. This is the end of a life chapter but the start of a lifetime friendship.

I would like to thank all my friends, you were a family for me: Pepe, Lau, Sandy, Luis, Alan, Moni, Miriam, Carlos, Viteri, Lalo, Omar, Toño, Adrian, Chuga, Pozoles, Steveo, Greenteam, Erika, Fabian, Rikeiks, Fedo, Ulises, Cony, Paulina, Liliana, Samanta, Marissa, María, Figueroa, Javi, Juanfran, Julio, Nicanors, Gen, Alejandro, Yessi. To Yuli Takataka for being so supportive and lovely. You gave me hope and happiness when I least expect it. I express my gratitude to CONACYT Mexico for their financial support, without this help, this work would not have been possible.

Finally, I would like to deeply thank my family. They have always supported me by all possible means in every step of my life. Papá thank you for guiding me and believing in me. Mamá thank you for your infinite love. Itzel and Juan thank you for always being by my side. I dedicate this thesis to all of you.

Abstract of Thesis

Vibration-based condition monitoring is a technique that contributes to the reliability of rotating machinery. Wireless sensor nodes can be used for continuous machine health monitoring in automotive, industrial or aerospace sectors. Consider that random packet loss and signal recovery are common issues in wireless sensing, especially under these types of scenarios. Conventionally, to compensate for these issues, lost data packets are retransmitted, the signal is boosted or the communication channel is changed. However, these techniques may not be enough or convenient to alleviate the packet loss problem as energy conservation in sensor nodes is a critical aspect to face as they are generally powered by batteries or energy harvesters. More importantly, the signal recovery problem needs to be addressed as wireless retransmissions may be limited in aerospace applications. Hence, a different approach is desirable.

This thesis presents a framework that mitigates the random packet loss problem, performs data compression, recovers the signal and increases energy savings at the sensor nodes. The focus is on energy conservation and increased signal recovery performance in wireless vibration sensing systems directed to support equipment health management in aero-engines. The presented framework is divided into vibration data encoding and vibration data decoding. In the former, local signal processing in the frequency domain and compressive sensing occurs at the wireless sensor nodes. For the latter, a novel signal recovery algorithm is used to decode the signal at the base station. The proposed algorithm enhances the performance of the standard orthogonal matching pursuit algorithm for recovery of sparse vibration signals.

The wireless vibration sensing system was successfully demonstrated on an active Trent 1000 gas turbine engine running on a testbed to collect real vibration data. This data was used as prior frequency support for the proposed signal recovery algorithm. The inclusion of prior information improves system performance by reducing the number of samples required for signal recovery. Energy is conserved at the wireless sensors by reducing the amount of data to be sent for vibration signal recovery.

Contents

List of Figures

List of Tables

List of Acronyms

DPCM	Differential Pulse Code Modulation
DSP	Digital Signal Processor
E-OMP	Enhanced Orthogonal Matching Pursuit
EHM	Equipment Health Management
EMD	Empirical Mode Decomposition
EMU	Engine Monitoring Unit
MEMS	Micro-electromechanical System
PDF	Probability Density Function
PE	Piezoelectric
PR	Piezoresistive
PRD	Percentage Root-mean squared Difference
SPI	Serial Peripheral Interface
TH	Threshold
VC	Variable Capacitive
WSN	Wireless Sensor Networks
WVS	Wireless Vibration Sensing

Chapter 1

Introduction

1.1 Motivation

Vibration-based condition monitoring is a technique that contributes to the reliability of industrial rotating machinery. It can help prevent unforeseen machinery failure and reduce the risk for workers. Traditional vibration monitoring is based on the deployment of wired sensors on the static housing of machinery [1]. However, the installation and maintenance of these wired sensors result in added weight, complexity and cost [2]. Wireless Sensor Networks (WSN) make it possible to overcome wired sensors limitations such as weight and cost derived from wiring, connectivity issues and deployment in rotating machinery [2]. Wireless sensors have been identified as an attractive alternative for industrial and factory automation, automotive systems, distributed control systems and networked embedded systems [3]. Important benefits include weight reduction, mobility, scalability, reduced cabling and installation costs [4].

Wireless sensor nodes can be used for continuous machine health monitoring in noisy propagation environments such as those found in the automotive sector, oil and gas industry or gas turbine engines. However, random packet loss is likely to occur under these types of noisy scenarios due to interference, obstacles and multipath propagation among others [5]. Furthermore, wireless sensor nodes are severely constrained in terms of computational capabilities, storage resources, communication

bandwidth and power supply [6]. Sensor nodes are often battery powered or a type of energy harvester is used as a main source of power. Even when using energy harvesting, it is necessary to use techniques involving power management since the available energy differs over time and in function of the sensor nodes location [7]. Hence, data reliability and energy conservation through low power consumption are fundamental requirements for wireless sensor nodes in long-term and continuous vibration based condition monitoring. If the wireless sensors are to be installed within a gas turbine engine it is useful to identify the main sources of vibration from an aircraft and understand the principles of condition monitoring based on vibration. Then, techniques to perform signal processing on wireless sensors for data encoding and signal recovery methods for data decoding are explored.

In summary, wireless vibration sensors were deployed on an active gas turbine engine to collect vibration data. During this test, it was noted that the wireless communication was affected by random packet loss causing several packet retransmissions, unexpected time delays, affected data integrity and wasted energy resources from the sensor nodes. This was the main motivation for proposing a framework to mitigate the packet loss problem and signal recovery problem. For the former, current practical approaches involve using the resources of the transceiver. For instance, increasing the output transmission power, migrating to different channels or allowing data retransmissions. This situation is undesirable, especially in autonomous sensors where the energy is severely limited. The desired scenario is to encode the data in a way that the vibration signal can be recovered even after suffering from random packet loss. For the signal recovery problem, there are sophisticated methods to recover signals from compressed sensing measurements. However, they are computationally expensive and information about the application is not considered. The desired situation is to capture the signal characteristics of the application or use prior information that can help the recovery algorithm to look in the frequency regions of interest where most of the energy is expected to be located. By dealing with these two problems will result in increased energy savings and improved performance in the wireless vibration sensing system.

1.2 Airplane Vibration

Some types of vibration on airplanes can be expected occasionally and are considered normal. However, cases of abnormal vibration require prompt detection and subsequent timely maintenance action.

Normal and abnormal vibrations may happen for several reasons. For instance, mechanical malfunctions, aerodynamics and external factors such as atmospheric turbulence may cause airplane vibration. All vibrations have associated frequencies and magnitudes that may be detected through vibration sensors [22].

Normal vibration: Each airplane has a characteristic signature of normal vibration. This is because of mass distribution and structural stiffness which results in vibration modes at certain frequencies. Very low-level vibrations result when external forces act on the airplane, such as normal airflow over the surfaces. Typically, this is known as background noise. Also normal but more noticeable, is the reaction of the airplane to turbulent air.

Abnormal vibration: This type of vibration typically has a sudden start and may be accompanied by noise. The vibration may be steady or intermittent with a distinct frequency. When the start of abnormal vibration can be associated with a previous event, the source may be evident. However, some vibrations are subtle and require diagnostic methods to determine their probable causes.

Abnormal vibration usually is associated with causes such as engine rotor imbalance, mechanical equipment malfunction, airflow disturbances or control surfaces that have excessive wear among others [22]. The use of vibration sensors for condition monitoring allows the detection of abnormal vibrations and enable preventive maintenance to preserve assets and reduce downtime.

1.3 Vibration-based Condition Monitoring

Many deviations from normal conditions in rotating machinery such as an unbalanced rotor, shaft bending, and ball bearing faults can be detected and diagnosed by

measuring its vibration. Vibration-based condition monitoring is a technique that involves sensing and analysis of the system characteristics in a given domain such as time or frequency. The purpose is to detect changes with respect to the characteristic vibration signatures that machinery exhibits during normal operation. The machine structure and its internal components contribute to the overall vibration signature which is unique among machines [33]. Moreover, the machinery vibration reflects changes on which the condition of one of its components changes. A vibration condition monitoring procedure typically consists of three main steps [10-12] as shown in Figure 1.1. The procedure starts by collecting vibration data from the vibration source, this data is then processed to extract meaningful information. Finally, the extracted features are compared to known signatures [13-14] for fault diagnosis. The remaining useful life of the machine can be estimated using an additional prognosis step [15].

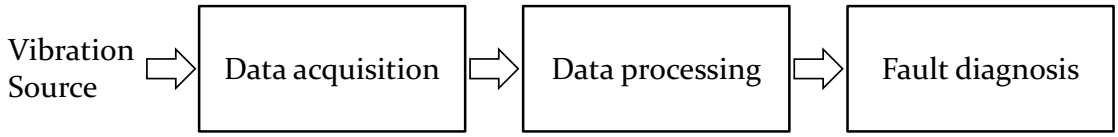

Figure 1.1: Block diagram of a typical condition monitoring system.

Traditionally, vibration is measured indirectly. For instance, to measure shaft vibration, the sensor is placed on a plummer block or house bearing unit as shown in Figure 1.2, this pedestal provides support for a rotating shaft. There are cases on which the vibration is measured directly from the shaft itself. Mitchell [16] discusses arrangements for measuring vibration on frequently monitored machinery such as centrifugal pumps, fans, axial compressors, generators and so on. The summary of his major guidelines are as follows:

1. *Indirect shaft vibration* in machinery may be captured efficiently by placing an accelerometer on the bearing as shown in Figure 1.3a. In machines supported by flexible foundations, the rotor generates dynamic force, much of it is transmitted to the supporting structure through the bearings and then dissipated

Figure 1.2: Structure of a plummer block [16].

in the form of structural vibration. The indirect measurement should follow the ISO-10816 standard [17].

2. *Direct rotor vibration* in machines may be measured by a proximity probe mounted on the bearing pedestals as shown in Figure 1.3b. For machinery with relatively large casing-to-rotor weight ratios supported on rigid foundations, the energy is expected to be dissipated by the rotor vibration itself and a minimal amount is transferred to the bearing [17].

3. *Combined vibration measurements* may be performed by proximity probe and accelerometer together. If the vibration quantity is equally divided into bearing and shaft vibrations, both can be measured and combined. The direct/combined measurement should follow the ISO-7919 standard [17].

The vibration condition monitoring method, as described, is a reliable tool for condition monitoring. However, some limitations are identified:

- Experienced personnel are required for data collection and analysis.
- On-bearing sensors are typically subjected to structural noise that propagates through the machine hull.
- The number of sensors can be increased to enhance fault diagnosis [18]. However, exhaustive signal processing work would be required.
- Cost, maintenance and space needed for system components and cabling.

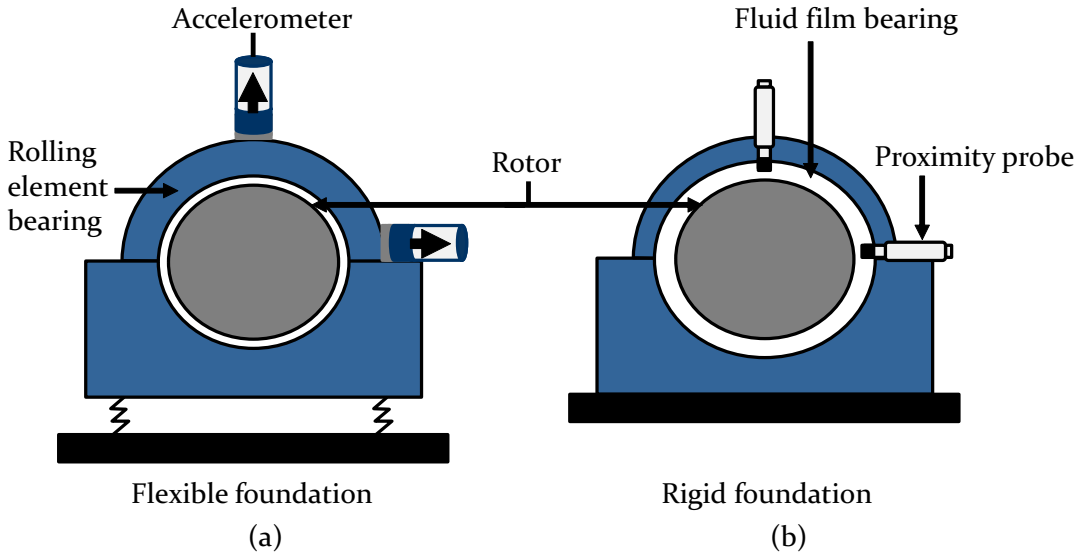

Figure 1.3: Indirect (a) and direct (b) vibration measurement arrangements.

Due to these reasons, an ideal scenario for vibration analysts would be to use a method to capture shaft vibration directly without being affected by bearings and structure imperfections, bearing damping, structural noise and so on. Another objective is to reduce the number of sensors to minimise system maintenance cost and exhaustive signal processing.

Vibration can also be measured on-shaft, acquiring vibration at its source. Sensors may be placed at the rotor where the amplitude is maximum and fault symptoms may be more identifiable.

The advances in wireless technology and sensing capabilities enables to attach a wireless vibration sensor on the rotor [19] as shown in Figure 1.4 (right) which may help to detect a wider range of faults and replace two wired sensors per bearing as opposed to the case shown in Figure 1.4 (left).

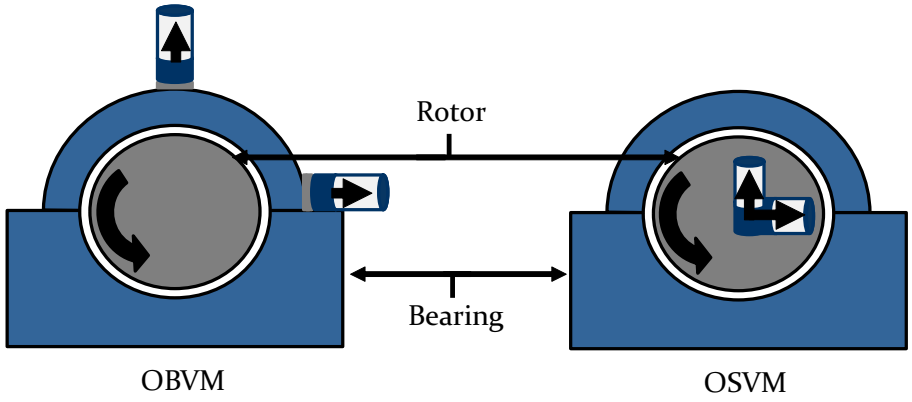

Figure 1.4: Sensor position in on-bearing vibration measurement and on-shaft vibration measurement with a wireless sensor.

1.4 Research Objectives

A Gas Turbine Engine (GTE) is one of the most important aviation components. The core of this propulsion system is the gas producer that turns fuel into mechanical energy. However, several LRUs (Line Replaceable Units) contribute to the remaining useful life of the propulsion system and overall health. LRUs such as fuel and oil pumps, starters, actuators, sensors, gearbox, etc. do not directly form part of the core engine but are necessary to support its operation. The use of wireless sensor nodes with vibration-based condition monitoring can be used to monitor machine health on different LRUs or accessories within a GTE. After the deployment of wireless sensor nodes on an active gas turbine engine test, it was noted that during wireless data transmission, the data integrity, energy efficiency and availability of data was affected by random packet loss, causing multiple data packet retransmissions and unexpected time delays. To bridge these issues, this research presents a suitable framework for Wireless Vibration Sensing (WVS) systems considering the following objectives:

1. Meet system requirements: Investigation of the wireless vibration sensing process. Demonstrate that the selected hardware meets the specific requirements for the wireless sensor infrastructure through research, simulation and experimental analysis.

2. Collection of real vibration data from a gas turbine engine and capture signal

characteristics from the application: Identification of issues and limitations in WVS in noisy environments and development of adequate solutions. Conduct experimentation in a Laboratory environment and in a Gas Turbine Engine to identify potential flaws, conduct simulations based on real data and capture the frequency structure from the application to use it as prior information to improve system performance.

3. Signal encoding at the sensor nodes to compress data, promote energy savings and mitigate random packet loss: Energy efficiency is fundamental in WVS systems because the available energy is limited and varies over time because batteries and/or energy harvesting are used as the main power supply source. Develop a solution that considers the available energy at the sensor node, incorporates local signal processing and compressed sensing prior to wireless transmission.

4. Efficient signal decoding at the base station and minimisation of the number of measurements required for vibration signal recovery: Stability and performance in a WVS system for machine health monitoring are affected by time delays and wasted resources which may be derived from unexpected wireless retransmissions and prolonged signal recovery of vibration signals at the fusion centre. Propose a signal recovery algorithm that improves system performance and energy savings from the sensor nodes by reducing the number measurements required to recover the vibration signal.

1.5 Contributions to Knowledge from this Research

The developed framework mitigates the effect of random packet loss, performs data compression, and increases signal recovery performance in wireless vibration sensing systems to support Equipment Health Management (EHM). It is divided into two main procedures: vibration data encoding and vibration data decoding. In the former, the vibration data is encoded at the wireless sensor node through local signal processing and compressive sensing. In the latter, the vibration data is decoded at the base station using an enhanced signal recovery method for compressive sensing measurements.

The novel contributions contained within this thesis are as follows:

1. Wireless vibration data collection within a running gas turbine engine and estimation of energy distribution across the frequency spectrum from the application: It was demonstrated that the proposed wireless sensing system is capable of meeting the specific requirements of a system requirements document generated by Rolls-Royce for the wireless sensor infrastructure, achieved through a set of experiments conducted in sensor nodes using professional equipment provided by Rolls-Royce (Objective 1). To our knowledge, this is the first time self-powered wireless vibration sensors have been successfully demonstrated on an active civil gas turbine. The wireless vibration sensing system was tested on a Trent 1000 aero-engine running on a testbed to collect real vibration data and then capture signal characteristics from the application (Objective 2). This information is then used as frequency support in the proposed signal recovery algorithm mentioned in contribution 2. The signal encoding strategy for local signal processing at the wireless sensor nodes (Objective 3) presented in [21] includes frequency domain analysis, automatic signal sparsity adjustment and compressed sensing.

2. The second main contribution is a novel algorithm that enhances the standard Orthogonal Matching Pursuit method used for signal recovery of compressed vibration data (Objective 4). The improvement in the performance of this signal recovery algorithm is achieved by including prior information in the form of frequency support structure. This additional input to the recovery algorithm in the form of prior corresponds to the estimated probability density function (energy distribution in the frequency domain) from real vibration data collected during the active Gas Turbine Engine test mentioned in contribution 1. The proposed algorithm uses fewer measurements than the standard OMP for signal recovery. This results in energy savings at the sensor nodes as the data transmitted via wireless is reduced. Also, this situation reduces time delays and increases reliability in the wireless vibration sensing system. This work has been submitted to peer review to the IEEE Industrial Electronics Journal.

1.6 Thesis Layout

The remainder of this thesis is structured as follows:

In Chapter 2, a literature review from vibration sensing technologies and its inclusion in Wireless Sensor Networks (WSN) is presented. The design objectives, related work and challenges of WVS systems applied in industrial environments are also described. The concept of compressive sensing, its relevance in WSN and method selection for signal recovery using CS are also introduced.

In Chapter 3, the signal encoding strategy is presented. The selected hardware for vibration sensing, wireless communication and the system architecture is described. The method used for local signal processing at the sensor node through the Fast Fourier Transform is presented. The selection and implementation of the random sensing matrix used for compressive sensing are shown. Also, an algorithm that increases power efficiency is described, it adjusts signal sparsity dynamically in function of the available power at the sensor node. Furthermore, the power savings from using this algorithm in conjunction with compressive sensing are discussed.

In Chapter 4, the signal decoding method is presented. The set of vibration signals collected during the running aero-engine test are presented. The procedure to estimate the Probability Density Function (PDF) from this set of signals is described and the PDF output is illustrated. The estimated PDF was used to produce a set of 1000 synthetic signals with the same frequency support as the real data for packet loss simulation and experimentation during signal reconstruction procedures. More importantly, this PDF was used as frequency support structure and given as an additional input to the widely used Orthogonal Matching Pursuit (OMP) algorithm. The description and procedure of this Enhanced-OMP (E-OMP) algorithm is shown in this chapter. The E-OMP meets a given recovery percentage using a reduced number of compressive sensing measurements in comparison to the standard OMP method.

Chapter 5, presents the experimental setup. Also, the power consumption savings derived from using compressive sensing and adaptive sparsity adjustment at the sensor nodes prior to wireless data transfer are highlighted. Moreover, the reconstruction results from the received measurements at the receiver side when using the standard

and modified OMP algorithm are compared and presented. The performance and accuracy of the enhanced OMP algorithm are illustrated and discussed.

Finally, in Chapter 6, the findings from previous chapters are discussed, and final conclusions presented. Also, avenues of future work identified from the current research work are outlined.

Chapter 2

Literature Review and Technical Background

2.1 Introduction

Condition monitoring evaluates the internal condition of machinery to increase the useful life and prevent faults [22]. Vibration analysis is recognised as the most widespread method to perform machine condition monitoring [22]. Through vibration analysis, the machine health condition may be evaluated by tracking changes with respect to the characteristic vibration signature that the machine exhibits during normal operation. Vibration-based condition monitoring contributes to the reliability of rotating machinery. Wireless vibration sensing allows remote condition monitoring and overcomes the constraints of wired sensors in terms of added weight, installation risks in rotating components, complexity and cost [2]. For instance, wireless sensors can be used for continuous machine health monitoring in noisy environments such as in the automotive sector, oil and gas industry or gas turbine engines. Packet loss is likely to occur randomly during wireless transmissions under these types of conditions. The data integrity, energy efficiency and availability of data can be affected by random packet loss, causing multiple data packet retransmissions, wasted energy and unexpected time delays. A suitable framework for wireless vibration sensing can provide the means to help mitigate the random packet loss effect through

vibration data encoding and increased energy savings by using an efficient signal recovery method that exploits the application characteristics.

This chapter presents the literature review and technical background related to the work developed in this thesis. This chapter is structured as follows:

- Section 2.2 presents the reliability challenges when using wireless vibration sensing in harsh environments and related work. Furthermore, previous studies about local signal processing in wireless sensor nodes and characteristics of existing hardware for wireless vibration monitoring are presented. The compressed sensing technique is described including foundations, current research studies, applications and requirements. The available signal recovery methods to recover the signal from compressive sensing measurements are also presented in this section.
- Section 2.3 presents the technical background to understand the wireless vibration sensing system analysed in this thesis. In summary, this section presents the concept and importance of Machine Health Monitoring (MHM), an analysis of vibration sensing technologies including characteristics and types of accelerometers, an overview of wireless sensor networks including network characteristics, applications and main design objectives.

2.2 Literature Review

The following section presents the benefits and drawbacks of using wireless sensing for machine health monitoring in harsh environments. Next, previous research work on local signal processing in wireless sensor nodes is presented along with assumptions, weaknesses and conditions not considered in their methodology. The principles and related work behind the encoding and decoding strategies for the wireless vibration sensing system are presented including compressive sensing and signal recovery methods and requirements. Finally, the major challenges, critical factors for wireless sensing in rough environments and approaches taken by previous studies are analysed in order to identify gaps in the literature. The literature review and technical background presented in this section helped to define a suitable framework

for wireless vibration sensing systems capable to perform condition monitoring in harsh environments considering data integrity, power savings and efficient signal recovery.

2.2.1 Vibration Sensing for Machine Health Monitoring

Machine Health Monitoring (MHM) provides efficient methods to preserve equipment and minimise downtime. Vibration monitoring enables preventive maintenance on almost any type of machine in applications such as aerospace, civil engineering, oil & gas, rail, robotics, unmanned vehicles, etc [57-62]. To perform condition monitoring, the sensors are fixed to the mechanical parts of the machines to track failures and malfunctions.

In industry and aero-engines, sensors may be mounted on machinery and/or Line-Replaceable Units (LRU). An LRU is a modular component of an airplane or spacecraft designed to be replaced quickly at an operating location [63]. LRUs include parts that do not directly form part of the core engine but that are required to sustain its operation, such as starters, fuel and hydraulic pumps, fuel/oil heat exchangers, valves, actuators, gearbox and so on [63].

Vibration sensing technologies

An accelerometer is a device that measures changes in gravitational acceleration in the device or machine it may be installed in. Accelerometers are used to detect and monitor vibration in rotating machinery. Single and multi-axis models of accelerometers are available to detect direction and magnitude of acceleration, as a vector quantity, and can be used to sense orientation, coordinate acceleration, vibration, shock and falling. To sense motion in multiple directions, the accelerometer requires to be designed with multi-axis sensors or multiple linear axis sensors. To measure movement in three dimensions, three linear accelerometers are adequate.

Accelerometers have multiple applications in industry and science. For instance, high sensitive accelerometers are components of inertial navigation systems for aircraft and missiles [81-82]. Other applications include the measurement of vehicle acceleration, structural monitoring, medical applications and machine health monitoring

[83-85]. Here, the accelerometers are used to report vibration and its changes in time of shafts at the bearings of rotating equipment such as turbines, pumps, fans, compressors or faults on bearings. The selection of the most appropriate sensor for an application is based on requirements.

MEMS Accelerometers

Micro-electromechanical System (MEMS) Accelerometer or microelectromechanical system is a technique of combining mechanical and electrical components together to form small structures. Miniaturization reduces cost by decreasing material consumption. Furthermore, it increases applicability by reducing size and mass allowing to place MEMS in areas where a traditional system doesn't fit.

MEMS accelerometers are extensively used in applications such as shock detection, tilt control and vibration monitoring among others [86]. MEMS accelerometers feature small size, negligible weight and onboard signal conditioning. For instance, Kok et al [87-88] integrated a complete wireless data acquisition system containing a MEMS accelerometer, a microcontroller and an RF transceiver. They demonstrated that its overall weight is virtually negligible.

One may question the efficiency of MEMS accelerometers. For instance, Ratcliffe et al. [89] demonstrated their capability for machine health monitoring applications. Thanagasundram et al. [90] evaluated MEMS technology conducting analysis techniques to evaluate the properties of these sensors without causing damage, also known as nondestructive testing. They also conducted spectral analysis of vibration signals from a dry vacuum pump, obtaining satisfactory results.

Continuous research attempt to further develop MEMS accelerometers. For instance, Badri et al. [91] proposed modifications to the structure of the moving plates of a variable capacitance MEMS accelerometer to improve the proportionality between proof mass motion and measured capacitance, and thus improve acceleration measurement. Additional improvements may involve the on-shaft sensor equipped with an RF antenna to receive power from a close transmitter via wireless [92-93]. The advances in MEMS accelerometers and wireless technology allow performing wireless vibration sensing for MHM in harsh environments [67].

2.2.2 Wireless Sensor Networks for MHM

The deployment of vibration sensors and supporting instrumentation in rotating machinery requires to guarantee its safe and long-term operation. Therefore, the harsh conditions inside an engine need to be considered. More importantly, the deployment of traditional wired sensors on rotating machinery is not the best solution. The wear of the wiring after continuous machinery rotation may cause wires to break and cause a short circuit, damage to the machinery or personnel. Besides, the cabling is used to interconnect devices which lead to costly installation and maintenance, added weight, high failure rate of connectors, and so on. An early solution to solve the communication problem for on-shaft vibration measurement was to use slip rings [64]. A slip ring enables a stationary wire or set of conductors to transmit power or data signals to one that is rotating [65]. They are widely used in applications with wind turbines, brushed DC motors, assembly line machines, and so on [65-66]. However, slip rings are costly and the noise associated encouraged their replacement by miniaturized WSNs [67-68]. Hence, wireless sensor technology opens the possibility to mount sensors directly onto rotating components without needing these expensive and electrically noisy slip-rings.

The availability of WSNs bring a series of advantages over wired solutions including easier deployment of sensor nodes, this brings an alternative over the use of wired sensors which are expensive, complex and usually hard to install. Moreover, the use of wireless sensors brings the opportunity to place them in critical places, to lower the costs of operation in industrial environments, to deploy in large scale, etc. Additionally, the capabilities of self-configuration and self-organization in WSNs assures efficiency in energy services and reliable management [25, 26]. The environment within a GTE presents harsh conditions. This type of atmosphere may be subject to noise from machinery rotation, metallic reflections and frictions, noise generated from nearby equipment, engine vibrations, variations in temperature, channel interference and obstacles among others [59]. Thus, these severe situations may cause wired system solutions to be unsuitable in some applications and require cabling isolation. Reliability in wired systems could be enhanced by adding redundant wires although it would result in added complexity, weight and cost. Additionally, it is not a suitable solution if the machinery or equipment connected by these wires need to be relocated. As a result, using wireless alternatives appears as a viable solution to be

used in atmospheres under these conditions [23].

The use of wireless sensors for machine health monitoring eliminates physical connectors and wiring that could be exposed to hazardous environments. Hence, they enable to monitor systems that could not be monitored previously due to high maintenance cost or personnel risk exposure to repair these systems. Also, wireless sensors allow monitoring of systems where external connections are impossible or impractical [69]. However, this technique requires the collection of a large amount of vibration data from the machinery or accessory of interest to facilitate accurate fault diagnosis. This situation is not always practical in a wireless environment due to sensor node limitations such as limited memory size, lengthy transmission time caused by low transmission rate and data packet retransmissions derived from random packet loss when installed in noisy environments. Hence, energy consumption and wireless transmissions may be minimised through local digital signal processing and data compression.

In wireless MHM, Fault Diagnosis may occur at the base station after the vibration signal is acquired, conditioned, processed and transmitted from the sensor node. It is desirable that signal postprocessing occurs at a dedicated BS because there are typically no constraints on power consumption to carry out computationally intensive algorithms and methods to diagnose faults. There exist two main approaches for this purpose: signal-based and model-based. In the case of the model-based method, a fault can be detected from continuously comparing the difference between the actual machine response and the model. The reliability of this method is dependent on the conformance or match between the real machine and the model, boundary conditions and the accuracy of materials parameters [70], more details in [71-72].

In the signal-based approach, a vibration signal is used to diagnose faults without the need to model the machine dynamics. The overall level of vibration is a robust indicator to determine machinery condition and to decide if a check-up is required [73]. Later, to determine a fault type, the signal may be analysed in the frequency domain. Detailed tables about common faults linked to their spectral representation can be found in [73-74].

Although the fault detection methods are out of the scope of this research, they were introduced for the interest of the reader with references to literature that cover these

topics in more detail. The focus of this research work is on energy efficient encoding procedures for vibration signals acquired from sensors prior to wireless transmission to increase robustness to random packet loss and data compression to minimise the number of transmitted samples. Also, the focus is to recover the signal with high accuracy and speed.

Opportunities and limitations in wireless sensor networks

Wireless Sensor Networks (WSN) have been extensively considered one of the most important new technologies of the present century [33]. The current evolution in MEMS and wireless communication technology have allowed the deployment of small inexpensive smart sensors in a physical area, these sensors networked using wireless links and Internet have opened opportunities for a variety of military and civilian applications such as environmental monitoring, battlefield surveillance and process control in industries [34].

WSNs have received great interest from both industry and academia around the world. However, WSNs present unique characteristics and constraints that should be considered when building a model for a specific application, those include limited power source, small memory space and constrained processing power, those characteristics including higher unreliability on sensor nodes differentiate WSNs from traditional wireless communication networks such as cellular systems and ad hoc networks [35]. Extensive research activities have been conducted to attempt to solve design and application issues, resulting in considerable advances in the deployment and development of WSNs. It is predicted that in a near future WSNs will be globally used in diverse civilian and military applications, revolutionizing the way we interact with the physical world and our quality of life [36].

WSN Network Characteristics

The sensor nodes communicate the sensed data over a short distance through the wireless medium and cooperate to achieve a common task such as battlefield surveillance, environmental monitoring and industrial process monitoring and control in remote locations [95-97].

A WSN typically consists of a collection of low cost, low power and multifunctional spatially distributed sensor nodes (SNs) that monitor and collect data from the

environment or area of interest in which they are deployed [94]. The SNs are small in size but incorporate sensors, embedded microprocessors and radio transceivers. Consequently, WSNs include sensing, data processing and communication capabilities. The sensor nodes communicate the sensed data over a short distance through the wireless medium and cooperate to achieve a common task such as battlefield surveillance, environmental monitoring and industrial process monitoring and control in remote locations [95-97]. A WSN system also includes a manager node or gateway which provides wireless connectivity back to distributed nodes and the wired world such as the Internet, a personal computer to display the data on a graphic user interface (GUI) or an Engine Monitoring Unit (EMU) in the case of a Gas Turbine Engine. The selected wireless protocol depends on the application requirements [98].

WSN Applications

Wireless sensor networks are typically distributed over a region of interest where they perform sensing, processing and communication tasks. The sensors can be used to monitor physical or environmental conditions such as temperature, pressure, sound, light, and vibration among others. The advantage of not requiring cabling to communicate and report sensed data within the existing network and the low cost of available sensors have allowed the creation of a variety of applications such as environmental monitoring [96], military applications and outdoor surveillance [95], healthcare monitoring [99], habitat monitoring [100], home automation and indoor surveillance [101], industrial process control [97] and aircraft health monitoring [102] among others. The previous applications, as well as many others, benefit from wireless data acquisition capabilities and deployment in many environments such as battlefields, outer space, oceans and machinery in remote locations.

2.2.3 Local Signal Processing in WSN

The installation of wireless sensor nodes for vibration monitoring in rotating machinery such as gas turbines [27], rotating shafts in the industrial sector [28], rotor blades in helicopters [29] and so on, appears as the only feasible solution. This is because the installation of wired sensors is unviable or hazardous for that purpose. Wireless sensors provide potential advantages over wired sensors. The use of WSNs

help to avoid associated issues regarding wired analogue sensors such as weight reduction, lower installation cost, increased data acquisition flexibility, scalability, easier setup processes and reduced complexity. Furthermore, by using WSNs, physical connectors and wiring exposed in hazardous environments are eliminated [30].

Condition monitoring based on vibration sensing is a technique that allows assessing the operating conditions of any moving mechanical system or rotating machinery. Monitoring these vibration signals using WSNs results can help to improve diagnosis, and therefore, machinery failure can be prevented. Typical vibration monitoring is performed using low integrated piezo-electric accelerometers [31]. The raw vibration data acquired from these types of sensors is then transmitted to a Base Station (BS) for further signal processing. However, the power consumption in wireless sensor nodes is considerably increased when the radio transceiver is continuously active to send the raw vibration data to the BS. Moreover, to ease reliable machine health assessment, sensor nodes should acquire the vibration based signals at a high sampling rate which generates large data packets. These situations become impractical in a wireless data transmission due to the characteristic low transmission rate and prolonged transmission time [32]. For continuous vibration monitoring, it is fundamental to minimise power consumption on sensor nodes. One way to reduce power consumption is proposed by Chan et al. [32] where the sensed data is compressed prior to wireless transmission. A novel data compression algorithm combining Empirical Mode Decomposition (EMD) and Differential Pulse Code Modulation (DPCM) is implemented for that purpose. EMD is used to decompose and identify instant non-linear changes and non-stationary signals caused by abnormal operation in the machinery. On the other hand, DPCM is applied for further data compression by using a linear predictor and quantizer before wireless transmission occurs. However, this study does not consider local signal processing on sensor nodes, packet loss, interference, security issues during transmission and reliability reduction due to a high compression ratio. A more suitable alternative is to reduce the continuous transmission of raw data by analysing the signal locally on the sensor nodes using signal processing methods.

Other studies, attempt to implement local signal processing through dedicated algorithms for vibration monitoring. However, it is challenging to embed these type of algorithms on sensor nodes (SNs) due to constraints on processing power, memory and limited energy source [33]. Additionally, algorithms to monitor vibration can

be resource intensive and complex depending on the reconstruction requirements and signal characteristics. For instance, Merendino et al. [34] implement a discrete wavelet transform and time sample averaging in a microcontroller to detect faults in gears. Other studies use a Field Programmable Gate Array (FPGA) or a dedicated Digital Signal Processor (DSP) to run signal processing algorithms [35]. Even if these processors offer high performance, speed and computational power to perform signal processing, FPGA or DSP are not the best solutions for local signal processing at wireless sensor nodes due to their high power consumption, cost and size [36].

Existing commercial wireless vibration monitoring systems found in the literature do not perform local processing on sensor nodes. The WiMon100 sensor node by ABB group [37] is used to improve maintenance of electrical motors and rotating equipment. The transducer type that performs vibration measurements is a piezoelectric accelerometer, raw vibration data is transferred to the BS to perform further signal processing. The data received runs own developed software for data analysis, storage, graphical user interface and decision making [37]. The V-Mon 4000 by Inertia Technology [38] sensor node is used for industrial vibration monitoring, it transmits the vibration signals to the BS for further processing and condition monitoring of the machine. This sensor node claims to achieve real-time transmission of vibration signals due to the powerful ARM Cortex-M4 processor used. Complex signal-processing techniques such as wavelet transform, time domain averaging and empirical mode decomposition are carried out on the base station. The VIBConnect sensor node by Pruftechnik is used for condition monitoring and diagnosis. However some drawbacks were identified, the radio module and sensors are physically separated and connected by short cables, in case the sensor node is installed in a hazardous environment the cabling is exposed to damages. Moreover, the output signal from the accelerometer is a relative simple output of 35 mV/g, which means that the sensor does not provide application-specific analysis such as embedded frequency domain processing or any other type of signal processing. The raw vibration data acquired by the accelerometer is transmitted to the base station for further analysis, visualization, reporting and archiving [39]. The WiVib 4/4 Pro by Icon Research is a battery-powered device with multiple inputs, this device is used to measure vibration and parameters from machinery and mechanical systems. It allows four standard integrated circuit piezoelectric accelerometers to be connected to any of the 4 channel inputs. The acquired data is transferred over a wireless standard WiFi

802.11 to a host computer for processing and display, no local signal processing is performed at the sensor node [40]. The next subsection presents the current challenges and approaches to perform wireless sensing for condition monitoring in harsh environments.

2.2.4 Challenges and Approaches

Manufacturing plants, companies and industry in general, rely on the data collected from the networks of distributed sensors located in strategic zones. The advantage to sense, measure and monitor data from hard to reach areas using simple procedures or infrastructures have made this technology popular nowadays. Many industries such as power plants, oil and gas pipelines, chemical and industrial companies among others have deployed wireless networks to monitor different parameters. These parameters are fuel levels, pipe flow, air pressure, electrical current, temperature, vibration [41] together with data that represent the machine status. The collected information allows tracking the effectiveness and efficiency of a given process, factors that are fundamental for safe operation.

There exist applications of WSNs that have replaced wired sensors to make space for temperature and vibration sensors, which are used for vibration monitoring in motors [42-46] this is because of the infeasibility to install wires in some areas. WSNs are used for condition monitoring on which data is reported periodically regarding the status of motors and tool performance statics on machines [47]. The sensors support machine maintenance since they generate alarms when an unexpected event occurs. Then, the measurements taken are sent to the sink or controller to take immediate actions. Additionally, WSNs open opportunities to perform in situ or local signal analysis infeasible using wired sensors, some of the applications that take advantage of this features include steady state motor analysis and onboard oil analysis [48].

Condition monitoring and machine prognostic analysis using WSNs are becoming a common area in manufacturing centres and plants involving critical operations. For instance, Jardine et al. [49] refer to the use of wireless technology in nuclear power plants to increase the accuracy in multisensory systems for machine prognostics and health management. There exist similar applications that use WSNs for machine tool monitoring, Wright et al. [50] use wireless sensors to monitor temperature for end

mill inserts. In a similar way, Sundararajan et al. in [48] use condition monitoring based on vibration sensing to avoid breakage of tools.

Reliability can be enhanced through control mechanisms to handle timing and frequency bandwidth efficiently. For example, in [51] Kunert et al. propose control techniques to improve throughput and enhance reliability. In this study, reliability is guaranteed by retransmitting messages when necessary, important assumptions in this study include predictable access to the wireless medium and admission control in real time. Other approaches to improving reliability include the use of probability functions and estimation techniques. In [52] an analytical model is proposed to estimate the probability of failures during wireless data transmission in the industrial domain. This systematic approach estimates the desired reliability by means of packet success rate estimation, and a suitable number of message retries is configured as a result. In [53] an interesting contribution by Fischione at al. involves the design and implementation of a protocol used to guarantee reliability and delay requirements in wireless sensor networks for control and actuation applications. This protocol considers routing, duty cycling, and medium access control all combined to maximise the network lifetime and improve energy efficiency. The main objective of this approach is to optimize energy consumption considering factors such as packet reliability and time delays.

Reliability, timing and accuracy [54] are probably the most critical factors that should be guaranteed when using wireless sensor networks to transmit data in harsh environments such as the industrial domain or within a gas turbine engine. It is essential to ensure that the measurements obtained from the sensors are accurate, transmitted reliably and received by the base station or the destination node at the appropriate time. Meeting time deadlines regarding data transmission is a crucial factor in process automation [55], [56] where unexpected time delays or interrupted communication may cause failures in the production line, discontinued services, damage on machinery or even cause a risky situation for the workers. On the other hand, transmitting inaccurate data due to a faulty sensor or the random packet loss effect caused by interference or noise in the wireless medium may result in defective condition monitoring or may cause the actuators to have an unexpected behaviour since they may respond as a result of the data measured by the sensors. An approach to meet time deadlines and mitigate packet loss during wireless transmission is required to increase reliability in the wireless sensing system. These may be achieved

by implementing a strategy for signal encoding through local signal processing and compressive sensing in the wireless sensor nodes for data compression and help deal with random packet loss.

Conventional digital signal processing

In digital signal processing, a real-world signal such as temperature, voice, position, pressure, vibration, etc. is digitised and then mathematically manipulated. Signals are processed in order to be displayed, stored, compressed, transmitted or analysed using advanced signal processing methods available only for data in digital format [79]. For instance, a continuous signal is converted into a discrete signal that is finite and equally spaced in time because it is uniformly sampled at or above the Nyquist rate [80]. Conventional signal processing follows the Shannon- Nyquist theorem for sampling signals. Many samples are generated using this method because the sampling rate should be more than twice the maximum frequency present in the signal. Opposed to this conventional sampling approach, a novel signal acquisition and recovery method is proposed by Compressive Sensing (CS) theory [80]. This signal processing technique efficiently acquires a signal using fewer samples than traditional methods [80]. In summary, CS theory asserts that if a signal is compressible or sparse in a given basis, the signal can be reconstructed from fewer measurements in comparison to the conventional Nyquist case, this topic is covered in more detail in the next section.

2.2.5 Compressive Sensing for Signal Encoding

Conventional signal processing follows the Shannon-Nyquist theorem for sampling signals [113]. The data is sampled at least twice the highest frequency component found in the signal, the so-called Nyquist rate. This method generates many samples as the sampling rate should be more than twice the maximum frequency present in the signal. In modern compression technology, this signal is compressed for a smaller representation as shown in Figure 2.1. For example, in image compression, in jpeg, most of the image components are discarded using the wavelet transform [107].

One may question the utility of acquiring so many measurements if most of them are discarded in the subsequent processing stage. In contrast, Compressive Sensing (CS)

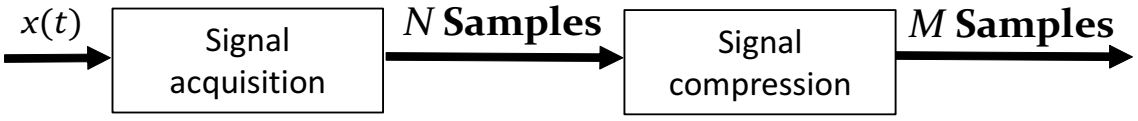

Figure 2.1: Conventional signal sampling and compression.

asserts that a signal/image can be sampled at a subnyquist rate (lower than Nyquist rate) while reducing computational complexity and without affecting signal recovery [105]. In [106], it is shown that CS achieves higher peak signal-to-noise ratio and lower reconstruction error in comparison to traditional compression methods such as Discrete Cosine Transform (DCT) and Joint Photographic Experts Group (JPEG). Compressive sensing is based on three principles/rules to perform successfully. These principles include incoherent subsampling, transform sparsity and signal reconstruction [107] which are presented in the next subsections. In this thesis, compressive sensing was used for signal encoding in the wireless sensor nodes to help deal with the packet loss problem and for signal compression.

2.2.5.1 Introduction to Compressed Sensing

Suppose that sampling and compression are required for an application so only the coefficients of higher magnitude are kept for a given data set. According to Shannon-Nyquist sampling theory, in order to accurately recover/reconstruct a signal/image without losses, it should be sampled at a rate of at least twice the maximum frequency in the signal. It is challenging to reduce the Nyquist rate through undersampled measurements. Although storage and computational power may be reduced, the reliability of the reconstructed data can be affected because the recovered signal may differ considerably from the original one and distortion effects such as aliasing may occur [108].

Studies in [107, 109, 110] present a promising technique called compressive sampling or Compressed Sensing (CS) in which the number of samples is reduced significantly while compression of sparse data occurs. This recent paradigm used for data acquisition and processing was originally developed to efficiently store and compress digital images. In the proposed theoretical model, it is shown that CS exploits the sparsity nature of images where most of the energy in the signal is concentrated in

a few non zero elements/coefficients as shown in [111]. Moreover, it is not required for the signal itself to be sparse but compressible or sparse in some known transform domain or basis. For instance, transforming images into Fourier or wavelet basis may reveal the relevant content or energy concentrated in a few elements, which will be a suitable sparse representation for CS. In the case of time-based signals, they may not appear to be sparse in its original domain as shown in Figure 2.6a but they may be when they are transformed to the frequency domain as shown in Figure 2.6b through the Fourier Transform. Here, a few frequencies or non-zero elements capture most of the energy in the signal, this is the case for the current application presented in the following chapters within this thesis. Subsequently, during the sampling process, CS compresses the signal using much fewer measurements to represent the complete set of signals. For instance, in image processing applications [109], this procedure occurs when the image is projected onto a random subspace through a random sensing matrix of smaller size in comparison to the size of the image without having any prior knowledge of the image itself. Furthermore, in WSN, CS enables to execute simple computations at the encoder side where the battery-powered/energy harvested wireless sensors are located. Whereas computationally intensive recovery methods to reconstruct the signal or image occur at the base station which is not typically constrained by battery usage. In other words, this method reduces the dimensionality of the image/signal by projecting high-dimensional data onto a lower-dimensional space while preserving relevant information. In this thesis, we denote the dimension of high dimensional space by N and the dimension of low dimensional subspace by M.

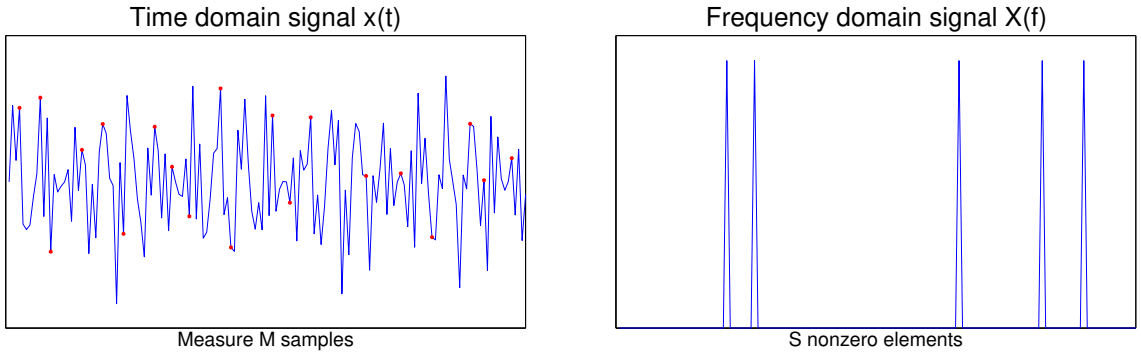

(a) (b)

Figure 2.2: Samples in time domain (a) and frequency domain (b).

2.2.5.2 Applied Principles in Compressed Sensing

Compressive sensing (CS) states that certain signals and images can be reconstructed from far fewer samples or measurements than the conventional Nyquist case if the signal is compressible or sparse in a given basis [107]. For example, if the signal requires to be sparse in some domain, techniques like the Discrete Fourier Transform (DFT) or Wavelet transform can be used over the original signal or image. After transformation, the coefficients or elements in the signal that capture most of the energy can be identified [107]. This concept is relevant to the application of wireless vibration sensing for condition monitoring in industrial plants, gas turbine engines and so on. The electrical noise propagation in these environments affects the wireless communication producing random packet loss. However, the sparsity in a vibration signal on a given basis can be exploited to help deal with this problem. This effect can be minimised through the use of inertial vibration sensors with embedded frequency domain analysis which outputs a nearly sparse signal that can be used in conjunction with CS. The received signal at the fusion centre can be recovered from fewer samples than the conventional case without signal compression through random encoding.

One can recover certain signals and images from a fewer number of samples or measurements if two principles are followed during CS: sparsity, which requires the signal to be sparse in some domain, and incoherence, which refers to the sensing modality through the measurement/sensing matrix [107].

Sparsity

The concept of sparsity applies to images and signals [107, 109]. For instance, a signal or image is considered to be sparse when its informational content is reflected in a few data points. In other words, sparsity describes the density level of a signal or image on a given basis. Many natural signals in their original domain may seem dense but when they are transformed to a convenient domain using a suitable basis, the signals may become compressible or sparse. In simple words, the original signal/image is transformed into another representation or domain where it is simpler/easier to distinguish/differentiate between relevant and irrelevant information. For instance, this can be performed with the Fourier or Wavelet transforms. The new domain presents a concise summary of the elements contained in the signal. In image processing, this helps to easily define a threshold and to determine that all pixels

below that threshold contain information that is irrelevant. Similarly, in this research work, the original time-domain vibration signal is transformed into the frequency domain. Here, the frequency components below the defined threshold are discarded in order to make the signal sparse and to keep the components that capture most of the energy in the vibration signal. In both cases, either in images or signals, after transformation, the coefficients or elements capturing most of the energy or information in the signal/image can be identified and maintained. In the same way, the elements of lower energy (E.g.: near zero) may be discarded or set to zero without losing important information in order to increase the sparsity level and convert a nearly sparse signal into a sparse signal that can then be used in CS. This procedure typically happens in CS because of the low contribution of these elements/coefficients towards the signal or because they can represent noise.

Mathematically, a signal f is S-sparse [107] when it has at most S nonzero elements. We let the vector $f \in \mathbb{R}^N$ be the signal of interest which can be expanded in an orthonormal basis (such as Fourier or wavelet basis) $\Psi = [\psi_1 \psi_2 ..... \psi_N]$ as follows:

$$f = \sum_{i=1}^{N} z_i \psi_i, \tag{2.1}$$

where z is the coefficient sequence. It is convenient to express f as Ψs, where Ψ is the NxN matrix containing $\psi_1, ..., \psi_N$. The idea of sparsity is clear, when the signal is transformed to obtain a sparse expansion, small coefficients can be discarded without much loss because the energy that those coefficients capture or their contribution to the signal is minimal. Consider f_s the vector obtained when the S largest values/coefficients of z_i in (3.2) are maintained while the rest are set to zero. This vector f_s is sparse because all elements are zero except for a few nonzero entries. From now on, S-sparse refers to objects with at most S nonzero elements. An example of the effect of discarding the vast majority of the coefficients in images can be observed in [107], the perceptual loss is hardly noticeable between the original image containing all the coefficients and the sparse image containing only the highest 2.5% coefficients while the rest of the coefficients are discarded. For instance, this principle is used in the majority of lossy coders such as JPEG-2000 [138].

Lossyness in Sparse Signals

In practical applications, the acquired CS measurements contain a large amount of data for storage and transmission. Hence, the lossy compression of CS is necessary for the CS acquisition process. An efficient lossy compression of CS acquisition requires to adaptively sparsify the image or signal of interest for better reconstruction [148]. At the stage of CS acquisition, it is known that a sparsity degree of the original signal is important for reconstruction from CS measurements. If the original signal is not sufficiently sparse, the reconstruction quality degrades due to the effect of noise folding. In [149], Arias-Castro et al. studied this problem in a practical system based on CS. Laska et al. [150] demonstrated that a compressible signal could only be recovered by part of its main coefficients, and the rest of the coefficients cause the noise folding effect, which in the end degrades the reconstruction quality considerably. To reduce that undesirable effect, the simple Discrete Cosine Transform (DCT) coefficients truncation method [151] was used in CS signal coding to improve its rate-distortion performance. However, in this study, the sampling rate variation is not considered which is the principal factor for deciding how many important DCT coefficients can be recovered from the original signal. In [152], Mansour et al. present an adaptive CS method which focuses on acquiring the large coefficients of a compressible signal to reduce the noise folding effect. In the wireless vibration sensing system presented in this thesis, the large magnitude frequency components are maintained as part of the signal encoding strategy. At the receiver, the encoded sparse signal is recovered at the base station, even under random packet loss. The signal can be recovered provided that enough number of CS measurements are received. More details in Section 2.2.5.5.

Sensing Matrix

Compressive sensing involves operation by a matrix on the signal or image of interest. Let x represent the signal of interest, where $x \in \mathbb{R}^N$ with sparsity S. Consider a system that acquires M linear measurements or samples. This process can be represented mathematically as

$$y = \Phi x, \tag{2.2}$$

where $\Phi \in \mathbb{R}^{MxN}$ and $y \in \mathbb{R}^M$. The sensing matrix Φ represents a dimensionality

reduction as we move from $\mathbb{R}^N$ to $\mathbb{R}^M$. The size of the vector of measurements y is produced as follows $y_{\{Mx1\}} = \Phi_{\{MxN\}} x_{\{Nx1\}}$. Where the number of measurements M are much smaller than the complete signal length N or $M \ll N$. In the standard CS framework, it is assumed that the measurements M are non-adaptive [139], this means that the rows of Φ are fixed and are not dependant on previously acquired measurements. However, in this research work, the number of measurements M are dynamic because they are selected based on the available power of the wireless sensor node, more details are described in Section 3.7.

Additional to sparsity in the signal, compressive sensing requires incoherence between the sensing matrix Φ and the sparsifying basis, like Discrete Fourier Transform or Wavelet basis. The sensing matrix Φ should preserve the information in the original signal or image during orthogonal projection [140]. Also, it should satisfy the properties shown by Donoho and Candes [113].

To generate a set of compressive sensing measurements, the dimension and type of sensing matrix Φ play an important role. First for appropriate signal encoding and subsequently for recovery of sparse signals. The selected measurement matrix Φ should meet the key properties such as RIP an incoherence sampling described below.

Restricted Isometry Property (RIP).- This property is fundamental in CS. The RIP requires a matrix Φ and any submatrix formed with Φ to be nearly orthogonal. In other words, each column in the sensing matrix Φ is almost orthogonal respect to the rest of the columns. In compressed sensing, random measurements are taken (from a sparse signal). This means that random columns of the sensing matrix Φ are selected to form a submatrix which is used to produce a vector of compressed measurements y, resulting in signal compression.

A matrix Φ meets the RIP if, for any S-sparse vector x, Φ obeys the following mathematical relation (3)

$$(1 - \delta_S)\|x\|_2^2 \leq \|\Phi x\|_2^2 \leq (1 + \delta_S) \parallel x \parallel_2^2 \tag{2.3}$$

where, δ_S is a particular positive constant, $0 < \delta_S < 1$. This means that the matrix Φ guarantees to only change the magnitude of any vector x to a small degree when signal

compression occurs. This is possible as long as the vector is S-sparse (containing at most S non-zero elements). In other words, the restricted isometry constant δ_S is the smallest number such that (3) is obeyed. If this occurs, it is said that Φ satisfies the RIP of order s with constant δ_S .

In order to reconstruct any S-sparse vectors x from measurements generated from $y = \Phi x$, it is required to be able to distinguish between different measurements. This allows to identify their origin and be able to recover them. For instance, say two sparse signals (x_1 and x_2) are compressed as $y_1 = \Phi x_1$ and $y_2 = \Phi x_2$ The measurements of any two sparse vectors x_1 and x_2 are required to be "sufficiently different". In case $y_1 = y_2$ (after signal compression through sensing matrix Φ) it would not be possible to distinguish them and reconstruct them uniquely. This may happen if the columns of Φ are not nearly orthogonal (redundant information exists) and probably Φ do not meet the RIP property. In simple words, the RIP property helps to design a convenient sensing matrix Φ such that the information in any compressible signal is not damaged by the dimensionality reduction as we move from $\mathbb{R}^N$ to $\mathbb{R}^M$ and then to recover the sparse signal from only M compressed measurements.

In compressed sensing, apart from meeting the RIP property, it is required to sample the data points randomly (incoherent sampling). When incoherence and subsampling are combined, they produce potential benefits. Firstly, subsampling increases speed because the fewer points sampled, the faster the acquisition. Secondly, with incoherence, the sparse signal can be reconstructed accurately with high probability using the CS framework [107].

In summary, the RIP property must be satisfied by Φ in order to successfully recover the signal. Given a Φ measurement matrix, it is NP-hard to compute the restricted isometry constants [118] to verify if that matrix obeys the RIP property. However, it has been shown that for many random matrices, they satisfy the RIP with high probability. These matrices include random Gaussian, Bernoulli and partial Fourier matrices [113]. Both the RIP and incoherence conditions can be met with high probability by choosing Φ as a random measurement matrix which is the case for the mentioned matrices [113]. This is achieved by letting the elements in the matrix Φ to be independent and identically distributed (iid) random variables.

The selected measurement matrix Φ should be fastly computable to encode the signal

and to recover it. Finally, it should be relatively easy to implement it in hardware [119].

2.2.5.3 CS Applications

Conventional signal processing techniques used in DSPs and FPGAs involve sampling data above the Nyquist rate, the generated data can then be sent to a base station for further signal processing and analysis [112]. Opposed to these typical techniques, CS theory is proposed as a novel signal acquisition and recovery method [113]. This signal processing technique efficiently acquires a signal using fewer samples than traditional methods [113]. The idea of compressed sensing is centred on the data structure rather than its bandwidth. In summary, CS theory asserts that if a signal is compressible or sparse in a given basis, the signal can be reconstructed from fewer measurements in comparison to the conventional Nyquist case. This directly benefits applications on which the number of measurements or samples are expensive or limited like in wireless sensor networks.

Compressive sensing allows to sense and to compress a signal simultaneously. This sensing modality [107] has been researched extensively for a wide range of applications from medical to military sectors [114, 115]. Fewer samples are used in CS than in traditional Nyquist case to represent a signal or image. This results in faster and more efficient signal acquisition methods because the signal is recovered using a reduced number of compressed sensing samples or measurements. For instance, applications that require fast sensing such as WSN or Magnetic Resonance Imaging (MRI) may benefit from CS [116]. The MRI technology allows producing detailed images of organs and structures inside the body through magnetic fields and radio waves. However, acquisition speed is a challenge, especially in anxious patients that cannot stay still or those with limited breath-hold capacity. CS may help to overcome those challenges because this technology helps to increase speed by decreasing considerably the acquisition time in MRI without sacrificing the quality of the image [116].

CS in Wireless Sensor Networks

Compressive Sensing has been used in many areas including wireless sensor networks [153-154] in static and mobile sensor networks [161]. The sensor nodes can acquire

a small number of measurements as linear projections of the raw signal and directly send these CS measurements via wireless to the fusion centre or base station without any additional processing at the sensor node [154], [156-157]. Other studies consider energy dissipation characteristics of WSNs using CS and compare it to two conventional approaches such as data acquisition without processing and data acquisition with transform coding. They show that compressive sensing extends network lifetime considerably compared to conventional approaches provided that the measured signals are sparse [112]. The work of Liu et al. [18] proposes a compressive data collection scheme for WSN focusing in a routing strategy without much computation and overhead to provide robustness for energy-conservation in practical applications. However, this study uses a convex optimisation method of traditional compressive sensing theory for signal recovery which can be computationally intensive and may cause unexpected delays. They also introduce conventional retransmission mechanisms for failed wireless data packets which are not desirable for data transfer in harsh environments such as in a Gas Turbine Engine. Other studies [158-159] attempt to reduce the energy spent on wireless transmissions between sensors in the network, also called distributed compressive sensing. This is developed to exploit the inter and intra sensor structure or correlation. However, the focus of this thesis is on a centralised architecture where each node in the network is independent and reports directly to the base station. In [160], it is shown that CS achieves great energy efficiency for sensing operations in WSN.

2.2.5.4 Theoretical aspects of CS

Let x be a sparse signal, where $x \in \mathbb{R}^N$ with sparsity S where $S \ll N$, that means, only S coefficients or elements of x are nonzero while the remaining are zero, thus the S-sparse signal x is compressible. CS asserts that sparse signals or images can be recovered with high probability from lower measurements in comparison to those dictated by Shannon-Nyquist theory [107] as long as the number of measurements meets a lower bound depending on the sparsity of the signal. Therefore, the sparse signal x can be recovered from a set of measurements of size M, where $M \geq S\log(N) \ll N$.

It is not required for the signal itself to be sparse in its original domain but compressible or sparse in some known basis or transform domain called Ψ. For instance, some

signals may be transformed to Fourier or Wavelet basis for a sparse representation to be used in CS [109, 113].

Suppose x is the sparse signal in Ψ domain, where Ψ is the transform basis used to sparsify the signal/image. The signal of interest x can be represented with fewer samples/measurements by computing the inner product between x and a random sensing matrix Φ. The resulting vector y contains the compressed sensing measurements. The number of required measurements depends on the sparsity level and signal length, more details in Section 2.3.4.6.

Regarding the sensing matrix Φ, it maps input vector to the measurement vector by linear weighted summation of the input. If the input signal is sparse in a given domain, then a sensing matrix can be used to generate the vector of measurements y. In other words, the sensing matrix Φ allows signal compression. The sparse signal x is encoded in the vector y. However, the sensing matrix Φ needs to satisfy the RIP property described in Section 2.3.4.2.

Mathematically, the encoding procedure can be represented as

$$y = \Phi x, \tag{2.4}$$

where $\Phi \in \mathbb{R}^{MxN}$ and $y \in \mathbb{R}^{M}$. The sensing matrix Φ represents a dimensionality reduction as we move from $\mathbb{R}^{N}$ to $\mathbb{R}^{M}$. $y_1 =< x, \phi_1 >, y_2 =< x, \phi_2 >, ..., y_m =< x, \phi_m >$. The process involved in CS is illustrated in Figure 2.3 [117], where it can be seen that the vector y contains M measurements resulting from a linear combination of Φ and elements of x.

2.2.5.5 Signal recovery of sparse signals

Overview

The idea of CS is that if a given signal has a structure or is sparse in a given domain, then this signal can be reconstructed even from fewer measurements [113]. This is particularly important for applications on which measurements are expensive or limited, such as the use of WSN and CS in a gas turbine engine. The received

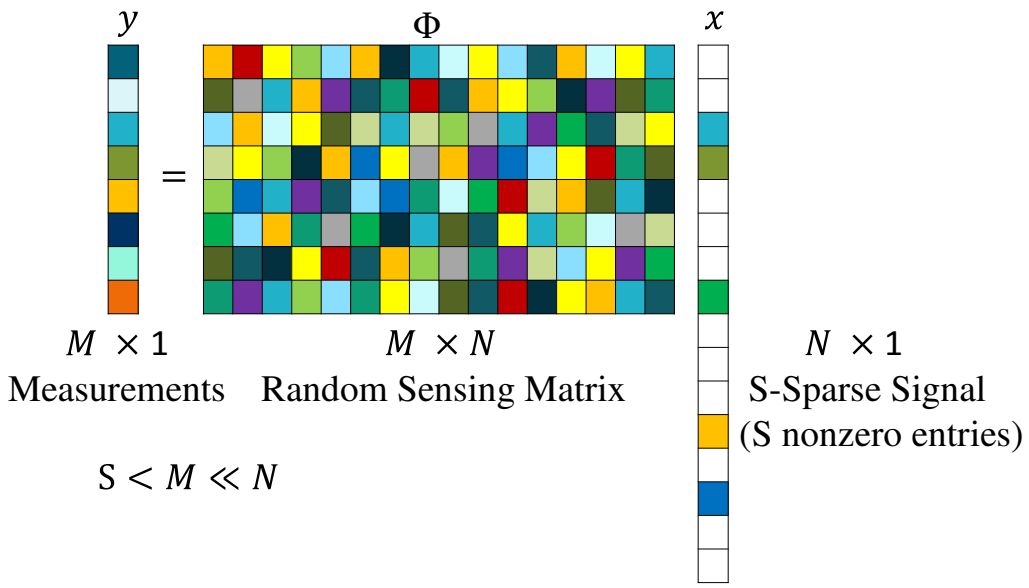

Figure 2.3: Compressive sensing measurement process with a random measurement matrix Φ and a sparse signal x with $S = 5$. The vector of compressed measurements y is the product of the sensing matrix Φ and the sparse signal of interest x. Here, x contains only zeros except for 5 nonzero components ($S = 5$).

measurement vector used for signal reconstruction is given by $y = \Phi x$, where x is the S-sparse signal and $\Phi \in \mathbb{R}^{MxN}$, the sensing matrix. More specifically, Φ and the sparse signal x are used at the transmitter to generate y, and at the fusion centre, the received vector y and Φ are used to recover the sparse signal x using a signal recovery method. During signal recovery, note that when the number of measurements M in the vector y is less than the dimensional space N of the signal x, the problem is an undetermined system of equations with fewer equations than unknowns, and x lies on an $N - M$-dimensional subspace which can be a line or a plane. However, under the assumption that x is likely to have small energy $||x||_{l2}$ as possible, the least squares solution is commonly used as the solving method [141]. Among all possible x that solve Φx= y , the purpose is to find the x that minimises the energy, the L2 norm or sum of squares of the coefficients given by:

$$x^* := \arg min_{x:\Phi x=y} ||x||_2 = \Phi^T(\Phi\Phi^T)^{-1}y, \tag{2.5}$$

where x^* is the least squares solution, the "best" guess for x. However, in many situations and applications, least squares is not satisfactory as it gives very poor

results, as the solution is almost never sparse. This effect is visible especially in the reconstruction of sparse signals and images [141], the recovered signal is not accurate. For instance, the signal reconstruction of a one-dimensional discrete signal f from a partial collection of Fourier measurements. The least squares solution is often very different from the original signal f when the number of measurements M is small compared to the original signal length N in f [125]. To reduce the noise and improve the signal reconstruction using the least squares method, more measurements M would be required. However, this is not a practical scenario if the number of measurements or samples are expensive or limited, such as in applications using medical resonance imaging or wireless sensor networks [142]. Hence, other methods are used for compressed sensing and signal recovery.

In summary, when the signal of interest is sparse, compressive sensing may be used to compress and encode the data [107]. However, a recovery method is required to decode and recover the original sparse signal. More specifically, in this application, the original time-domain vibration signal is transformed to the frequency domain to produce a nearly sparse signal. This signal is then thresholded to produce a sparse signal that can be used for CS. The threshold used to vary the sparsity level in the signal is selected in function of the number of allowed wireless transmissions which are dependant on the energy generated from the energy harvester/batteries at a given point in time. The produced S-sparse signal, $X_s \in \mathbb{R}^N$ and the random M x N measurement matrix Φ are used to generate M compressive sensing measurements which are transmitted to a base station via wireless in multiple data packets. The sparse signal is then recovered when the required number of CS measurements have been received at the receiver.

Number of measurements for signal recovery

Given a set of CS measurements, the problem of signal recovery is to determine the number of CS measurements needed to recover the original sparse signal and the recovery method to do it.

The number of compressed measurements M required for signal reconstruction through CS is determined by the sparsity level or compressibility of the signal, rather than its "size" or bandwidth [112]. The S-sparse signal (signal with at most S nonzero entries) can still be recovered if the number of samples/measurements received at the BS is at least M[107], given by:

$$M \geq C \cdot S \log(N/S), \tag{2.6}$$

where C is a constant value that depends on each instance [107], N is the signal length of X, S is the number of non-zero entries from the sparse signal and M is the number of measurements produced after CS. At the BS the M measurements received are used for signal reconstruction using L_1 minimisation or OMP [112].

A sparse signal has a concise representation when expressed in a suitable basis such as wavelet or Fourier transform [107]. For instance, if a discrete signal is changed from time to frequency domain through the DFT, relatively few coefficients capture most of the energy in the signal while most of the coefficients are small in magnitude [107]. Therefore, when a signal has a sparse expansion, it is possible to keep the large coefficients and discard small coefficients without significant loss such as the image reconstruction shown in [107]. In this application, the elements that capture most of the energy are kept through the proposed Algorithm 3.1 presented in Section 3.5.

The required number of measurements M may be different in real applications. For instance, in [107] the authors show that in practice, the number of measurements/samples of about $4\times$ the sparsity level are sufficient. This four-to-one practical rule indicates that four CS measurements for each unknown non-zero term suffice.

Methods to recover sparse signals

For sparse signal reconstruction from compressive sensing measurements, various techniques can be used. For instance, the sparse signal can be recovered at the receiver from the compressed measurements using popular numerical optimisation methods such as $L1$ norm minimisation [122], basis pursuit [123] or greedy algorithms such as Orthogonal Matching Pursuit (OMP) [124]. The papers [113], [121], [125] offer constructive demonstrations of the recovery phenomenon using numerical optimisation which can be computationally intensive. The algorithms found in literature range extensively in computational cost, empirical efficiency and implementation complexity. Therefore, it is valuable to explore and compare alternative approaches that are not based on optimisation. OMP is an effective greedy iterative algorithm that is commonly used to recover sparse signals from fewer measurements. It is widely used due to its simplicity, speed and ease of implementation [124]. In this

research work, compressive sensing and a novel algorithm are used to handle the signal recovery problem. The proposed algorithm is presented in Chapter 4. It considers the structure of the OMP algorithm and includes prior information in the form of frequency support structure which intends to improve the accuracy of signal recovery and to reduce the number of measurements required.

2.3 Technical Background

The framework presented in this thesis considers the signal characteristics of real vibration data collected from a running gas turbine engine. Prior to deployment, the available technologies were identified to perform local signal processing at the wireless sensor nodes. This section presents a brief overview of wireless sensor networks, vibration sensing for machine health monitoring and analysis of existing vibration technologies which were considered for the wireless vibration sensing system.

2.3.1 Machine Health Monitoring Architecture

Machine Health Monitoring is set up depending on the fault types to analyse, by measuring frequency ranges. Generally, spectrum analysis is used to identify different vibration frequencies. An example of a monitoring configuration is shown in Figure 2.4.

In this example, data acquisition occurs using a vibration sensor placed on a gearbox, a signal conditioner that amplifies the sensor output, a filter that removes unwanted frequency components from the signal and enhances wanted ones and an Analogue-to-Digital Converter (ADC) that converts the analogue sensor output to a digital form suitable for digital signal processing. For signal processing, the signal output is transformed by a Digital Signal Processor (DSP), generating a frequency spectrum for each sampling cycle. Then, this spectrum is compared to the component's reference spectrum, given by the component supplier. This operation allows determining whether a vibration frequency is caused by an actual fault or by the component monitored. In case the amplitude of a vibration exceeds a given threshold, an alarm is triggered and corresponding repairs are determined.

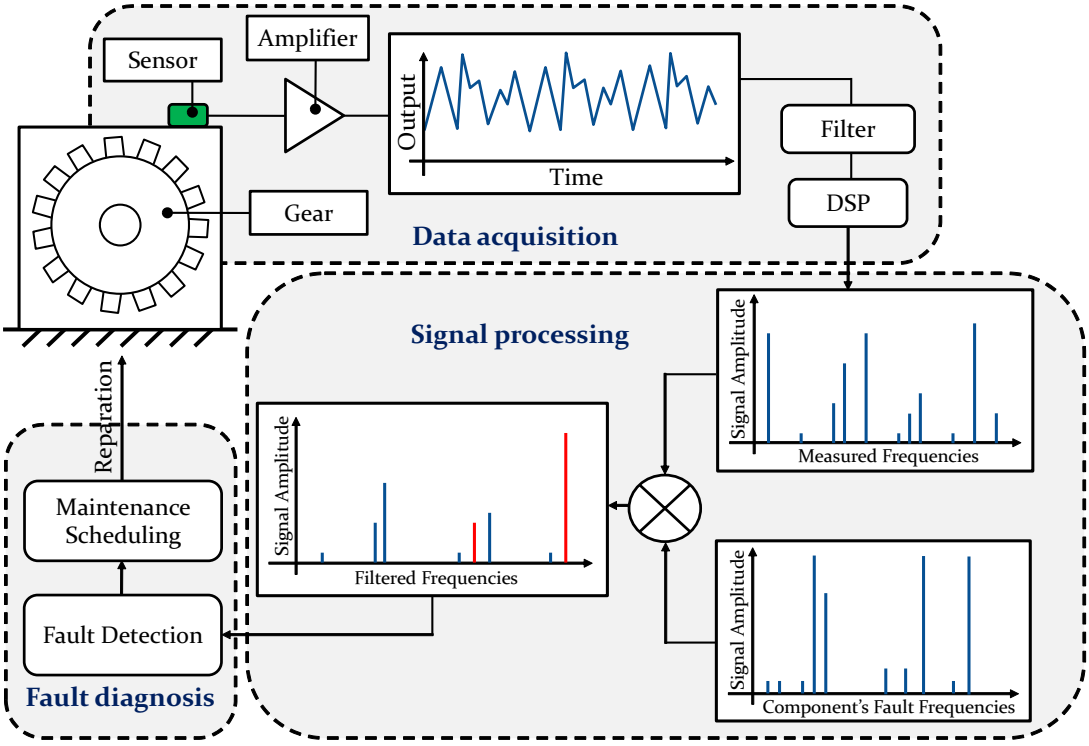

Figure 2.4: Example of a possible condition monitoring architecture.

The example described previously refers to MHM where a sensor or set of sensors are mounted on the housing of machinery [1]. For rotating machinery, as mentioned in Section 1.2, an ideal case for vibration analysis is to acquire vibration at the source. For instance, by placing the sensors directly on the rotor. This helps to capture shaft vibration at maximum amplitude and to avoid the effect of structural noise, imperfections in the machinery and bearings, etc. However, using wired sensors for condition-based monitoring in rotating machinery is not the best solution. The wear of the wiring after continuous machinery rotation may cause wires to break or machinery damage. The use of wireless sensors for machine health monitoring eliminates physical connectors and wiring that could be exposed to hazardous environments.

Digital Signal Processing

Signal processing refers to an operation over a signal of interest. The signal is converted from its physical form into a form on which it can be recorded and analysed. Signal processing is used in almost all disciplines of applied sciences such as electronics, mathematics, industry and engineering [75-77]. Analog signals found in nature may be present in different forms such as speed, acceleration, temperature,

resistance, voltage and so on. These analog signals need to be transformed in digital form in order to be processed by computers and digital microprocessors [78]. Unlike an analog signal, which is a continuous signal that contains time-varying values, a digital signal contains a discrete value at each sampling point. Therefore, a digital signal is easily represented using a computer because each sample can be defined with a series of bits that can take one of two possible states: 1 (on) or 0 (off). The signal precision is determined by the number of samples recorded per unit of time. Figure 2.5 shows an analog pattern which is represented as the curve, and the corresponding digital pattern, represented by discrete levels.

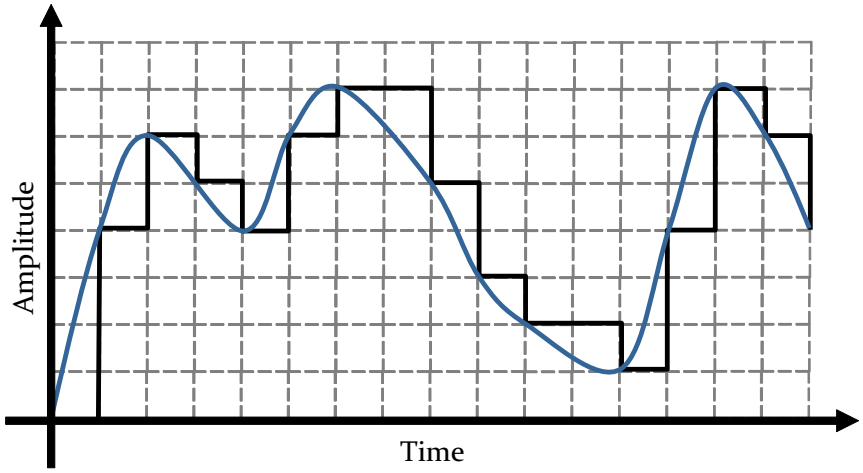

Figure 2.5: Example of an analogue pattern represented in digital form.

In digital signal processing, a real-world signal such as temperature, voice, position, pressure, vibration, etc. is digitised and then mathematically manipulated. Signals are processed in order to be displayed, stored, compressed, transmitted or analysed using advanced signal processing methods available only for data in digital format [79].

In digital signal processing, a continuous signal is converted into a discrete signal that is finite and equally spaced in time because it is uniformly sampled at or above the Nyquist rate [80]. Conventional signal processing follows the Shannon-Nyquist theorem for sampling signals. Many samples are generated using this method because the sampling rate should be more than twice the maximum frequency present in the signal. Opposed to this conventional sampling approach, a novel signal

acquisition and recovery method is proposed by Compressive Sensing (CS) theory [80]. This signal processing technique efficiently acquires a signal using fewer samples than traditional methods [80]. In summary, CS theory asserts that if a signal is compressible or sparse in a given basis, the signal can be reconstructed from fewer measurements in comparison to the conventional Nyquist case, this topic is covered in more details in Section 2.3.4.

2.3.2 Types of accelerometers

An accelerometer is a device that measures changes in gravitational acceleration in the device or machine it may be installed in. Accelerometers are used to detect and monitor vibration in rotating machinery. Single and multi-axis models of accelerometers are available to detect direction and magnitude of acceleration (or g-force), as a vector quantity, and can be used to sense orientation, coordinate acceleration, vibration, shock and falling. To sense motion in multiple directions, the accelerometer requires to be designed with multi-axis sensors or multiple linear axis sensors. To measure movement in three dimensions, three linear accelerometers are adequate.

Accelerometers have multiple applications in industry and science. For instance, high sensitive accelerometers are components of inertial navigation systems for aircraft and missiles [81-82]. Other applications include the measurement of vehicle acceleration, structural monitoring, medical applications and machine health monitoring [83-85]. Here, the accelerometers are used to report vibration and its changes in time of shafts at the bearings of rotating equipment such as turbines, pumps, fans, compressors or faults on bearings. The selection of the most appropriate sensor for an application is based on requirements. The different types of accelerometers are as follows.

There are three main types of accelerometers:

1. Piezoelectric (PE) Accelerometer. – This device makes use of the piezoelectric effect to measure dynamic changes in vibration, acceleration and shock. Most of this PE accelerometers are made of quartz crystals which produce an electrical

charge when they are exposed to a change in mechanical loading associated with a deformation in the crystal.

2. Piezoresistive (PR) Accelerometer. - This device also known as a strain gauge accelerometer is based on the piezoresistive effect. This effect describes the resistivity change of a semiconductor due to applied mechanical stress. In comparison to PE accelerometers, PR accelerometers use a piezo resistive substrate instead of a piezoelectric crystal, the force applied by the mass changes the resistance of the material, then a whetstone bridge network detects this change or deflection. PR accelerometers are chosen in high shock applications, they can also measure acceleration down to 0 Hz. Nevertheless, they have limited high-frequency response.

3. Variable Capacitive (VC) Accelerometer. – These devices sense a change in electrical capacitance, with respect to acceleration, this way varying the output of an energised circuit. Two parallel capacitors in differential mode are used as the sensing element. The peak voltage generated by an oscillator is altered when the structure is subjected to acceleration. A circuit detects and captures the peak voltage, a summing amplifier receives this as an input signal and outputs a final processed signal.

MEMS Technology

Micro-electromechanical System (MEMS) Accelerometer combines mechanical and electrical components to form small structures. This technology is now being used to manufacture state of the art MEMS-based accelerometers. MEMS-based accelerometers are available with different technologies. The most common one is based on capacitors such as the Analog Devices vibration sensor ADIS16227 used in this applied research work. MEMS-based accelerometer using capacitors is typically a structure that uses two capacitors composed by a movable plate held between two plates that are fixed. If zero net force is applied, the two capacitors are equal. A change in force displaces the moving plate closer to one of the fixed plates which increases capacitance. Conversely, when the moving plate is displaced away from the fixed plate causes a reduction in capacitance. After detecting the difference in capacitances, the signal is amplified to produce a voltage proportional to the

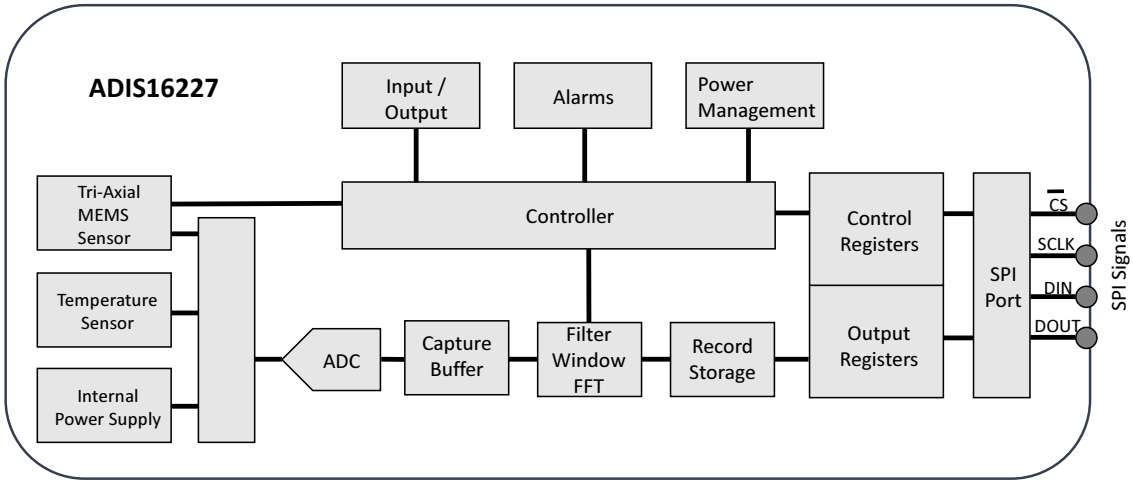

Figure 2.6: Functional block diagram of the ADIS16227 vibration sensor based on spec sheet.

acceleration sensed. An example of the internal structure of this type of MEMS VC accelerometer is shown in Figure 2.6.

MEMS accelerometers are extensively used in applications such as shock detection, tilt control and vibration monitoring among others [86]. MEMS accelerometers feature small size, negligible weight and onboard signal conditioning. For instance, Kok et al [87-88] integrated a complete wireless data acquisition system containing a MEMS accelerometer, a microcontroller and an RF transceiver. They demonstrated that its overall weight is virtually negligible.

One may question the efficiency of MEMS accelerometers. For instance, Ratcliffe et al. [89] demonstrated their capability for machine health monitoring applications. Thanagasundram et al. [90] evaluated MEMS technology conducting analysis techniques to evaluate the properties of these sensors without causing damage, also known as nondestructive testing. They also conducted spectral analysis of vibration signals from a dry vacuum pump, obtaining satisfactory results.

Continuous research attempt to further develop MEMS accelerometers. For instance, Badri et al. [91] proposed modifications to the structure of the moving plates of a variable capacitance MEMS accelerometer to improve the proportionality between proof mass motion and measured capacitance, and thus improve acceleration measurement. Additional improvements may involve the on-shaft sensor equipped with an RF antenna to receive power from a close transmitter via wireless [92-93].

2.3.3 Overview of Wireless Sensor Networks

The sensor nodes are small in size but incorporate sensors, embedded microprocessors and radio transceivers, consequently, WSNs include sensing, data processing and communication capabilities. A WSN system typically includes wireless sensor nodes and a manager node which provides wireless connectivity back to distributed nodes and the wired world such as Internet, a personal computer to display the data on a graphic user interface (GUI) or an Engine Monitoring Unit (EMU) in the case of a Gas Turbine Engine as shown in Figure 2.7. The selected wireless protocol depends on the application requirements [98].

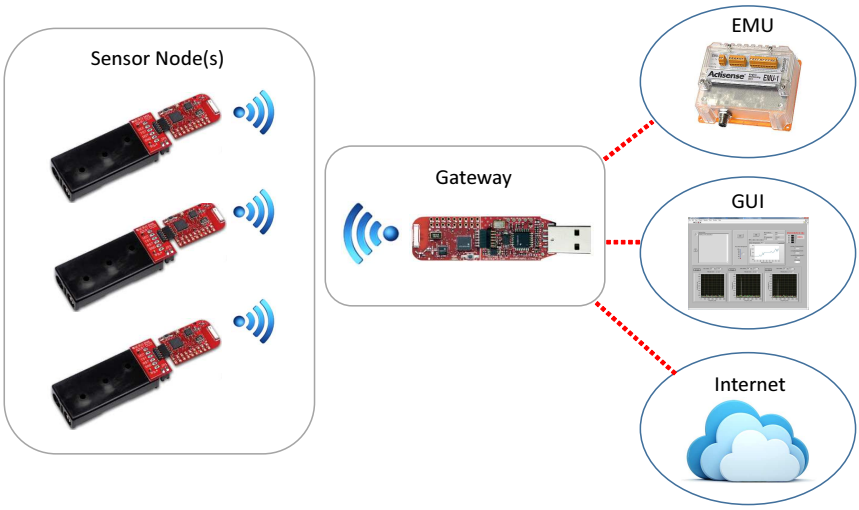

Figure 2.7: WSN Components, Gateway, Distributed Nodes and possible data outputs.

2.3.3.1 WSN Design Objectives

The majority of WSN applications are application specific and have specific requirements. Hence, it may be required by the application to meet some or most of the following main design objectives since it is not essential or practical to implement all of them in a single network [103].

- Low cost and small sensor nodes: Compact and low-cost sensor devices are primary design objectives to achieve large-scale deployment of WSN. Reducing the nodes size reduces cost, power consumption and facilitate node deployment.

- Low power consumption: It is essential to reduce the power consumption of sensor nodes since they are usually powered by batteries or by a type of energy harvester as the main power source. Hence, it is often impractical or impossible to charge or change the batteries, by reducing power consumption on sensor nodes, the lifetime of individual nodes and the complete network is extended.

- Scalability: Tens or even thousands of sensor nodes may exist in a sensor network, therefore the protocol of the network should be scalable to different dimensions of the network.

- Reliability: To ensure reliable delivery of data from sensor nodes it is important to implement a type of error control and correction techniques in the network protocol design.

- Fault tolerance: The installation of sensor nodes in harsh environments may cause the sensors to fail due to existing conditions and lack of maintenance. Hence, the sensor nodes should be tolerant to failures and should incorporate abilities for self-testing, self-calibrating and self-recovering [104].

- Channel Utilization: The narrowness of communication bandwidth in WSN demand improve channel utilization by using the available bandwidth efficiently.

- Quality of Service Support: The quality of service requirements in WSN applications may vary from one to another in relation to allowed tolerance to packet loss and data delivery latency. Hence, the network protocol design should consider the requirements of quality of service for a particular application.

- Security: A WSN is often vulnerable to security threats that can adversely affect the proper functioning of the network. This aspect is particularly important if the network is going to be used in highly critical systems. Hence, a WSN should implement security mechanisms to effectively prevent unauthorized access and external attacks.

For this research work, the focus is on low power consumption, reliability and quality of service support. The next sections present how these design objectives are considered to solve the packet loss and signal recovery problems considering energy conservation in the wireless sensor nodes.

2.4 Chapter Summary

In this chapter, the availability of vibration sensing technologies to perform wireless condition monitoring was shown, highlighting the importance and benefits of using MEMS accelerometers. In addition, a summary of wireless sensor networks was presented including its characteristics, objectives, challenges, applications in harsh environments and current research involving local signal processing in sensor nodes. The theoretical foundations of CS show that this method is a promising candidate to achieve the presented objectives in this research work. In summary, the CS paradigm is divided into three major parts: sparse signal representation, random measurement matrix and signal reconstruction method. Using CS enables high compression rate through simple computations at the sensor nodes. All the complex computation regarding signal reconstruction is performed at the receiver, where typically there are no power constraints due to a constant energy source. To sum up, the scope of this research work is to design an adaptive vibration sensing framework based on compressive sensing that can mitigate the random packet loss problem during wireless transmission, presented in Chapter 3. More importantly, to improve signal recovery performance by exploiting prior information from the application, presented in Chapter 4.

In the next chapter, the selected hardware for vibration sensing and wireless data transmission is introduced. Also, the architecture of the system is illustrated and all the phases involving local signal processing at the sensor node are presented such as onboard frequency domain analysis and compressive sensing. Moreover, the domain selected to identify the main frequency components, the generated and implemented random sensing matrix and the selected signal recovery method are described.

Chapter 3

Local Signal Processing for Wireless Vibration Sensing Systems

3.1 Introduction

A wireless sensor network is composed of sensor nodes deployed with the intention to monitor and record conditions at different locations [126]. These sensor nodes initialise a cooperative network and perform three basic functions: sensing, computation and communication [126]. As the sensor nodes are devices generally powered by batteries or through energy harvesting, a critical aspect is the energy consumption in sensor nodes to extend network lifetime [127]. Hence, there is the need to use techniques for energy efficient data acquisition and energy conservation. For wireless vibration sensing, effective utilization of limited power resources may include data encoding through frequency domain analysis and compressive sensing at the sensor nodes [128]. The former may be used to select a frequency bandwidth of interest, event detection and as a basis for compressed sensing [128]. Compressive sensing can be used for data compression and to help mitigate the packet loss effect during wireless data transfer [129]. The reduction in the amount of data transmitted via wireless and the minimisation of wireless retransmissions increases energy conservation in the sensor nodes [130].

This chapter presents the architecture of the system for vibration data encoding

at the wireless sensor node, including instrumentation used and its specifications. Local signal processing occurs at the sensor node by combining frequency domain analysis and compressive sensing. In compressive sensing, a sparse signal and a suitable sensing matrix are required [107]. Hence, an algorithm is proposed and presented in this chapter which reduces the dimensionality of the vibration signal (after transformation to the frequency domain) to induce sparsity while maintaining the main spectral components. For the case of the sensing matrix, a Bernoulli matrix was generated by sampling independent identically distributed binary entries with equal probability. This matrix was stored in the sensor node as part of the wireless vibration sensing strategy for signal encoding.

The proposed wireless sensor network presented in this chapter was used in a set of experiments to demonstrate that the selected hardware is capable of meeting specific requirements (see Appendix A) of a system requirements document generated by Rolls-Royce for the wireless sensor infrastructure [131]. This document defines the system level requirements considered to be fundamental for a WSN to ease wireless transmission of vibration and temperature data from a network of distributed "Smart Sensors" within a Gas Turbine Engine to support Equipment Health Management. It is important to note that the work presented throughout this thesis focusses on a single wireless sensor node transmitting vibration data directly to the base station. Although the strategies proposed could potentially be applied to a wireless sensor network.

This chapter is structured as follows:

- Section 3.2 presents the target board used for the wireless vibration sensing system.
- Section 3.3 presents the selected vibration sensor and its features.
- Section 3.4 presents the system architecture including the data flow description from the sensor node to base station.
- Section 3.5 presents a proposed algorithm to induce sparsity in the frequency-domain vibration signal while keeping the principal frequency components, this algorithm outputs a sparse signal ready for CS.

- Section 3.6 presents the selection, generation and implementation of the sensing matrix stored in the sensor node as part of the signal encoding strategy.
- Section 3.7 presents the summary of this chapter which essentially covers the set of processes and signal processing that occurs at the wireless sensor nodes. This section connects with Chapter 4 which presents the signal decoding at the base station to recover the vibration signal from compressed sensing measurements.

3.2 Wireless Target Board

The performance of the WSN was developed and evaluated using the eZ430-RF2500 development tool by Texas Instruments [132]. The eZ430-RF2500 is a wireless development tool that features a target board that can be either programmed to be used as an End Device (ED) or an Access Point (AP) commonly referred as the manager node. The Target Board including several key components is shown in Figure 3.1, the TB features an ultra-low power MSP430F2274 microcontroller to perform general processing tasks [133], a CC2500 2.4 GHz radio frequency transceiver chip to handle sent and received data packets [134], a Wurth chip antenna to transmit and receive wireless data [135] and a very low power crystal oscillator to handle Interrupt Service Routines and wake up the microcontroller when using low power modes. The target board can be connected to either a battery pack or a USB debugging interface which serves as a link between the PC and the AP target board, the possible connections as an ED or AP are shown in Figure 3.2.

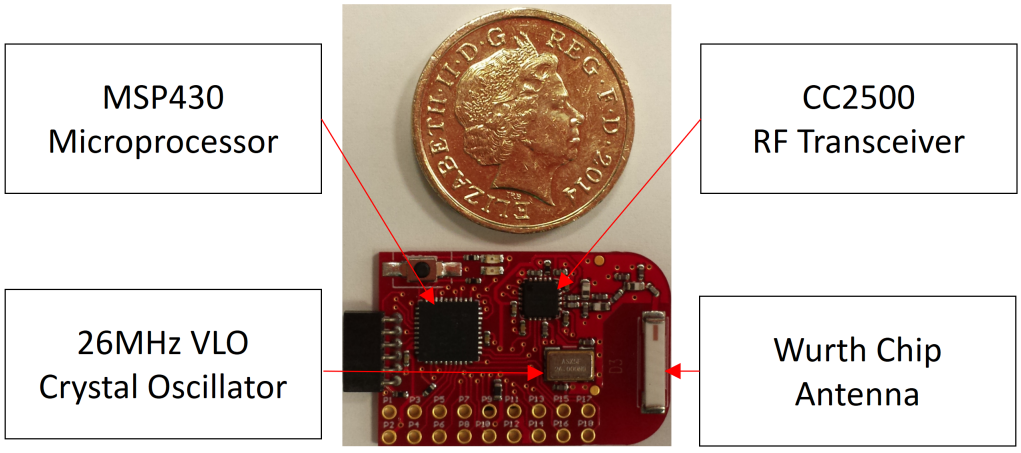

Figure 3.1: The eZ430-RF2500 target board.

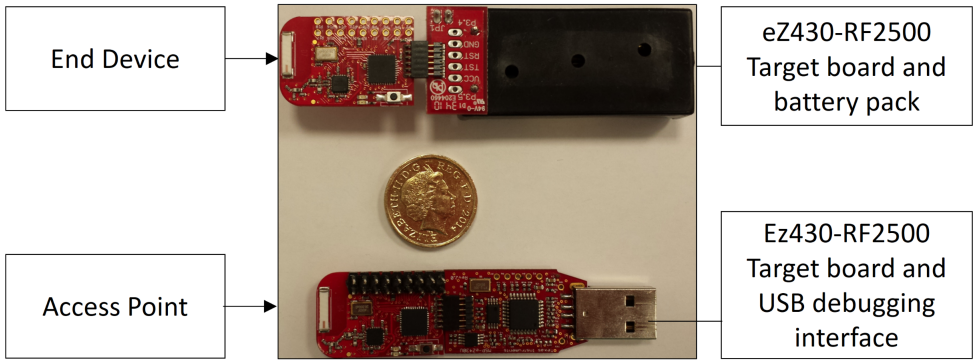

Figure 3.2: Connections on eZ430-RF2500 target board to be used as an ED or AP.

3.3 Choice of Vibration Sensor

The vibration sensor ADIS16227 developed by Analog Devices is a type of variable capacitance accelerometer [136]. This complete vibration sensing system incorporates wide bandwidth, tri-axial acceleration sensing with advanced time domain and frequency domain signal processing. Time domain signal processing includes a programmable decimation filter and selectable windowing function. Frequency domain processing converts a 512 point real-valued time domain signal into 256 point spectral domain data for each axis. The 16-record FFT storage system offers

the ability to track changes over time and allow to capture FFTs with multiple decimation filter settings.

The 22 kHz sensor resonance and 100.2 kSPS sample rate provide a frequency response that is suitable for machine-health applications. The aluminium core provides excellent mechanical coupling to the Micro-Electro-Mechanical Systems (MEMS) acceleration sensors. An internal clock drives the data sampling and signal processing system during all operations, which eliminates the need for an external clock source. The data capture function has three modes that offer several options to meet the needs of many different applications.

The ADIS16227 utilises an SPI interface and also includes a digital temperature sensor and digital power supply measurements. It has an extended operating temperature range of $-40°C$ to $+125°C$.

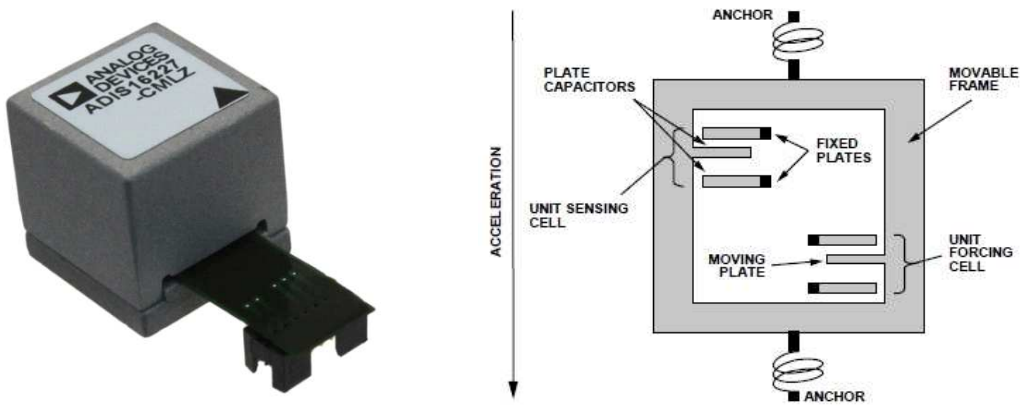

Figure 3.3: ADIS16227 Vibration Sensor [136].

The analog-to-digital converter (ADC) samples each accelerometer sensor at a rate of 100.2 kSPS. Four different sample rate options are provided for FFT analysis, SR0 (sampling frequency-fs), SR1 (fs/8), SR2 (fs/64), and SR3 (fs/512). The reduced rates are due to a decimation filter, which reduces the bandwidth and bin widths. The performance trade-offs related to each sample rate setting is shown in Table 3.1. For instance, SR1 was selected for this research work. This setting was determined to be appropriate for this application because the frequency target for this application is up to 3 KHz. Under SR1, frequencies of up to 6.262 KHz could be captured with

a ~25 Hz bin resolution. On the other hand, if finer resolution is required, SR2 can be selected, providing a 3.1 Hz bin resolution, however the bandwidth is reduced to under 1 KHz.

Table 3.1: Sample rate settings and filter performance [136].

Setting	Sample Rate (SPS)	Bin Width (Hz)	Bandwidth (Hz)	Noise (mg)
SR0	100189	196	26000	467
SR1	12524	25	6262	260
SR2	1566	3.1	783	100
SR3	196	0.38	98	38

The vibration sensing system ADIS16227 performs sampling, processing and storage of tri-axial vibration data into a buffer. When manual time mode is selected, each axis record contains 512 samples per axis. Otherwise, each record contains the 256-point FFT result for each accelerometer axis. Since the size of each data sample is two bytes long, a single vibration measurement will consist of 1536 bytes of data (1.5 kB), which corresponds to 0.5kB per axis. The next section presents the system architecture showing the functionality of the vibration sensor and the wireless target board for the wireless vibration sensing system.

3.4 System Architecture

WSN may consist of several end devices. A typical End Device (ED) consists of one or more sensor transducers, a microprocessor, an RF interface and a local power source (batteries or energy harvester) such as the eZ430-RF2500 end device presented in Section 3.2. The function of an ED is to measure a particular parameter (e.g. temperature or vibration) and convert that data into a format that can be transmitted wirelessly in short bursts. The ED may also optionally carry out some pre-processing of that information prior to transmission to reduce the amount of

data sent over the wireless channel (e.g. using a Fast Fourier Transform (FFT) to convert vibration data from the time domain into the frequency domain and then discretise that data into bins). Since the power resources of EDs are limited, they enter a low power mode to conserve power when they are not measuring, processing and transmitting data. An interrupt service routine wakes the ED periodically to carry out a measurement cycle.

An AP acts as a gateway or data concentrator. There is usually just one AP in a WSN. It is intended to be located at the site of the Engine Monitoring Unit (EMU) and is directly wired connection to it by way of an Ethernet or CAN port. The function of an AP is to establish a connection with any EDs that wish to join the WSN. It then remains constantly awake to receive transmissions from the EDs. Incoming data is handled and sent to the EMU. The AP may also be responsible for other tasks such as reporting node failure, choosing a suitable wireless channel and managing the power resources of EDs.

The architecture of the wireless vibration sensing system with a single sensor node is illustrated in Figure 3.4 and the data flow from the sensor node to base station in Figure 3.5. In a wireless sensor network, each sensor node may incorporate the signal encoding described. At the sensor node, the onboard Application-Specific Integrated Circuit (ASIC) (Figure 3.4B) integrated inertial sensor with embedded frequency analysis described in Section 3.3, computes the spectral representation of the measured vibration signal using the Fast Fourier Transform (FFT). The obtained frequency analysis of the signal is transmitted from the ASIC to the microcontroller's SN (Figure 3.4C). The DFT of the signal can be considered sparse in comparison to its time domain representation; using the CS framework the signal's sparsity is exploited by making random measurements of the signal, this is where the compression happens. All the CS processing occurs physically in the microcontroller's sensor node. A sensing matrix Φ (Figure 3.4A) was formed by sampling independent identically distributed (i.i.d.) binary entries from a symmetric Bernoulli distribution with equal probability, this matrix Φ was then stored in order to perform data compression. The compressed version of the DFT is then transmitted wirelessly using the board's transceiver. The data is received at the access point and can be transferred to an Engine Monitoring Unit (EMU) in an aeroengine or to a base station to reconstruct the signal using a signal recovery method such as the enhanced orthogonal matching pursuit presented in Chapter 4.

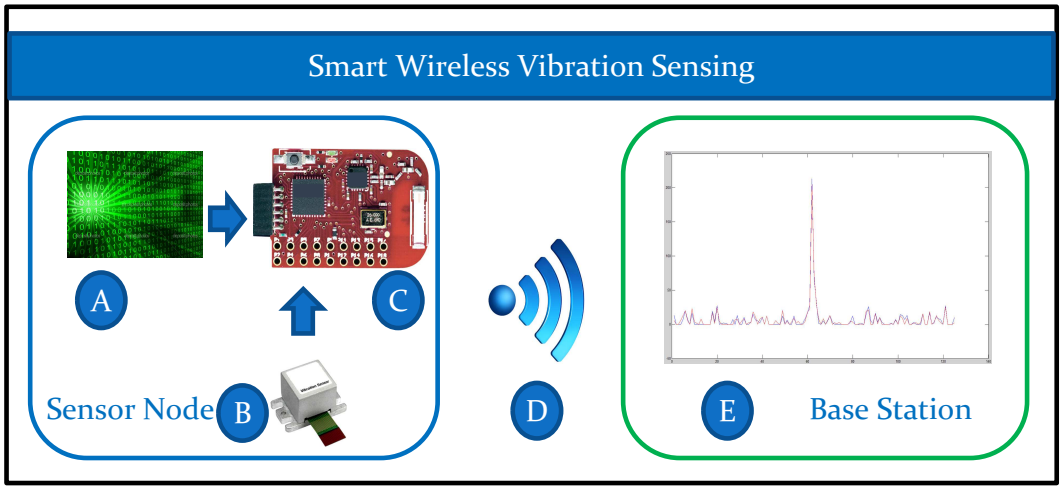

Figure 3.4: Wireless vibration sensing system architecture showing a random sensing matrix(A), ASIC (B), microcontroller's sensor node(C), wireless transmission(D), signal recovered at BS(E).

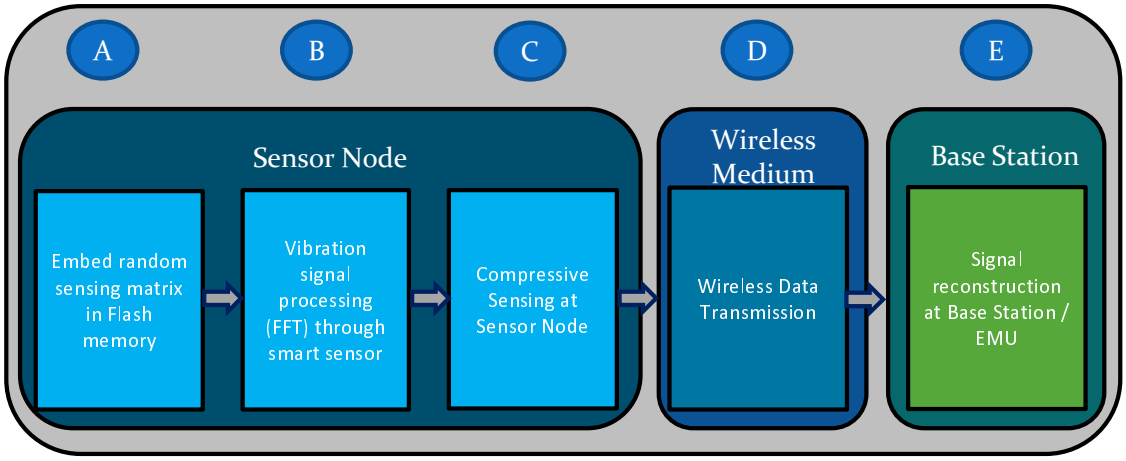

Figure 3.5: Data flow description from Sensor Node to Base Station.

The next section shows how the vibration signal was prepared to be used with Compressed Sensing (CS). In summary, the vibration signal is acquired and transformed to the frequency domain at the sensor node (a suitable basis for CS). Moreover, a proposed algorithm is used to induce sparsity in the vibration signal while maintaining the main frequency components. These procedures form part of the signal encoding strategy presented in this chapter.

3.5 Dynamic sparsity adjustment algorithm

In this application, the original vibration signal is transformed to a suitable domain for CS using the DFT which is defined as:

$$X\ [\omega] = \frac{1}{\sqrt{\mathrm{N}}} \sum_{\mathrm{n}=0}^{\mathrm{N}-1} \mathrm{x[t]e}^{-2\pi \mathrm{i}\omega \mathrm{t}/\mathrm{N}}, \quad \omega = 0, 1, 2, ..., \mathrm{N}-1 \tag{3.1}$$

where x[t] is a discrete-time signal of length N and $X[\omega]$ is the Fourier coefficients sequence in the frequency domain. Once all the N Fourier coefficients are obtained, it is straightforward to locate the non-zero frequencies and their coefficients. However, it may be required to compute a large number of zero coefficients or coefficients of low magnitude caused by noise in the application. In the scenario described, the DFT is computed by an inertial sensor with embedded frequency analysis described in Section 3.3. In a conventional scenario, the signal X may be compressed by identifying the S coefficients that capture most of the energy and their locations. This data can then be encoded and transmitted wirelessly to a base station [112]. However, this procedure requires knowledge of all N coefficients of X because the locations of the coefficients of higher magnitude may not be known in advance as they are signal-dependent [107]. An efficient signal compression technique should be used to reduce the amount of data sent via wireless and consequently increase energy savings. It is important to consider that in a real application, the wireless sensor nodes may be deployed in a noisy environment and the random packet loss effect may cause multiple data packet retransmissions which affects energy efficiency, produces unexpected time delays and reduction of SNs lifetime.

An efficient sampling and compression method is proposed by Compressed Sensing (CS) [107]. However, to use CS the signal is required to be sparse [107]. In other words, if the signal is dense and contains mostly non-zero elements, a threshold can be used to increase signal sparsity [137] by setting to zero the low energy components and maintaining the components of higher energy. However, using a threshold results in signal distortion. This is because the frequency components above the threshold τ are maintained while the frequency components below τ are discarded. Therefore, it is important to condition the S-sparse signal prior to wireless transmission through

adequate thresholding so that it can be recovered at the base station accurately with minimal distortion. This adaptive method increases signal sparsity and keeps only a few sinusoids that carry most of the signal information/energy. The energy consumption is reduced by sending only the number of measurements required for signal reconstruction of a particular S-sparse signal which in the end decreases the number of wireless data packet transmissions. The number of measurements sent by the wireless sensor node may be further reduced to minimise power consumption at the expense of increased distortion. In summary, the frequency components that capture most of the energy in the signal are maintained while most of the low magnitude components are set to zero. The proposed Algorithm 3.1 outputs a sparse vibration signal suitable for compressed sensing, it considers the available energy in the sensor node and a dense vibration signal with mostly nonzero elements as inputs.

Studies found in literature about compressive sensing [107, 109, 113] assume that the input signal is sparse in some basis. Essentially, this refers to a signal containing mostly zeros, except for a few nonzero elements. In real applications where the equipment is installed in noisy environments (such as in a gas turbine engine) this is rarely the case because most of the frequency components, if not all, are nonzeros (as shown in Section 4.3). In energy-constrained applications, the adaptive threshold Algorithm 3.1 can be used to discard low magnitude frequency components and make the signal sparse ready for compressive sensing. When the signal sparsity is increased (more zeros in the signal), the number of CS measurements to be sent are reduced which derives in less wireless data packet transmissions. In this application, the sensor node sleeps using low power mode and wakes up periodically to send data packets. The proposed algorithm presented considers the energy available from the battery or energy produced by an energy harvester prior to wireless data transmission. The number of compressed sensing measurements to send is determined and the signal sparsity is induced dynamically in each transmission using an adaptive threshold.

Motivation

A sparse signal is a requirement for compressed sensing (as explained in Section 2.3.4). However, in many real applications, a signal of interest may not be sparse. For instance, the signal may be dense even after the time-domain signal is transformed into the frequency domain. This means the signal in the frequency domain contains

mainly nonzero elements or even all. This situation may occur in noisy environments such as in a GTE where the noise is likely to generate components of low magnitude across the frequency spectrum. Algorithm 3.1 keeps the S frequency components of higher magnitude and sets the other elements to zero. The power available in the wireless sensor node is computed to adjust the signal sparsity in the output signal to increase the probability of successful signal recovery at the receiver.

In brief, the Algorithm 3.1 is proposed as it achieves the objective to output a sparse signal ready for compressed sensing from a dense input signal considering power available at the sensor node for sparsity adjustment. It adjusts signal sparsity dynamically maintaining the main components of higher magnitude and is also simple and straightforward to implement. Other sophisticated methods for thresholding [155] may be explored and selected based on application requirements and available resources.

In the proposed thresholding algorithm, the DFT is used as the basis to transform the signal into a different domain as the vibration sensor selected by the UTC-RR outputs the vibration signal in the frequency domain. Signal processing occurs in the vibration sensor shown previously in Figure 3.4B. Depending on the application, it may worth to explore other transformation alternatives such as wavelet transform, discrete cosine transform, etc. However, that would mean using valuable resources of the wireless sensor nodes to implement the wavelet transform or any other method. As mentioned throughout this thesis, it is important to use the resources in wireless sensor nodes efficiently considering their constraints regarding limited energy, storage capacity and computing power.

The proposed thresholding Algorithm 3.1 is as follows:

Algorithm 3.1 Adaptive Thresholding Procedure

Inputs:
a. A vibration signal in the time domain $x(t)$ or frequency domain $X(f)$.
b. Number of measurements mp that can be contained in a single data packet.
c. Maximum number of allowed wireless transmissions wt. This number is determined by the amount of power available at the sensor node.
Output:
A sparse vibration signal $X_S(f)$ for compressed sensing.
Procedure:
1. If the input signal is in the frequency domain go to Step 2. If not, compute the Discrete Fourier Transform (DFT) of the time-domain signal $X(f) = \text{DFT}(x(t))$.
2. Find the maximum value of the frequency domain signal $X_{max} = \max(X(f))$.
3. Calculate threshold step size which is equal to 1% of X_{max}. $TH_{size} = X_{max}/100$.
4. Calculate total number of measurements to be sent. $M = wt \times mp$.
5. Set number of maximum S nonzeros for the sparse signal $S \approx M/4$.
7. Initialise sparse vibration signal $X_S(f) = X(f)$.
8. Obtain number of nonzero elements N_Z in the signal $Xs(f)$.
9. If $N_Z \leq S$ go to Step 12. If not, continue to Step 10.
10. Increment threshold $TH \leftarrow TH + TH_{size}$.
11. Threshold signal $X_S(f) = Threshold\,(X(f), TH)$ and go to Step 8.
12. Output $X_S(f)$.

Assumptions

The sensor node includes a power supply sensor and the power consumption per wireless data packet transmission is known so that the number of allowed wireless transmissions can be defined for each S-sparse DFT signal.

Vibration data encoding/decoding

A flowchart of the vibration data encoding and decoding strategy of this research work is shown in Figure 3.6 along with the place where the proposed Algorithm 3.1 is used.

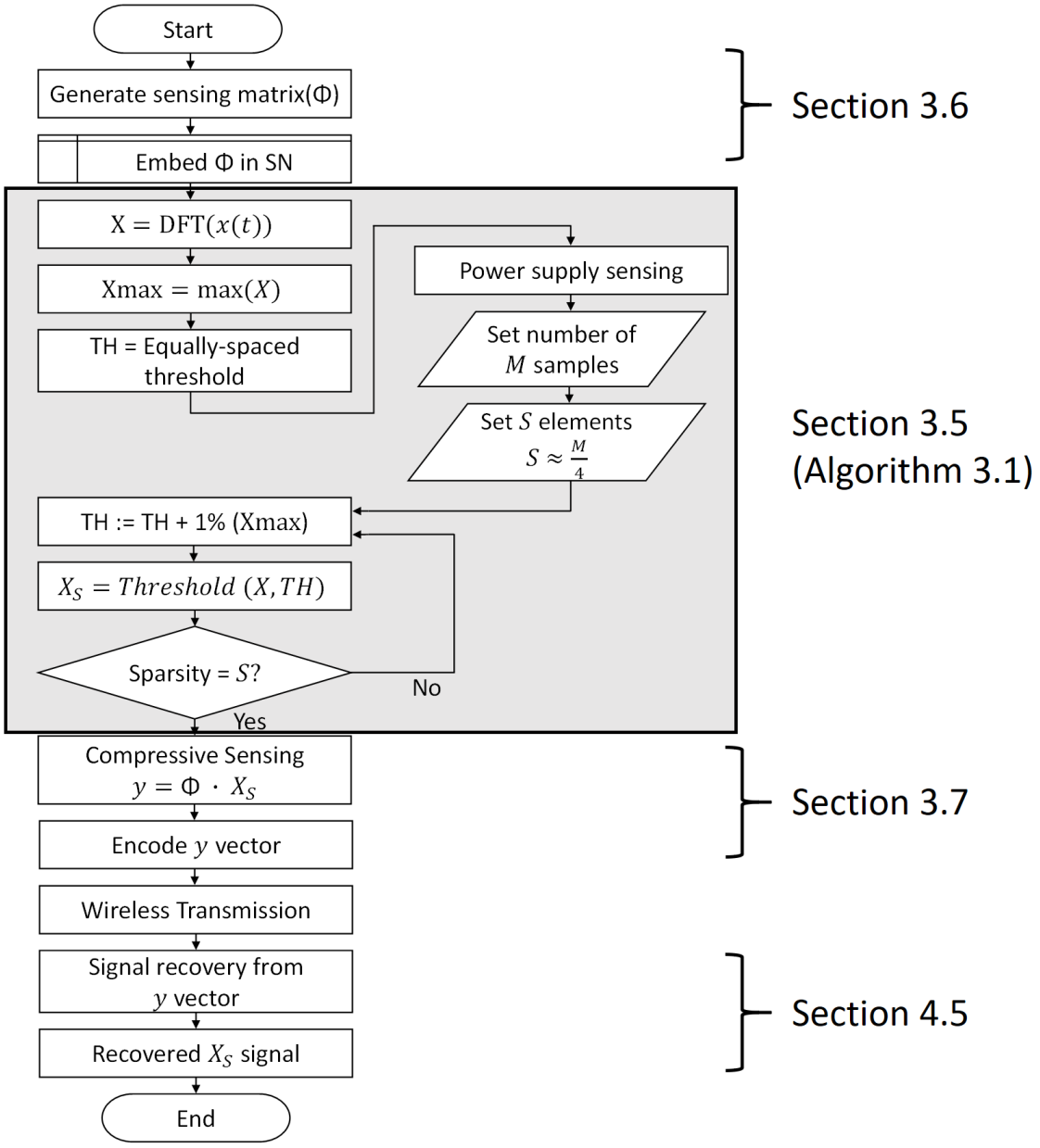

Figure 3.6: Flowchart of vibration signal encoding at the sensor node and vibration signal decoding at the receiver.

The set of processes of the signal encoding strategy at the sensor nodes are summarised as follows:

1. A suitable random sensing matrix Φ was generated with Bernoulli distribution as described in Section 3.6. This matrix was then embedded in the micro-

controller's SN. The same sensing matrix was used at the base station for signal reconstruction. This type of binary sensing matrix helps to reduce computational cost since the obtained measurement vector y is computed from Φx using only additions instead of multiplications as is the case with floating-point matrices.

2. The frequency-domain vibration signal X is obtained from a vibration sensor with embedded FFT analysis.

3. The magnitude value of the highest frequency component is computed, the location is not required under this scenario.

4. The sparsity level is modified through an equally spaced threshold (TH) produced from the dominant peak. The TH ranges from 1%-99% because at 0% would mean that the signal is not conditioned locally and the compression is null because none of the coefficients are discarded. In a real application most of the frequency components, if not all of them, contain non-zero values. In the case of 100% means that even the highest peak is discarded. According to [107] the number of measurements/samples of about $4\times$ the sparsity level are sufficient. This four-to-one practical rule indicates that 4 samples per unknown non-zero term (S) is sufficient. For instance, if 24 samples are to be sent, then signal sparsity is adjusted through thresholding so that the S-sparse signal contains the 6 non-zero S sinusoids/coefficients of higher magnitude.

5. A recursive TH is applied to the original FFT-based signal starting from 1% and stopping when the current number of S non-zero elements in the vibration signal is less or equal to the number of maximum S nonzeros for the sparse signal. The value of S for each FFT spectral measurement is determined by the power available at the sensor node prior to wireless transmission.

6. The measurements based on CS are encoded in multiple data packets and transmitted via wireless.

7. The vector of compressive sensing measurements y is received at the base station and a signal recovery method such as the enhanced OMP presented in Chapter 4 is used to recover the sparse vibration signal sent by the sensor node.

Compressive sensing requires a sparse signal and a sensing matrix [107]. This section presented how to make a signal sparse from a dense vibration signal in the time or frequency domain. The next section presents the selection and generation of the sensing matrix which was implemented in the sensor node for compressive sensing as part of the signal encoding strategy.

3.6 Selection and Implementation of Random Sensing Matrix

To generate compressive sensing measurements, a sparse signal and a random sensing matrix Φ are required [107]. This matrix Φ should satisfy the RIP shown in [113]. In [125] Candes and Tao define the properties required for random sensing matrices to be used for signal recovery. For instance, they show that both Bernoulli and Gaussian matrices satisfy the properties required for compressive sensing with high probability [107]. From the matrices that satisfy the RIP with overwhelming probability [107], the Bernoulli matrix was chosen. This matrix was selected, generated and implemented in this thesis as part of the wireless vibration sensing strategy for signal encoding at the sensor nodes. This matrix was selected and used as the sensing matrix Φ. It was selected over other matrices because it uses less memory when embedded in a wireless sensor node, the computation is reduced and the production of compressed measurements is faster than using floating-point matrices. This sensing matrix Φ was formed by sampling independent identically distributed binary entries from a symmetric Bernoulli distribution with probability $\mathbf{P}$=1/2, this matrix Φ is then stored in the sensor node. The product of this matrix Φ with a sparse signal x produces a vector of measurements y. The condition for that is $M = O(S \log (N/S)) \ll N$ as mentioned in [107]. Hence, as the sparsity increases the number of measurements M grows but only logarithmically in N, the signal length. An example of a test vector, corresponding to a single row in the sensing matrix Φ is shown in Figure 3.7.

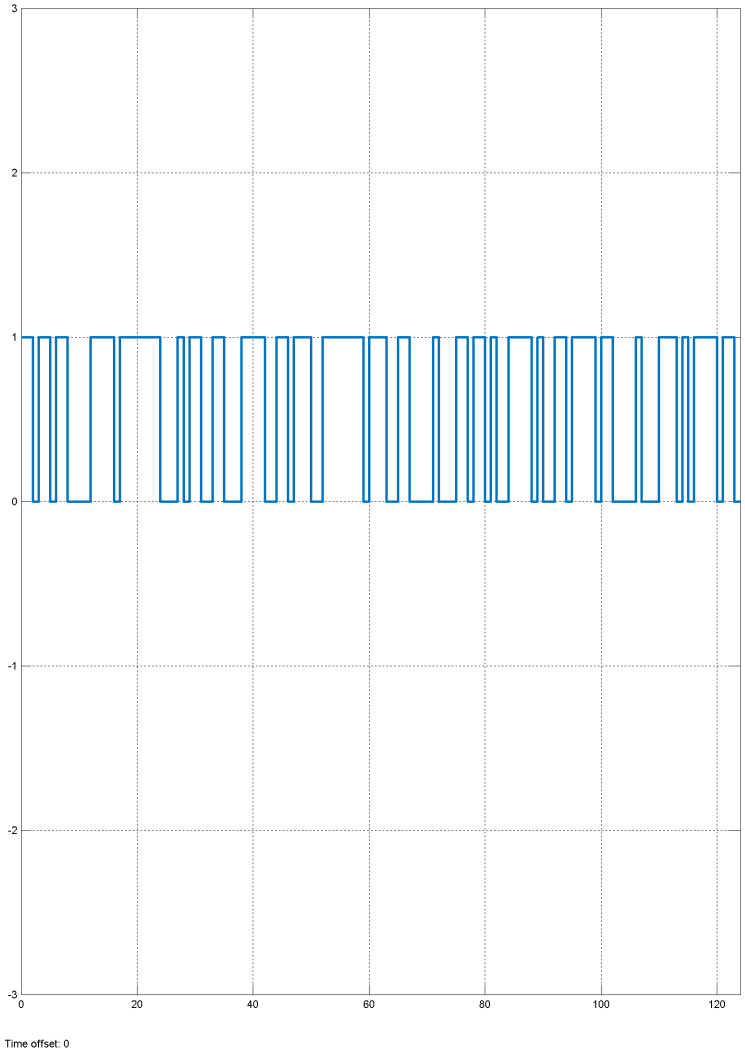

Figure 3.7: Example of a single binary test vector of length $N = 125$.

A Bernoulli binary generator in Simulink was used to generate all the test vectors for the sensing matrix Φ as illustrated in Figure 3.8, this function generates Bernoulli random binary numbers. The following parameters were used: probability of a zero=0.5, initial seed= from 1 to N (125), output data type: Boolean.

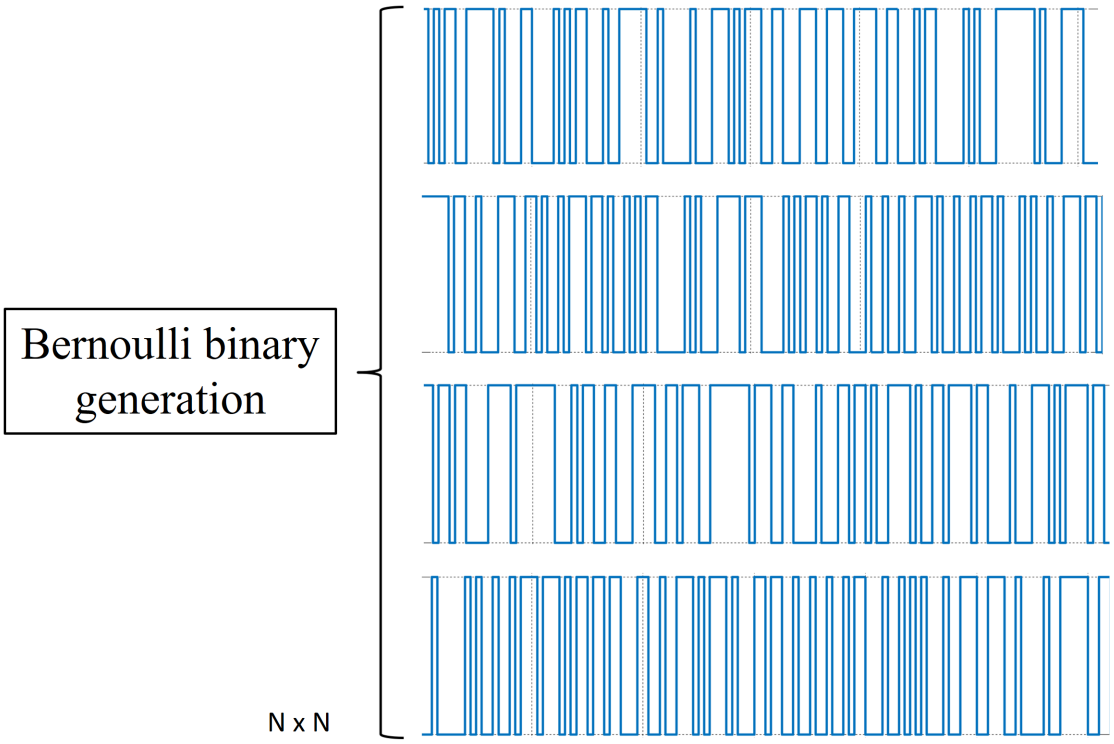

Figure 3.8: Examples of generated test vectors that form the Bernoulli Random Sensing Matrix Φ. Each binary test vector was embedded in the sensor node as binary entries as shown in Figure 3.9.

After the generation of the $N \times N$ sensing matrix Φ, it was then embedded in the microcontroller's flash memory of the sensor node to allow on-board compressive sensing. An example of a portion of the sensing matrix stored in the sensor node is shown in Figure 3.9.

$$\Phi = \begin{bmatrix} 1 & 0 & 0 & 1 & 0 & 0 & 1 & 0 & . & . & . & 0 \\ 1 & 0 & 0 & 0 & 0 & 1 & 1 & 0 & . & . & . & 1 \\ 1 & 1 & 0 & 1 & 1 & 0 & 1 & 1 & . & . & . & 1 \\ 0 & 0 & 1 & 1 & 0 & 1 & 1 & 0 & . & . & . & 1 \\ 0 & 0 & 1 & 0 & 1 & 0 & 0 & 0 & . & . & . & 0 \\ 1 & 1 & 0 & 0 & 1 & 1 & 1 & 1 & . & . & . & 0 \\ 0 & 1 & 1 & 0 & 1 & 1 & 1 & 0 & . & . & . & 1 \\ 0 & 0 & 0 & 1 & 0 & 0 & 1 & 0 & . & . & . & 1 \\ . & . & & & & & & & & & & . \\ . & & . & & & & & & & & & . \\ . & & & . & & & & & & & & . \\ 1 & 0 & 1 & 1 & 1 & 1 & 1 & 0 & . & . & . & 0 \end{bmatrix}$$

N (right) N (bottom)

Figure 3.9: A section of the implemented binary matrix in the sensor node.

This section presented the selected and generated random sensing matrix which was embedded in the sensor node as part of the compressed sensing procedure. This same matrix is also stored in the base station for signal recovery. To generate compressive sensing measurements, a sparse signal is required (e.g. the output signal X_S of the proposed Algorithm 3.1 in Section 3.5) and a sensing matrix Φ which can be generated as described in this section.

The next section presents the use of compressive sensing for signal encoding in the sensor node including how to generate a vector of compressive sensing measurements and the number of measurements required for signal recovery. Compressive sensing generates this vector of measurements y using a sparse signal (Section 3.5) and a sensing matrix (Section 3.6). This vector contains the encoded vibration signal which is transmitted by the wireless sensor node to the base station.

3.7 Chapter Summary

The framework proposed in this research work mitigates the effect of random packet loss and performs data compression by using local signal processing at the wireless sensor node through frequency domain analysis, adaptive thresholding and compressive sensing. More importantly, after wireless data transmission, the performance during signal recovery is increased. More details in Section 4. This thesis may be divided into two main sections: vibration data encoding which was presented in this chapter, and vibration data decoding procedures. The vibration data is encoded at the wireless sensor node (TX) through local signal processing and compressive sensing. To encode the vibration data at the sensor node, a spectral representation of the vibration signal through the Fast Fourier transform was used as the basis for signal compression using compressive sensing. Subsequently, the vibration signal dimension was reduced via an adaptive thresholding algorithm that induced sparsity while maintaining the main spectral components. To produce compressive sensing measurements, a sparse signal and a suitable measurement matrix are required. Hence, a Bernoulli matrix was generated and stored in the sensor node as part of the wireless vibration sensing strategy for signal encoding. For signal decoding, the vibration data received at the base station (RX) is decoded using an enhanced signal recovery method for compressive sensing measurements which is presented and described in the next chapter.

Chapter 4

Signal Recovery with Frequency Support

4.1 Introduction

Mitigating the effect of random packet loss during wireless transmissions is challenging especially if the data transmission occurs in noisy environments such as in a gas turbine engine. Chapter 3 presented the encoding procedure. The data packets are encoded at the sensor node through on-board frequency domain analysis, dimensionality reduction and compressive sensing prior to wireless vibration data transfer. These procedure aims to help deal with the packet loss problem through local signal processing and data compression. At the receiver, the data needs to be decoded to reconstruct the original signal sent by the transmitter.

The present chapter shows the set of steps for frequency domain sparse signal estimation and signal recovery at the receiver. The number of compressed sensing measurements required for signal recovery is reduced by exploiting prior information from the application. The methodology to achieve that is as follows:

1. Demonstrate that the selected hardware is able to collect, transmit and recover vibration data within a Gas Turbine Engine (Section 4.3).

2. Observe and analyse the collected vibration data to help identify patterns and zones of higher energy within the frequency spectrum (Section 4.3).

3. Propose a method to capture the signal characteristics from the application or frequency components where most of the energy is concentrated. The idea is to then use that information to recover the vibration signal accurately and reduce the number of samples required (Section 4.4).

4. Generate synthetic vibration signals to validate the proposed strategy (Section 4.5).

5. After validation, incorporate the prior knowledge obtained in Step 3 into the proposed signal recovery algorithm (Section 4.6).

In summary, this chapter presents the signal decoding procedure to recover the original vibration signal sent by the wireless sensor node is described. More specifically, the received vector of compressed sensing measurements is decoded using a proposed signal recovery algorithm. This algorithm is a novel contribution in this research work. It considers information from the real application and is used as prior knowledge to enhance signal recovery performance. This prior information refers to vibration signals collected from wireless sensor nodes deployed on a Trent1000 aeroengine during a running engine test. The structure of these frequency domain signals is extracted using a novel algorithm which outputs a probability density function which was used as frequency support for the proposed signal recovery algorithm.

This chapter is structured as follows:

- Section 4.2 presents the experimental methodology of the wireless vibration sensing system.
- Section 4.3 describes the deployment of wireless sensor nodes in the active Gas Turbine Engine and presents the collected vibration data.
- Section 4.4 introduces the properties of a probability density function followed by a proposed novel algorithm to estimate the Probability Density Function (PDF) for the frequency spectrum.
- Section 4.5 presents the procedure to generate synthetic vibration signals based on the same probabilistic structure from the collected data in the aeroengine.

- Section 4.6 presents a novel algorithm, the Enhanced Orthogonal Matching Pursuit which increases signal recovery performance including the PDF estimated in Section 4.4.
- Section 4.7 presents final remarks and summarises the impact of the proposed algorithm to enhance the performance during signal recovery of vibration signals from compressive sensing measurements.

4.2 Experimental Setup

The experimental setup is described as follows: the sensor node used for experimentation in laboratory and in a gas turbine engine includes the eZ430-RF2500 wireless development tool by Texas Instruments which features an ultra-low power MSP430F2274 microcontroller and a CC2500 2.4 GHz Radio Frequency transceiver chip. The vibration sensor used is the ADIS16227 developed by Analog Devices. This MEMS variable capacitance acceleration sensor was selected because it's an application-specific integrated circuit tri-axial sensor with embedded frequency analysis which computes the spectral representation of the measured vibration signal, using the Fast Fourier Transform. Moreover, this representation is suitable to be used in conjunction with compressive sensing [107]. This sensor was placed on top of an LDS V406 permanent magnet, electrodynamic shaker as shown in Figure 4.1a. This shaker was selected as it is designed for vibration testing of small components, laboratory experiments, structural analysis, etc. This shaker produce forces up to 196N (44 pound-force lbf). The purpose of using this shaker was to evaluate the vibration sensor and replicate vibration amplitudes of gearbox mounted accessories that are likely to find in GTE or the industrial sector [146]. The sensor nodes were tested on the LDS shaker before deployment on the gearbox of an active gas turbine engine as shown in Figure 4.4.

4.3 Data collection in a Gas Turbine Engine

Initially, the sensor nodes with incorporated vibration sensing were tested in Laboratory using the electrodynamic shaker provided by RR and described in Section

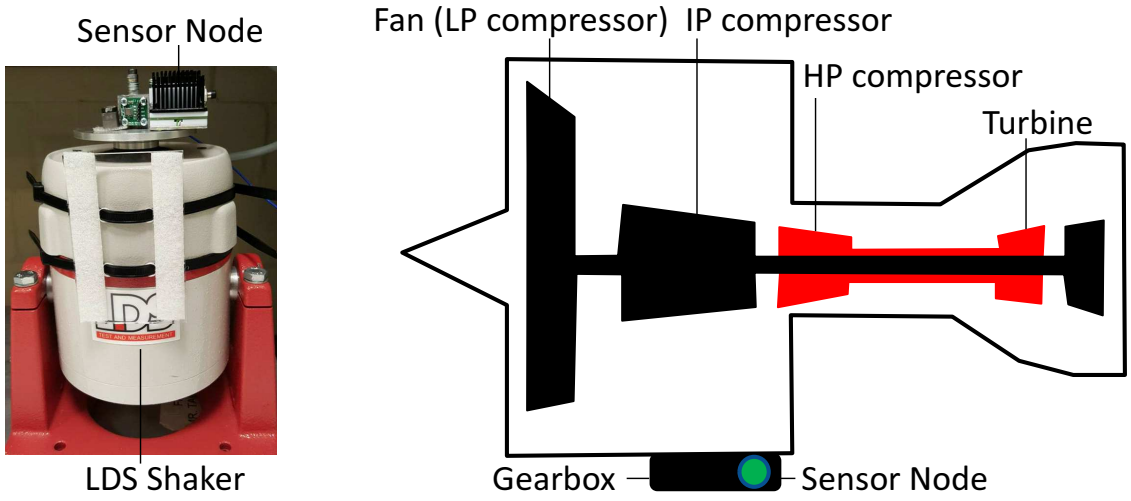

(a) (b)

Figure 4.1: LDS shaker used to evaluate the vibration sensor (a) and deployment illustration of the sensor node on a GTE gearbox (b).

4.2. After evaluation, a wireless vibration data collection test was carried out in a running gas turbine engine at INTA, Madrid. The purpose was to collect data from a real scenario and evaluate the performance of the wireless sensing system. A set of wireless sensor nodes were deployed on a Trent 1000 aeroengine (see Figure 4.1) on different LRUs such as the fuel pump, oil pump, and Fuel-Oil Heat Exchanger for temperature sensing and on the gearbox for vibration sensing. For instance, the deployment of a sensor node on the gearbox is illustrated in Figure 4.1b while the actual installation of sensor nodes on the aero engine are shown in Figures [4.2-4.4].

The availability of energy was limited because the self-powered sensor nodes incorporated energy harvesting through a thermoelectric generator. More importantly, the overall wireless communication was affected by random packet loss which resulted in multiple data packet retransmissions, unexpected time delays and wasted energy. The information of each FFT-based vibration signal computed at the sensor node was distributed in multiple data packets and sent via wireless to the receiver. Each data packet contained information about a portion of the frequency spectrum. Hence, under this approach, at the base station, it was required to receive all data packets for each independent vibration signal in order to reconstruct it. An effort was made to mitigate the packet loss effect by using features of the transceiver in the sensor

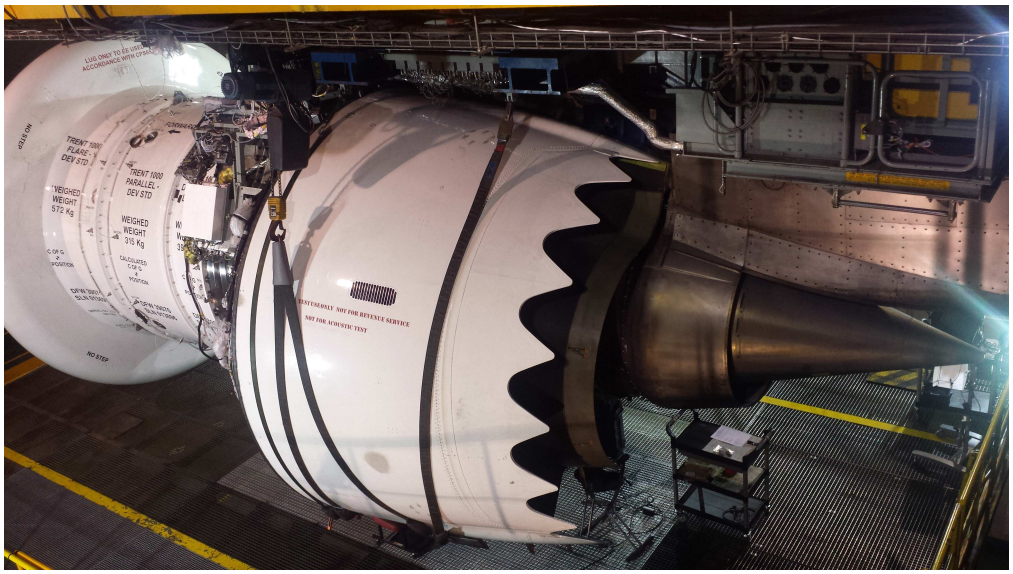

Figure 4.2: The Rolls-Royce Trent 1000 turbofan engine on which the wireless sensor nodes were installed.

node. For instance, the output power was automatically increased in case of a poor received signal strength. Additionally, the sensor nodes migrated among different channels to avoid channels subject to noise or interference. However, the use of these techniques was not enough to solve this issue.

An example of a vibration signal affected by poor signal strength resulting in random packet loss is depicted in Figure 4.5. For this single spectral measurement, about 70% of the data packets were received at the receiver side while 30% were lost randomly. The gaps in the image in Figure 4.5b represent a portion of the frequency spectrum that is missing due to lost data packets. Under this scenario, it is not possible to infer the information that corresponds to these gaps from the received/available data. Even if a single data packet is lost for a given vibration signal, it is not possible to determine the magnitude of the lost frequencies covered by that lost data packet. As a result, on this GTE test, all incomplete FFTs were discarded. The situation for these cases is far from ideal because the time and energy spent by the sensor node for vibration signal acquisition, conditioning, encoding, transmission, reception and decoding at the base station for all the received data packets are wasted, not counting any failed wireless retransmissions. As mentioned throughout this thesis, in wireless sensing applications it is vital to conserve energy and maintain the reliability of the system. That was the main reason for considering local signal processing at the sensor

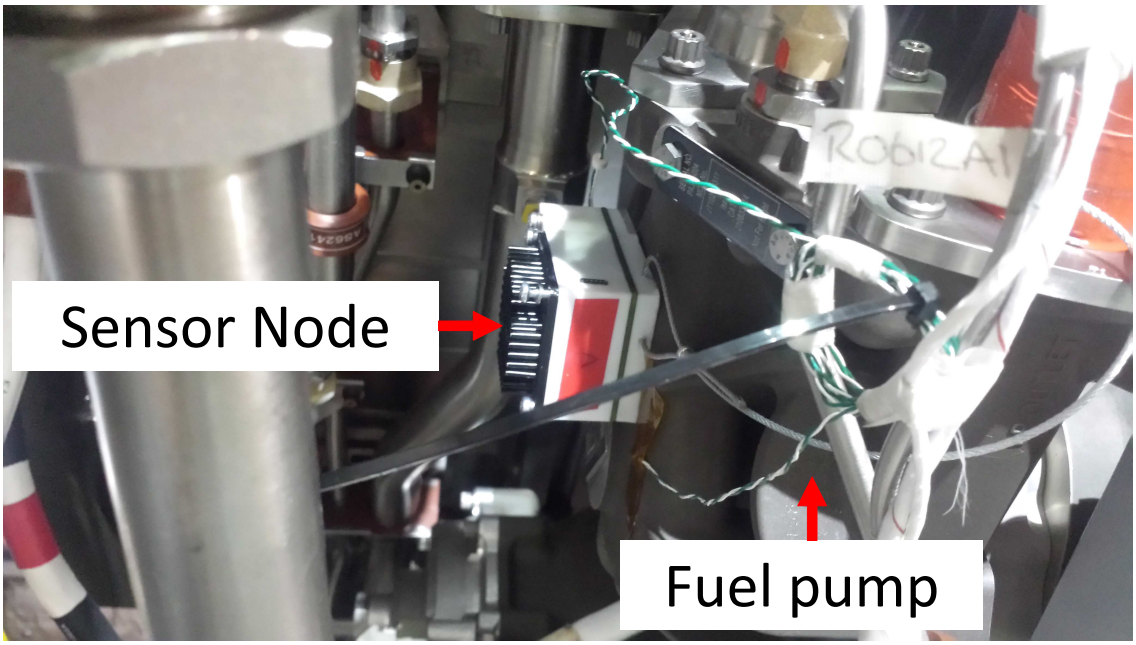

(a)

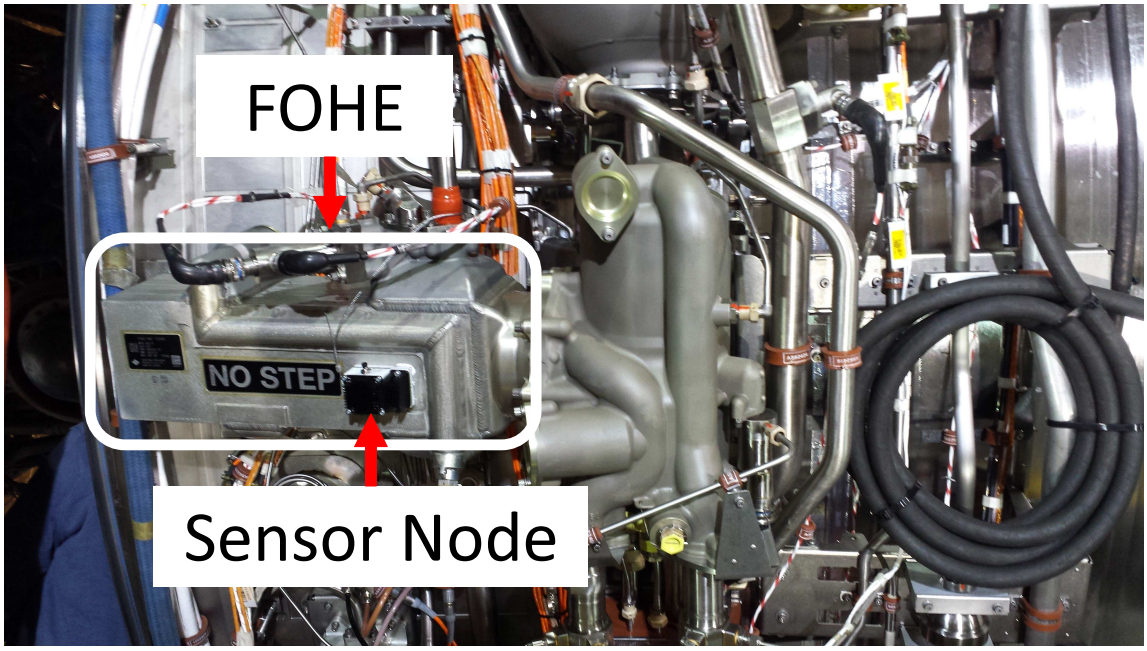

(b)

Figure 4.3: A wireless sensor node placed on the fuel pump (a) and on the Fuel-Oil Heat Exchanger for temperature sensing (b).

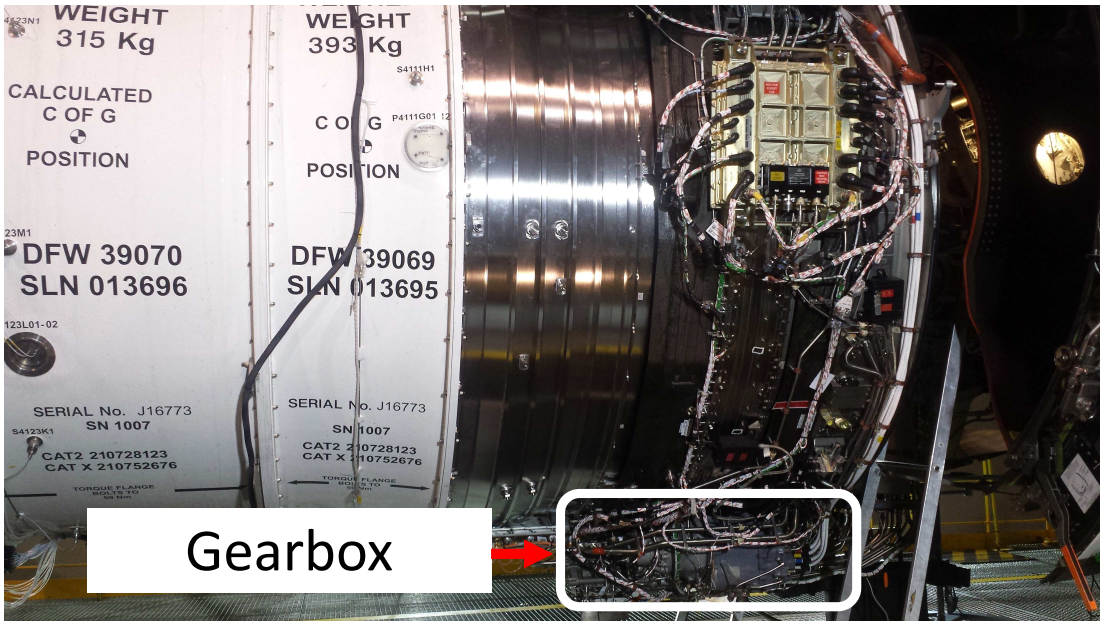

(a)

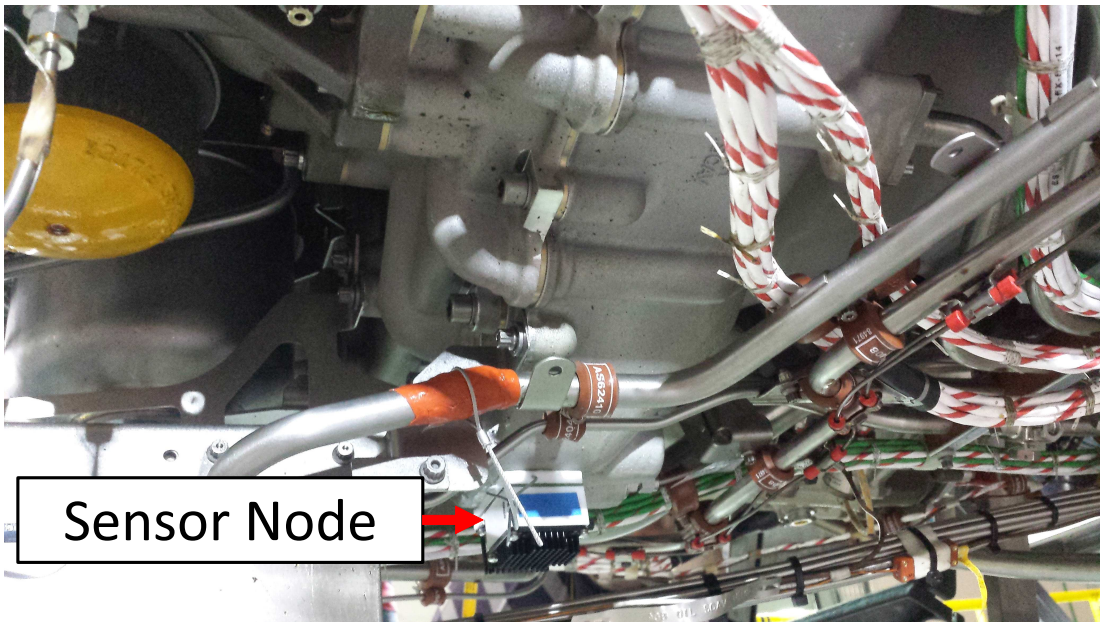

(b)

Figure 4.4: Deployment of a wireless sensor node on the gearbox for vibration sensing, distant view (a) and close-up view (b).

node to provide signal compression through random encoding and mitigate the effect of random packet loss. Moreover, the collected real data was used to generate prior information which was then used as frequency support for the recovery algorithm at the receiver side for signal decoding as described in Section 4.6. This resulted in an improvement in performance and reduction in the number of measurements required for a recovery percentage target.

Some of the complete FFT-based signals acquired by the sensor node and recovered at the base station are shown in Figures [4.6-4.8]. These vibration signals correspond to the data received from the wireless sensors at the running engine test for different levels of thrust. Figure 4.9 presents all the vibration signals received at the base station.

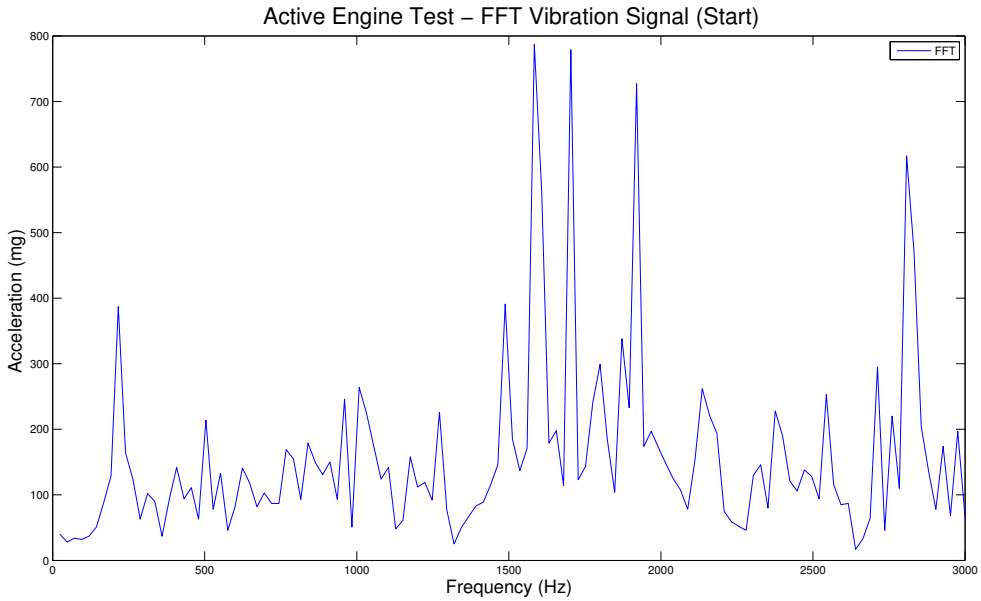

Figure 4.6: Example of an FFT collected during the Active Engine Test (low thrust).

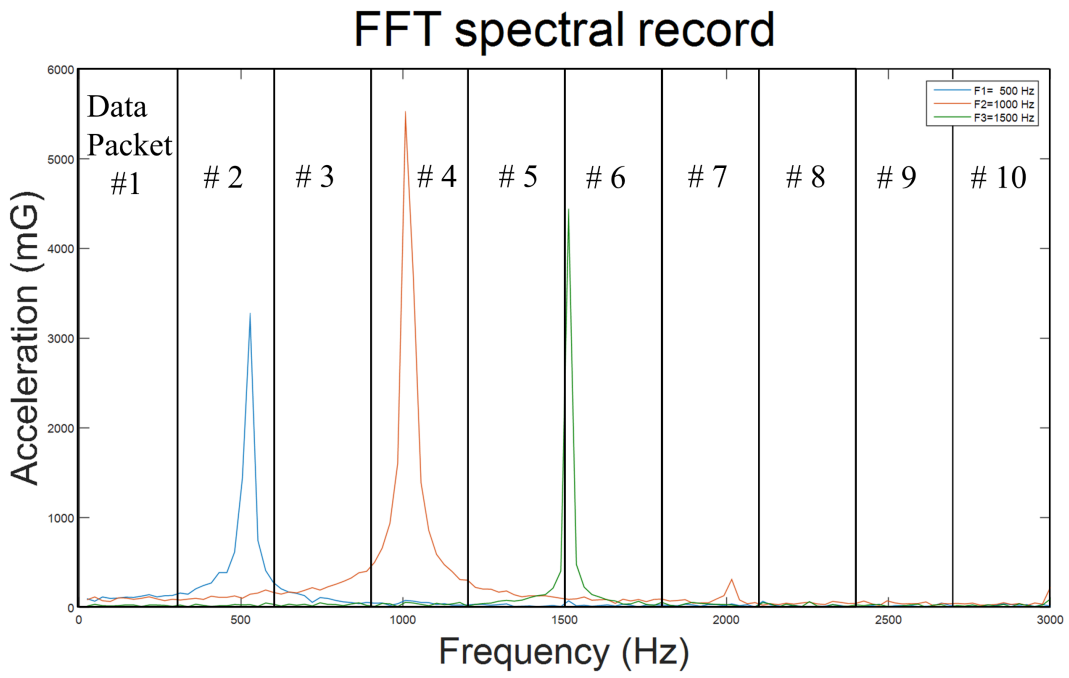

(a)

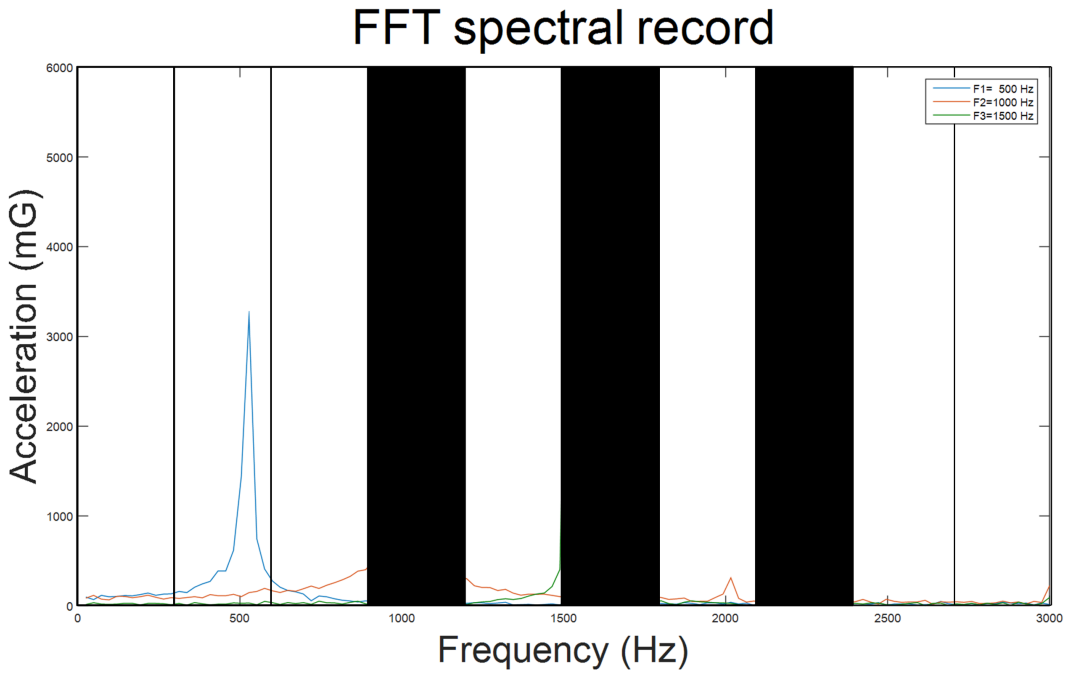

(b)

Figure 4.5: Example of vibration data acquired from LDS shaker which was recovered at the base station with all data packets received (a) and incomplete vibration signal under packet loss effect, packets lost #4, #6, #8 (b).

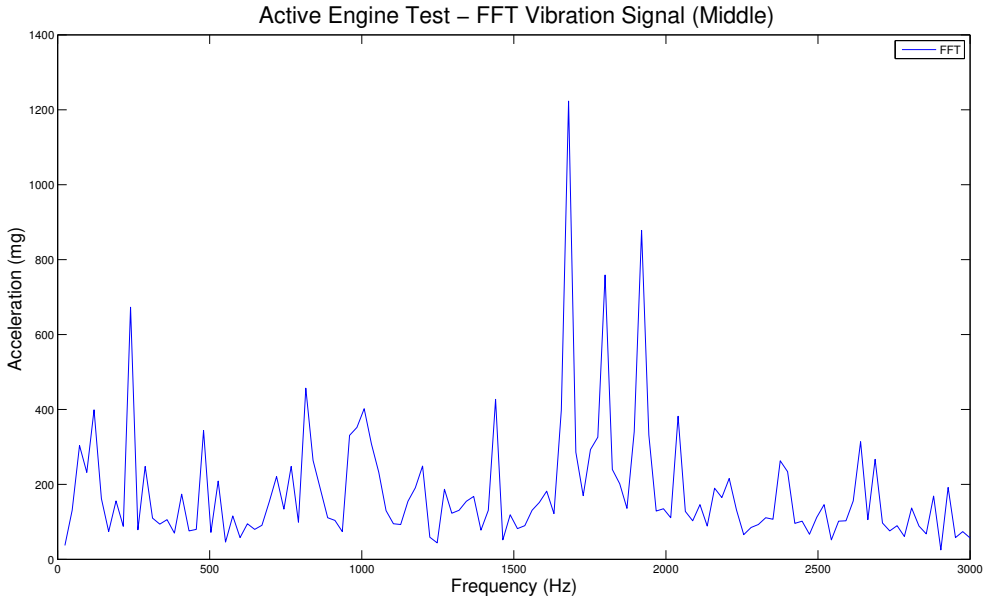

Figure 4.7: Example of an FFT collected during the Active Engine Test (medium thrust).

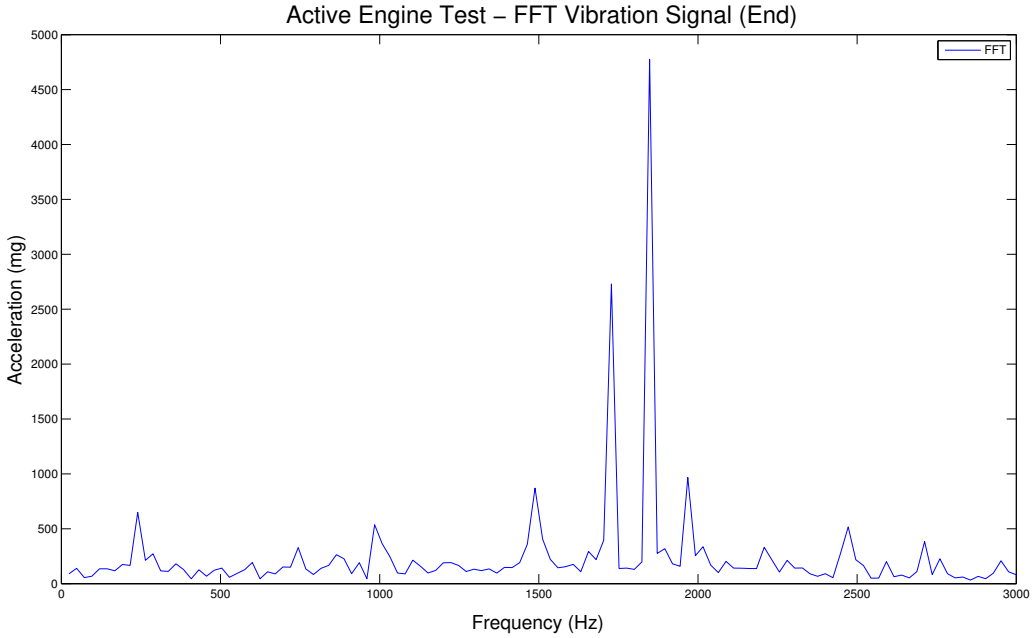

Figure 4.8: Example of an FFT collected during the Active Engine Test (high thrust).

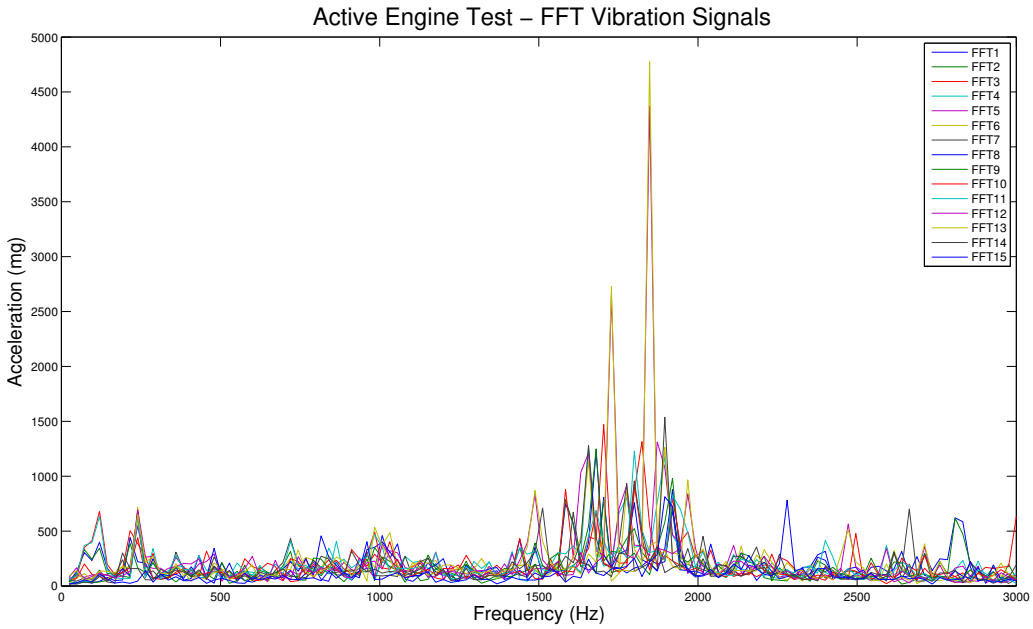

Figure 4.9: All FFTs collected in the Active Engine Test.

The vibration signals in Figures [4.6-4.8] are samples of the FFTs computed at the wireless sensor node and received at the base station during the active engine test mentioned at the beginning of this section. The thrust was gradually increased throughout the running engine test (acceleration profile). Figures 4.6-4.8 correspond to the collected data from the vibration sensor at different points in time when different levels of thrust were applied to the engine. The difference in increased acceleration is visible in these figures. The dominant peak is probably the vibration mode of the shaft (acceleration increases in response to the thrust). However, the vibration sources are not described in this research work as this proprietary information was not shared. If that information was available, it would be useful for fault diagnosis and prognosis. In summary, the objective of the presented figures is to show how the vibration profile changes depending on the applied thrust and that the highest amount of energy seems to be concentrated in some frequencies.

As can be seen from Figure 4.9, the dominant peaks from the vibration signals in this application seem to be concentrated within some frequency regions. Particularly, approximately around 1.5–2 KHz and in second place around 1 KHz. In other words, most of the energy is contained in certain areas of the frequency spectrum.

These characteristics presented an area of opportunity to propose an algorithm that captures and assigns different weights to each frequency bin considering energy levels. To achieve it, a probability density function was estimated and used to enhance signal recovery. This procedure is explained in the next section.

4.4 Probability Density Function Estimation using Gas Turbine Engine Data

As mentioned in the previous section, if the signal characteristics of the application are captured, it can be beneficial for signal recovery. For instance, that information can be used by the recovery algorithm as prior information to recover the sparse vibration signal using less measurements. This means performance improvement for signal recovery and energy savings at the wireless sensor nodes by sending a reduced number of measurements which translates into less wireless transmissions.

The situation presented in the previous section was the motivation to exploit prior information from the application to enhance signal recovery. This prior may be captured by estimating the Probability Density Function from the collected vibration signals. Hence, the algorithm selected to recover the vibration signal takes into account this frequency support structure as an additional input. The signal characteristics are captured from the collected vibration signals through a PDF. The performance of the signal recovery algorithm may be improved by increasing the probabilities of an accurate signal approximation. The following section presents the procedure to estimate the PDF from the collected vibration signals during the running aeroengine test.

This section introduces the Probability Density Function, followed by a novel algorithm to estimate the PDF from the vibration data collected in the Gas Turbine Engine. The estimated PDF captures the probabilities that a given random frequency is contained within the expected frequency regions of higher energy. This PDF is used as an additional input for the proposed signal recovery algorithm presented in Section 4.6.

4.4.1 Properties of a PDF

The Probability Density Function (PDF) $P(X)$ or density of a continuous random variable X is a statistical function that describes all possible values and likelihoods that X can take within a given range. In other words, this function links each outcome of a statistical experiment with its probability that it occurs. All the set of possible outcomes of the observed random phenomenon are contained within a sample space. More precisely, the PDF specifies the probability of a random variable to appear within a range of values. This probability is the result from computing the integral of this variable's PDF over that range. A PDF has the following properties:

1. The PDF is always non-negative.
2. The integral over the entire space is always equal to one.
3. The probability of a random variable to take a value between two points a and b is given by the area under the density function between the lowest and greatest values of the range.

$$
\begin{aligned}
&(1)\ f(x) \geq 0 \\
&(2)\ \int_{-\infty}^{\infty} f(x)\,dx = 1 \\
&(3)\ P(a \leq X \leq b) = \int_{a}^{b} f(x)\,dx = area\,under\,f(x)\,from\,a\,to\,b
\end{aligned}
\tag{4.1}
$$

4.4.2 PDF based on Collected Vibration Data

After signal compression occurs at the sensor node, the generated compressed vector is sent via wireless in multiple data packets. At the receiver, the selected signal recovery method is used to recover the original sparse vibration signal from this vector of CS measurements. The speed and performance are fundamental for applications that require fast signal recovery such as wireless vibration sensing to support EHM. This was the motivation to explore a suitable alternative to enhance the widely used

OMP signal recovery method. This was achieved by including an additional input to the algorithm as prior information. This prior was given as frequency support structure in the form of a probability density function which was estimated from the collected vibration data presented in the previous Section 4.3.

Kernel Density Estimation

Kernel Density Estimation (KDE) is a nonparametric way to obtain an estimation of the PDF of a random variable [143]. In other words, the objective of KDE is to find the PDF for a given dataset, it uses a kernel smoothing function [143]. Unlike a histogram approach, which places the data values into discrete bins to produce a discrete PDF, KDE creates an individual density curve using a smoothing function for each data value and then sums the smooth curves resulting in a single smooth continuous PDF for the dataset.

Given a discrete dataset, there are ways to know the data distribution by doing a form of density estimation such as histograms or KDE [143]. However, there are quite a few well-known problems with histograms [143]. Two of the main problems with histograms are the bin size (binwidth) and the end points of the bins. Histograms present challenges as they are not smooth, dependence on end points of bins and dependence on binwidth. The first two problems can be alleviated by using KDE. The dependence on endpoints of the bins is removed. Each of the blocks at each data point is centred instead of fixing the endpoints of the blocks [143]. The density estimate is continuous and allows to extract the density structure. A smooth kernel is used as the building block to produce a final smooth density estimate. Unfortunately, in KDE the problem of dependence on the bandwidth exists (equivalent to a histogram's binwidth). In this research work, the bandwidth selected produces a smooth curve and is theoretically optimal to estimate densities for the normal distribution [147].

In this application, the kernel distribution is estimated at 125 points from the input data, which refers to the total number of FFT bins that cover a frequency bandwidth of 3KHz (25 Hz per bin). However, it can be noted from the resulting PDF in Figure 4.10, that this function represents the set of possible values that the random variable can take in terms of magnitude. In other words, this PDF shows the probability that a random frequency falls within a given range of magnitude. In this case, the maximum occurs between a range of 100-200 mG. Therefore, most of the nonzeros are

contained within this range of magnitude. This PDF would be useful for applications that require to recover all the frequency components in vibration signals regardless of its magnitude. However, some frequency components may contain noise floor or their magnitude/energy may be too low to be of interest for a given application.

In this thesis, KDE is introduced for the interest of the reader as the KDE standard procedure was not modified. It was used as a tool to estimate the PDF based on the input data. The novelty of the proposed Algorithm 4.1 lies in the form that the vibration signals are sparsified (estimating the density distribution of the data in terms of frequency instead of magnitude) and then how the resulting PDF is used in the E-OMP recovery algorithm (Algorithm 4.3, explained in Section 4.6) to enhance performance and recover the vibration signal with less measurements.

PDF estimation in sparse signals based on the frequency spectrum

The final estimated PDF from the real vibration data (non-sparse) is shown in Figure 4.10. As mentioned in Chapter 3, to generate compressed sensing measurements, the input signal is required to be sparse. Essentially, the frequency components of higher magnitude in the original signal are kept while most of the components of lower magnitude are set to zero. In other words, the original signal is thresholded to make it sparse and suitable for CS.

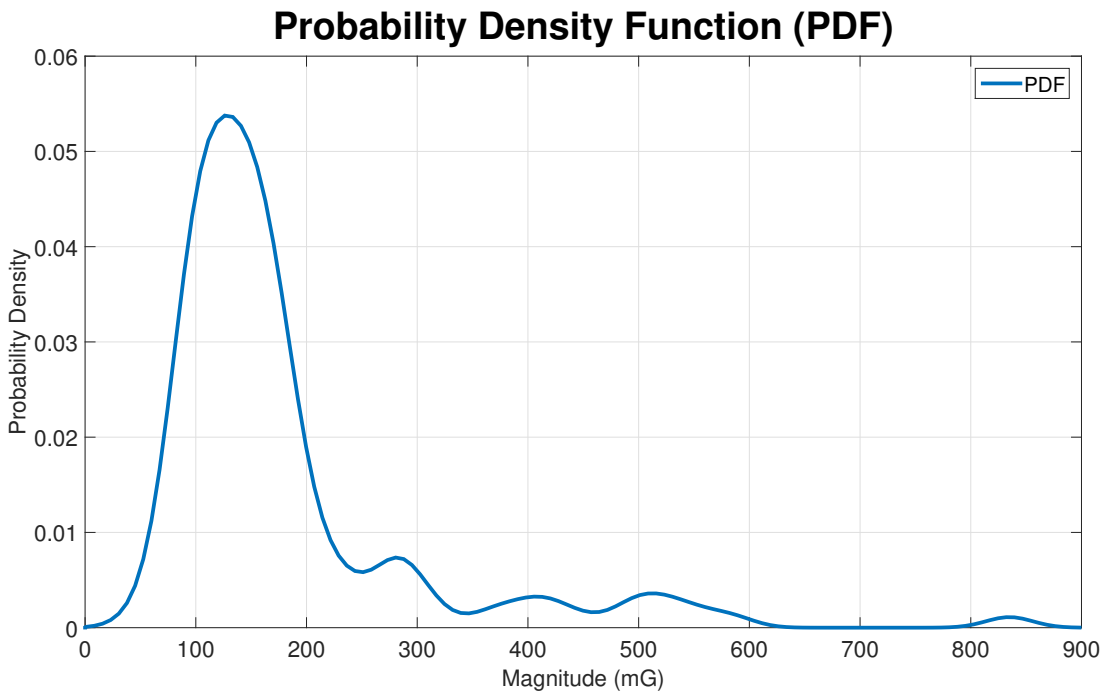

Figure 4.10: The density distribution of the original vibration data collected from the Trent1000 aeroengine gear box, the x-axis is the acceleration in mG and the y-axis is the probability density function.

When a signal is made sparse using a threshold, all the components below the selected threshold τ (distortion level) are not recoverable and as a consequence, they should not be considered to estimate the PDF. This thresholding procedure may help to remove noise from the signal. For instance, if the noise floor level is known, the value of τ may be set at that magnitude level and all frequency components below τ may be zeroed out to reduce the dimensionality of the signal and increase signal sparsity. Another case would be for instance to set τ to a level on which the resulting sparse signal contains S nonzero components. Figure 4.11 illustrates this situation, the average of the frequency domain vibration signals (from collected real data) in its original form and the resulting sparse signal (with $S = 36$ non-zero components) after using $\tau = 175mG$ are shown. The PDF produced based on this sparse vibration data is shown in Figure 4.12. The resulting PDF is more representative of the sparse vibration data, most of the components are zero except for S non-zero elements. However, this distribution function shows the probabilities of a random variable in

terms of magnitude and not respect to frequency. To exemplify this situation, the area of the averaged FFT from the real data is presented in Figure 4.13. It can be observed that most of the energy is concentrated between the frequency range of 1.5-2 KHz. To enhance the standard OMP algorithm, the PDF used as frequency support should model the true distribution of the signal capturing the zones of higher energy.

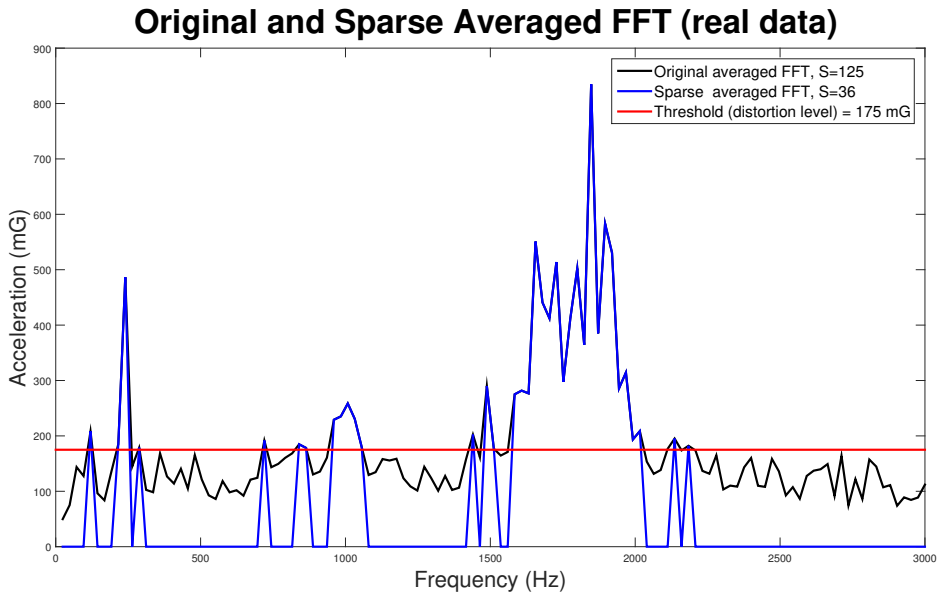

Figure 4.11: The averaged FFT-based signal from the original vibration data (black) collected from the Trent1000 aeroengine gearbox and the resulting sparse signal (blue) after using τ=175 mG (red).

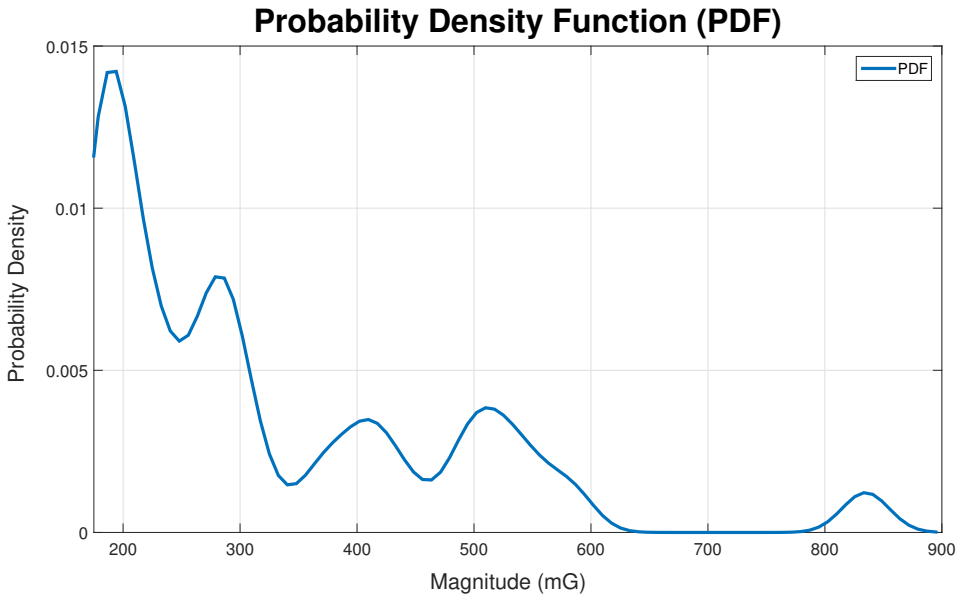

Figure 4.12: The density distribution of the thresholded sparse vibration data from Figure 4.11. In contrast to Figure 4.10, this PDF is the resulting distribution after the same vibration data is made sparse (blue signal in Figure 4.11). All components of lower magnitude are removed except the nonzero frequencies above the threshold, where $= 175$mG.

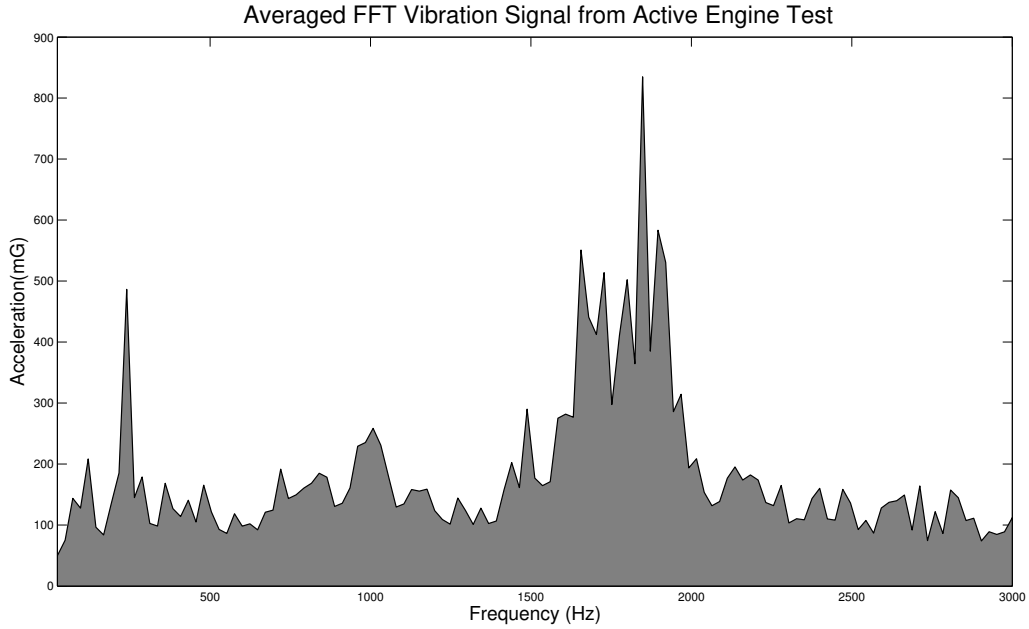

Figure 4.13: Resulting FFT from averaging all FFTs collected in the Active Engine Test.

The signal recovery algorithm can be enhanced by including an estimated PDF that captures the energy distribution across all the frequency spectrum. This is because at the base station, the received data from a wireless sensor node contains the vibration signal encoded in a vector of compressive sensing measurements. In CS, a sparse signal and a measurement matrix Φ are used to generate this vector of CS measurements. Hence, at the receiver, it is important to detect the contribution of Φ in the received vector. Finding the contribution of Φ, allows recovering the vibration signal with high accuracy from the received vector. The estimated PDF is used as prior frequency support to increase the probabilities of finding the right set of columns in Φ that contributed to the received vector through a weighted selection (more details in Section 4.6). This results in efficient signal recovery because less measurements are used to recover a vibration signal in comparison to the standard OMP signal recovery algorithm. Using less measurements to recover a signal means fewer wireless transmissions are needed, which results in important energy savings for the wireless vibration sensing system.

The proposed iterative Algorithm 4.1 to estimate the PDF from the collected vibration data is as follows:

Algorithm 4.1 PDF Estimation based on Frequency Spectrum

Inputs:
a. A $P \times N$ matrix of collected signals Γ, where the entries are nonzero elements. P is the number of collected signals and N is the signal length.
b. A desired number of S nonzero elements when the signals are made sparse.
Output:
An estimated probability density function P.
Procedure:
1. Initialise the iteration counter $k = 1$ and residuals matrix $R^{(k)} = \Gamma$.
2. Initialise the selection matrix $W^{(k)} = \mathbf{0}_{P \times N}$, where $W^{(k)}$ updates in each iteration with the selected entry from $R^{(k)}$.
3. Find the maximum in residuals matrix $w_k^{(k)} = max(R_{kj}^{(k)})$, where $j = 1, 2, ..., N$. If maximum occurs for multiple indices, then break the tie deterministically.
4. Update the selection matrix element $W_{k\,jmax} = w_{k\,jmax}$, where $jmax = j \mid max(R_k^k)$.
5. Set $R_{k\,jmax}^{(k)} = 0$. The chosen column is set to zero to not consider it in next iterations.
6. Increment k and return to Step 2 if $k \leq P$. If not, continue to Step 7.
7. Calculate the average of the rows in W. Consider $W = \begin{bmatrix} \alpha_1 \\ . \\ . \\ . \\ \alpha_P \end{bmatrix}$ to form the averaged vector $W_{avg} = \frac{1}{P} \sum_{q=1}^{P} \alpha_q$.
8. Initialise the PDF counter $t = 1$.
9. Estimate the Probability Density Function P_t with KDE, using W_{avg} as the sample data input.
10. Increment t. If $t \leq S$, $k = 1$ and go to Step 2. If not, continue to Step 11.
11. Sum the S estimated PDFs. $\sum_{v=1}^{S} P_v = P$.
12. Normalise and return P.

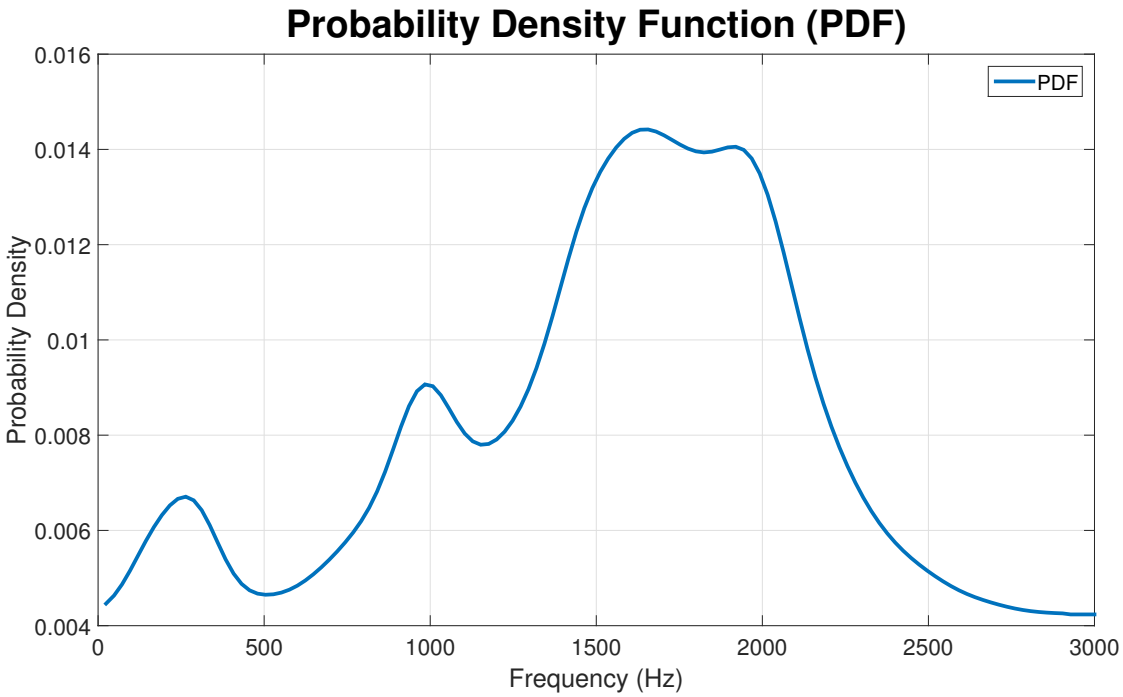

Figure 4.14: The estimated PDF of the sparse vibration data collected from the Trent1000 aeroengine gearbox in terms of frequency. The x-axis is the frequency in Hertz and the y-axis is the probability density function.

The PDF shown in Figure 4.14 is the resulting density estimate in function of the frequency. In other words, it represents the probability that a given random measurement falls within a given frequency. This PDF is representative of the sparse vibration signals (real data from this application) as it captures the frequency regions of higher energy. The estimated PDF was used as an additional input to the novel algorithm presented and described in Section 4.6. Due to the limited number of collected signals during the Gas Turbine Engine test, a set of synthetic vibration signals were generated to validate the proposed algorithm. The following section describes how the synthetic vibration signals were generated.

4.5 Generation of synthetic signals based on Active Engine Test data

As presented in Section 4.3, the data collection from the active engine test included only 15 FFT-based vibration signals. Due to the limited number of real vibration signals, a set of synthetic signals were produced based on the same probabilistic structure found in the collected vibration data. The objective was to produce frequency domain vibration signals which contain most of the energy in the same frequency regions as the vibration signals obtained from the aeroengine. This increased number of vibration signals were generated to test signal recovery methods.

Algorithm 4.2 indicates the inputs, outputs and steps in order to generate synthetic signals.

Algorithm 4.2 Synthetic Signal Generation Procedure

Inputs:

a. A $P \times N$ matrix of collected vibration signals Γ in the frequency domain. Where the entries are nonzero elements. P is the number of collected signals and N is the signal length.

b. A number of sinewave components Sc per synthetic vibration signal.

c. Minimum probability threshold value M_{TH}.

Output:

An averaged FFT-based synthetic signal F.

Procedure:

1. Calculate the average of frequency components in Γ to form the averaged vector x_{avg}. Consider $\Gamma = \begin{bmatrix} \eta_1 \\ . \\ . \\ . \\ \eta_P \end{bmatrix}$ to form the vector $x_{avg} = \frac{1}{P}\sum_{q=1}^{P} \eta_q$.

2. Estimate the Probability Density Function E using KDE as mentioned in Section 4.4.2 with x_{avg} as the sample data input.

3. Threshold the PDF E as: $E_{TH} = \begin{cases} E & E > M_{TH} \\ 0 & E \leq M_{TH} \end{cases}$

4. Sum the probabilities in the thresholded PDF $P_{TH} = \sum E_{TH}$.

5. Calculate the required size Sv of the set V as: $Sv = (100/M_{TH}) \times P_{TH}$ to accommodate the frequencies above M_{TH}.

6. Generate a vector $\mathbf{V}_f$=$[V_z]$ where $z = 1, ...Sv$. Where each V_z is repeated $E_{TH}(V_z) \times Sv$ times. The number of times a frequency appears in V_z is given by the thresholded PDF E_{TH} from Step 3.

7. Initialise the sinusoids counter $sel = 1$.

8. Select a random frequency f from $\mathbf{V}_f$.

9. Generate a sinusoidal wave $sw = A\sin(2\pi ft)$. Where the amplitude A is given by x_{avg} at frequency f.

10. Increment sel, and return to Step 9 if $sel \leq Sc$.

11. Sum the Sc sinusoids $\sum_{i=1}^{Sc} sw_i = S_{avg}$.

12 Calculate the FFT F from S_{avg} and return F.

The Algorithm 4.2 outputs an averaged FFT-based synthetic signal. Samples of the generated vibration signals from this algorithm are shown in Figures [4.15-4.17].

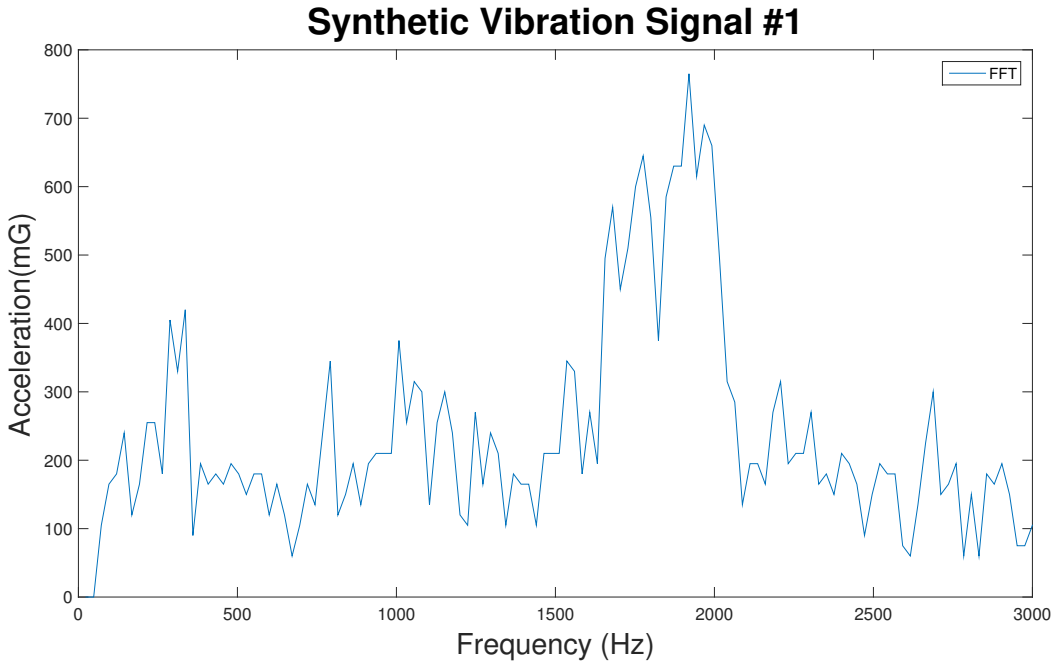

Figure 4.15: Example 1 of an FFT-based vibration signal generated synthetically using Algorithm 4.2.

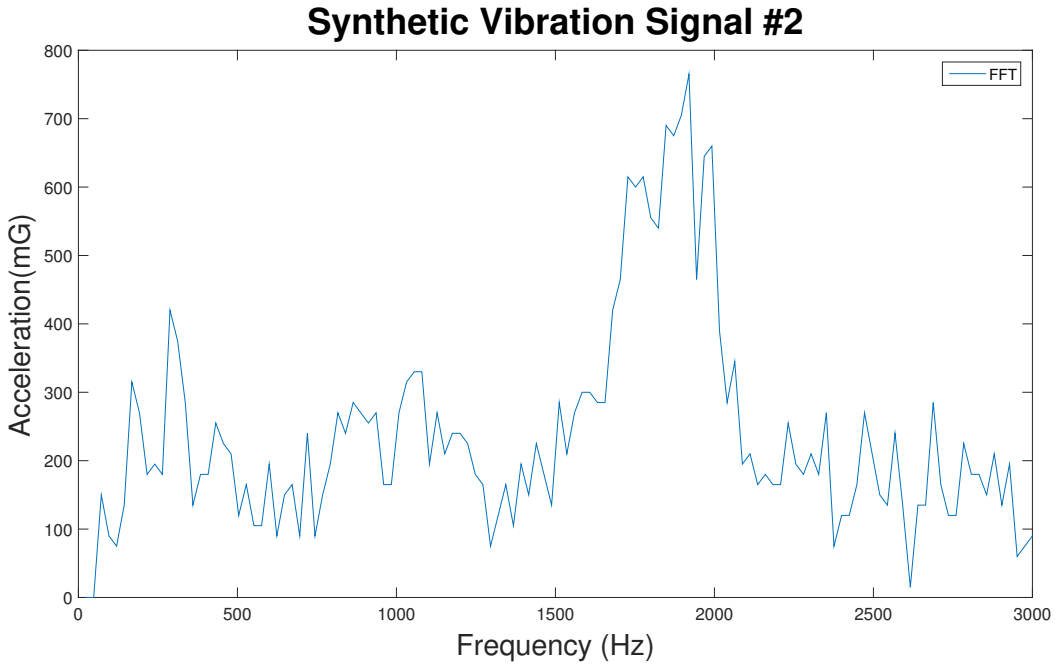

Figure 4.16: Example 2 of an FFT-based vibration signal generated synthetically using Algorithm 4.2.

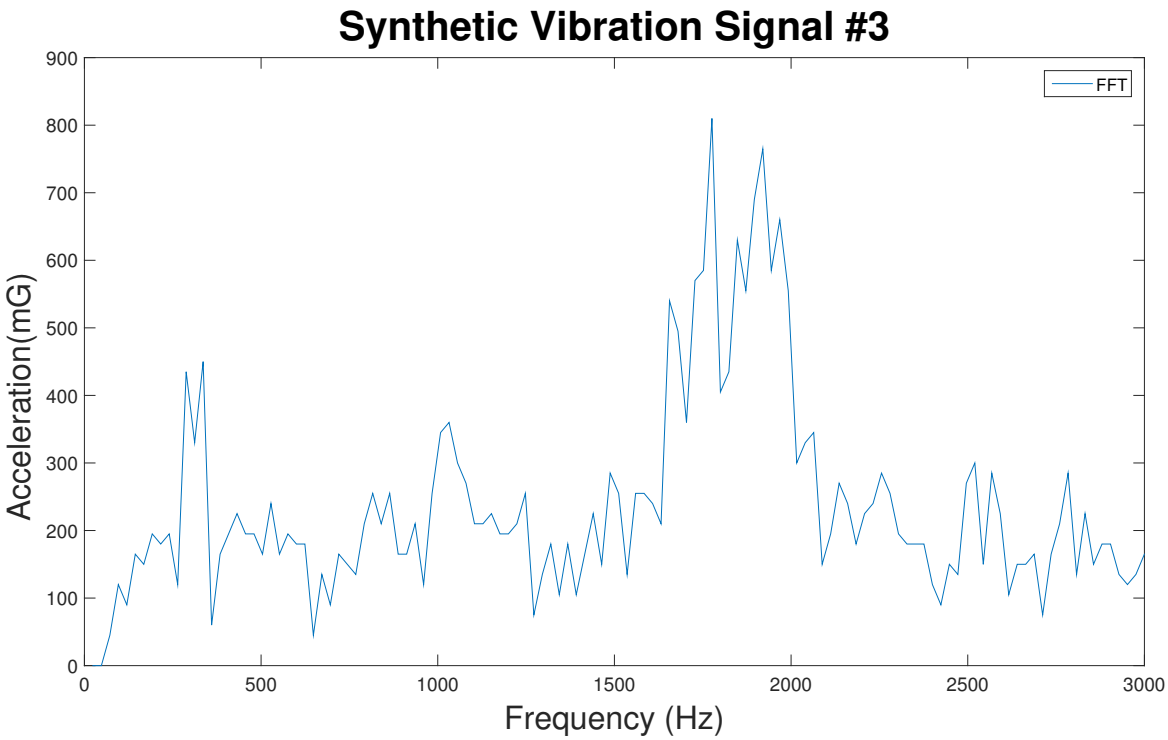

Figure 4.17: Example 3 of an FFT-based vibration signal generated synthetically using Algorithm 4.2.

As described in Section 4.4.2 and shown in Figure 4.13, in this application most of the energy is concentrated in frequency regions of the frequency spectrum. The generated synthetic signals follow the same probabilistic structure as the real vibration signals which was fundamental to perform simulations and evaluation of signal recovery methods. The following section introduces the Orthogonal Matching Pursuit (OMP) algorithm and presents the proposed novel algorithm which outperforms the performance of the standard OMP to solve the signal recovery problem.

4.6 Signal Recovery with Enhanced OMP

To recover sparse signals, sparse approximation algorithms can be selected. The most popular approaches are Matching Pursuit (MP) [162] and Basis Pursuit (BP) [123]. Mallat et. al [162] introduced MP, which was a pioneering work in greedy pursuit algorithms. Using MP and Orthogonal MP (one of its variants), the sparse signal is

built iteratively by selecting an atom that maximally improves the representation at each iteration step. In the case of BP, it looks for the vector that minimises the $L1$ norm coefficients, which is computationally expensive to obtain. Various techniques based on BP are commonly used for sparse signal recovery [123]. Although sparse signals or images can be recovered with high probability using BP [123], it may not be the best solution for applications that require fast signal recovery. In this thesis, OMP [124] was selected as it is simpler, faster, more efficient and easier to implement [144]. Moreover, the transparency of this algorithm motivated to propose a novel greedy algorithm named Enhanced Orthogonal Matching Pursuit (E-OMP) presented in Section 4.6.2.

4.6.1 Introduction to Standard OMP

The OMP is a variant of MP. At each iteration step in MP, the atom with the strongest correlation with respect to the residual signal is chosen. This is what the term matching refers to. Note that MP selects atoms among the complete dictionary at each iteration step. This means that an atom may be selected more than once, slowing down the convergence.

Orthogonal matching pursuit (OMP) [124] overcomes this problem by projecting the sparse signal onto the subspace spanned by the chosen atoms. Under this restriction, OMP implies that no atom is chosen twice. The resulting approximation of the signal is optimal in the least squares sense. Hence, to converge, fewer steps are required.

Like many methods, OMP presents some drawbacks. It has been demonstrated [124] that if OMP selects a wrong atom in some iteration step, the original signal may never be recovered. Moreover, OMP is computationally more demanding than MP but OMP makes sure that no repeated atoms are selected. Finally, the sparsity level of the signal is required which may not be known in advance. Despite the mentioned flaws, OMP is said to be the algorithm with better performance from the complete family of matching pursuits [124].

4.6.2 Development of Enhanced OMP

The selection of a wrong atom in some iteration step in conventional OMP is likely to result in inaccurate signal recovery. To improve the sparse signal recovery and mitigate this issue, it is proposed an algorithm called Enhanced OMP (E-OMP) (described in detail in Algorithm 4.3). The OMP and E-OMP are both iterative greedy algorithms. A greedy algorithm makes a local optimal selection with the intention to find the global optimum when the algorithm finishes its execution. The OMP selects at each iteration step, the dictionary element most correlated to the residual of the signal. Then, it results in a new approximation by projecting the signal onto the dictionary elements that have already been chosen. The main difference between OMP and E-OMP is that E-OMP considers prior information from the application (estimated PDF from Algorithm 4.1) in order to increase the probabilities of selecting the right column of the dictionary at each iteration step. Then, as OMP does, a new approximation is produced by projecting the signal onto the dictionary elements that have already been chosen. The running time of the standard OMP is dominated by Step 2. The E-OMP includes the estimated PDF in this step but no additional instructions or steps are added in comparison to conventional OMP. Hence, the running time is not altered due to the modifications introduced.

E-OMP for recovery of sparse vibration signals

In this research work, this greedy algorithm is used to recover sparse vibration signals from a vector of compressed sensing measurements y sent by the wireless sensor nodes. An accurate signal recovery occurs when all the columns from the measurement matrix Φ that contributed to the vector y are identified. Therefore, the importance to accurately select the correct columns at each step iteration. In this research work, vibration data was collected from an active aeroengine (Section 4.3). From this data, the probability density function was estimated (Section 4.4.2) and given as an extra input to the algorithm to enhance the selection of columns from Φ.

The steps to implement the algorithm used for the signal recovery problem are described as follows. Assume the vibration signal is in S-sparse representation. Let X_S be the S-sparse signal of interest in $\mathbb{R}^N$, and form an M x N matrix Φ referred as the measurement/sensing matrix whose rows $\{x_{1,}..., x_M\}$ represent a set of M

measurement vectors, where each vector lives in $\mathbb{R}^N$. The M measurements of the signal can be collected in an M-dimensional vector of data $y = \Phi \cdot X_S$.

Signal recovery may be seen as a sparse approximation problem. Since X_S contains only S nonzero elements. Through a linear combination of S columns taken from Φ, the measurement vector $y = \Phi \cdot X_S$ is constructed. In sparse approximation, it can be said that y contains an S-term representation in the dictionary represented by Φ.

In order to find the sparse signal X_S, the columns of Φ that are contained in the measurement vector y, need to be identified. An optimal column from the measurement matrix Φ is selected at each iteration with the intention to find the correct set of columns in Φ that contributed to the data vector y (this vector contains the encoded vibration signal). The vector y contains the encoded vibration signal, which may be decoded with high accuracy at the receiver when the right set of columns in Φ that contributed to y are found. For instance, when one or more columns in Φ are incorrectly chosen by the algorithm, results in an imprecise signal approximation. Therefore, it is vital to make an accurate column selection. The performance of the standard OMP algorithm increased because the likelihood of choosing the precise column at each instance augmented through a weighted column choice. This was achieved by including frequency support in the form of a PDF in the OMP algorithm.

The purpose of the OMP algorithm [124] is to pick a column of Φ at each iteration. The column chosen is the one that reflects the strongest correlation with the remaining part of the vector y. Then this contribution is subtracted from y and iterates on the residual until all the columns of Φ that participate in the measurement vector y are identified [124]. It is expected that the algorithm identifies the correct set of columns after S iterations. By using this algorithm, the original sparse signal can be recovered. The proposed novel algorithm 4.3 includes frequency support structure, it outperforms the performance of the standard OMP by allowing a weighted selection of columns of the measurement matrix which increase the probabilities of successful signal recovery. The steps to implement the Enhanced OMP (E-OMP) algorithm are given as follows:

Algorithm 4.3 E-OMP Algorithm for Signal Recovery

Inputs:

a. An M-dimensional measurement vector y.

b. A measurement matrix Φ of size: $M \times N$.

c. Sparsity level S of the signal to be recovered.

d. An N-dimensional vector containing the Probability Density Function P of the signal, estimated in Algorithm 4.1.

Outputs:

a. An estimate $\hat{X_S}$ in $\mathbb{R}^N$ for the optimal signal.

b. A set Λ_S containing the S indices of selected columns in Φ from $\{1, ..., N\}$.

c. An M-dimensional residual r.

Procedure:

1. Initialise the value of the residual $r_0 = y$, the index set $\Lambda_0 = \emptyset$, and the iteration count $c = 1$.

2. Select the index λ_c that solves the optimisation problem $\lambda_c = \arg \max_{i=1,...N} |\langle r_{c-1}, \varphi_i \rangle| \cdot P(i)$. If maximum is found for multiple indices then break the tie deterministically.

3. Augment the index set $\Lambda_c = \Lambda_{c-1} \cup \{\lambda_c\}$ and matrix of chosen columns Φ_c.

4. Acquire the new approximation of the signal by solving the least square problem: $x_c = arg\ min_x \|y - \Phi_c x_c\|_2$.

5. Calculate the new estimate of the data and the new residual: $a_c = \Phi_c x_c$ and $r_c = y - a_c$.

6. Increment the iteration counter c, and go back to step 2 if $c < S$, where S is the sparsity level or number of non-zeros.

7. The estimated sparse signal has nonzero indices at the elements listed in Λ_S.

Enhanced OMP: The step 2 is fundamental to enhance the performance in signal recovery as prior information about the signal in the form of Probability Density Function (PDF) is included. In other words, the index that solves the optimisation problem is found. The absolute value of the dot product between the residual and the columns of the measurement matrix Φ is calculated, the maximum value is selected which means maximum correlation. This corresponds to the position of the candidate column. This step was modified to include the PDF of the signal, this allows to include the frequency support structure, allowing a weighted selection (expectation) of candidate columns when prior information is known. The improved performance in signal recovery for signals with different sparsity levels is shown in the next chapter when using the standard OMP and Enhanced-OMP (E-OMP) with prior information.

4.7 Chapter Summary

This chapter has presented the procedure to modify the selected standard OMP algorithm for sparse signal recovery. Furthermore, samples of vibration signals collected from sensor nodes installed in an active aerospace gas turbine engine have been shown. Likewise, the estimated PDF from these signals was presented. It has been identified that the performance of the standard OMP algorithm was enhanced by adding frequency support in the form of the estimated PDF. The improvement in the standard OMP performance was derived from the inclusion of the PDF in the OMP as an additional input. This prior information allowed a weighted selection of columns of the measurement matrix that contributed to the vector received from the wireless sensor nodes. This resulted in a more accurate local optimal selection of columns which enabled an accurate signal recovery (global optimum, after algorithm finishes its execution) using a reduced number of measurements in comparison to the standard OMP without prior support. The next chapter presents the evaluation and comparison of both OMP and E-OMP algorithms for signal recovery of sparse vibration signals. The aim is to highlight the benefits of E-OMP in terms of energy savings and performance improvement when prior frequency support from the application is included in order to recover sparse signals.

Chapter 5

Experimental Results and Discussion of WVS Framework

5.1 Introduction

As mentioned throughout this thesis, autonomous wireless vibration sensing systems require to use techniques for energy conservation and tolerance to random packet loss, especially if the wireless sensors transmit data within harsh environments such as in a Gas Turbine Engine. Chapter 3 presented the system architecture and set of strategies for signal encoding at the sensor nodes through local signal processing to help mitigate the random packet loss problem and data compression to conserve energy by reducing the amount of data to be sent to the base station. Chapter 4 presented the proposed strategy to deal with the signal recovery problem and further promote the conservation of energy at the wireless sensor nodes by reducing the number of measurements required to recover the vibration signal sent by the sensor nodes. This was achieved by extracting the signal characteristics of the application through the estimated PDF which captures the energy distribution across the frequency spectrum. This information is then included in the proposed algorithm to recover sparse vibration signals.

This chapter presents the experimental results from the evaluation of the standard OMP (without frequency support) and E-OMP (with frequency support) to recover

sparse vibration signals from compressive sensing measurements. The purpose of this chapter is to show the enhancement of signal recovery performance comparing both algorithms. Energy savings and improved signal recovery are aims that are achieved through E-OMP. This happens because the number of measurements required at the receiver to recover a vibration signal using E-OMP is reduced in comparison to OMP for the same probability of successful recovery for all sparsity levels. More details, tables and resulting graphs are presented in this chapter.

5.2 Performance Evaluation

The performance is evaluated in terms of Percentage Root mean-squared Difference (PRD). The recovered signal $\hat{X_S}$ is compared against the original sparse signal X_S to verify the reconstruction accuracy using the PRD given by:

$$PRD = \sqrt{\frac{\sum_{n=1}^{N}(X_S(n) - \hat{X_S}(n))^2}{\sum_{n=1}^{N}(X_S)^2(n)}} \times 100, \tag{5.1}$$

where $X_S(n) \in \mathbb{R}^N$ represents the original signal, $\hat{X_S}(n) \in \mathbb{R}^N$ represents the recovered signal and N represents the signal length. If the PRD or error between the original and recovered signal is less than 1% then it is considered that the algorithm succeeded. For each triple (S, M, N), a total of 1000 independent trials were performed.

Sparse Signal Recovery using different Algorithms

As presented in Chapter 2, compressive sensing is used in a wide variety of applications including imaging, radar, wireless sensing and many more. Given a sparse signal in a high-dimensional space, the objective is to recover that signal accurately and efficiently from a number of linear measurements much less than the actual dimension of the signal. This is clearly possible in theory [107]. However, the difficulty lies in building efficient signal recovery algorithms. There have been two distinct major approaches to sparse signal recovery: Basis Pursuit and Matching Pursuit, each presents different advantages and shortcomings. This section presents three different algorithms for sparse signal recovery from CS measurements.

- Basis Pursuit (BP): Basis Pursuit or minimisation based on the L1 norm was one of the first methods suggested for signal recovery in the compressed sensing problem [123]. This method uses linear optimisation to recover sparse signals. Although this method provides strong guarantees and stability, it relies on the use of linear programming, lacks a strong bound on its runtime and is computationally expensive [145].

- Orthogonal Matching Pursuit (OMP): OMP has been described in Section 4.6.1. OMP is a representative method of the family of greedy algorithms. This greedy algorithm iteratively finds the solution by correlating the signal residual with the columns of the measurement matrix. The greedy approach is quite fast both in theory and in practice, efficient, simple and easy to implement [124]. However, it requires somewhat more measurements for signal recovery compared to L1 minimisation [145].

- Enhanced Orthogonal Matching Pursuit (E-OMP): The E-OMP algorithm proposed in this thesis is a variation of the standard OMP. In contrast to OMP, E-OMP considers prior information from the application in the form of frequency support structure which contains the estimated energy distribution of the frequency spectrum. This additional input allows a weighted selection of columns from the measurement matrix to the residual which results in an increased recovery probability in comparison to conventional OMP. From another perspective, if the recovery probability is fixed, then E-OMP requires a fewer number of CS measurements to recover the signal compared to standard OMP without prior frequency support.

The plot in Figure 5.1 shows the signal reconstruction results for different sparsity levels using the above-mentioned algorithms. It describes the situation in dimension $N = 125$ using three signal recovery algorithms. It shows the percentage (out of the 1000 trial signals) of signals recovered correctly as a function of M, the number of measurements. It provides a graphical comparison between the standard OMP, the Enhanced-OMP (E-OMP) (with prior support) algorithm proposed in this thesis and presented in Section 4.6.2 and $L1$ minimisation. Each curve denotes a different sparsity level S. As predicted, more measurements are required to ensure signal recovery when the number of nonzero elements increases. The performance to recover sparse vibration signals using the standard OMP, E-OMP and $L1$ minimisation can

be compared in Figure 5.1. From the results, the recovery probability is higher using the proposed E–OMP algorithm in comparison to the standard OMP for all sparsity levels using the same number of measurements (same conditions for both scenarios). The improvement in performance is because prior information in the form of frequency support structure is considered in the proposed E-OMP algorithm. As described in Section 4.4.2, the regions of higher energy in the frequency spectrum for a given vibration signal are estimated in the form of a Probability Density Function (PDF). This PDF estimated from the application is used as prior information for the proposed E-OMP algorithm (Section 4.6.2) as an additional input, resulting in improved performance compared to standard OMP without frequency support. Also, as expected, $L1$ minimisation (basis pursuit) clearly requires fewer measurements than OMP and E-OMP. However, as mentioned in this thesis and as shown in the literature, $L1$ minimisation is computationally expensive and in many applications, OMP is preferred over basis pursuit [145]. Hence, a different approach not based on optimisation was selected. The structure of OMP was chosen for this application as is widely used due to its simplicity, speed and ease of implementation [124]. Moreover, the transparency of this method presented an opportunity to include prior information from the application to improve signal recovery performance. The following plots and tables presented in this chapter compare OMP and E-OMP from different perspectives to show the benefits of the proposed algorithm.

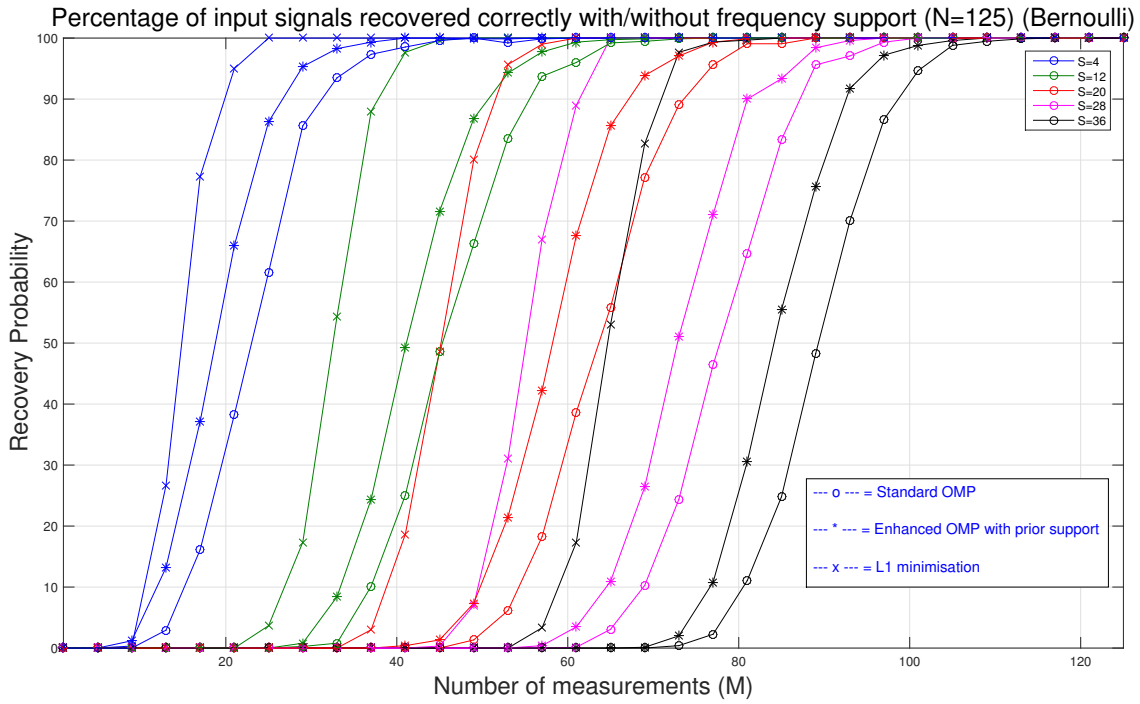

Figure 5.1: The percentage of 1000 input signals correctly recovered as a function of the number of measurements M for different sparsity levels S in dimension N =125. The signal recovery algorithms used include variations of Matching Pursuit (OMP and E-OMP) and Basis Pursuit (L1-minimisation).

Table 5.1 presents data extracted from Figure 5.1. It shows the number of measurements required to recover an $S-$sparse signal with a fixed rate of success. For instance, to recover a signal with >95% recovery probability, it can be noted that the number of measurements needed is less for the case of the proposed E-OMP algorithm (in average, ~5% less measurements) compared to standard OMP for all sparsity levels.

Table 5.1: The number of measurements required to recover a $S-$sparse vibration signal with >95% recovery probability in dimension $N = 125$ using standard OMP, the proposed E-OMP and L1-minimisation.

Standard OMP		Enhanced OMP		L1-minimisation	
Sparsity Level (S)	Measurements (M)	Sparsity Level (S)	Measurements (M)	Sparsity Level (S)	Measurements (M)
4	35	4	28	4	21
12	59	12	53	12	41
20	77	20	71	20	55
28	90	28	85	28	64
36	101	36	95	36	73

Figure 5.2 shows another view of the data. It presents what percentage of signals were recovered correctly as a function of S, the sparsity level. The recovery probability increments as more measurements are taken given a fixed sparsity level. This figure shows a situation that is significant in applications. For instance, assume there is enough space to save only $M = 50$ measurements in memory or there is enough time to collect and process only $M = 50$ pieces of information. In dimension $N = 125$ using standard OMP and the proposed E-OMP, we should expect to recover a signal with 10 nonzero terms in ~90% of instances for standard OMP and ~97% for enhanced OMP. A signal with 13 terms in ~50% of instances for standard OMP and ~76% for enhanced OMP.

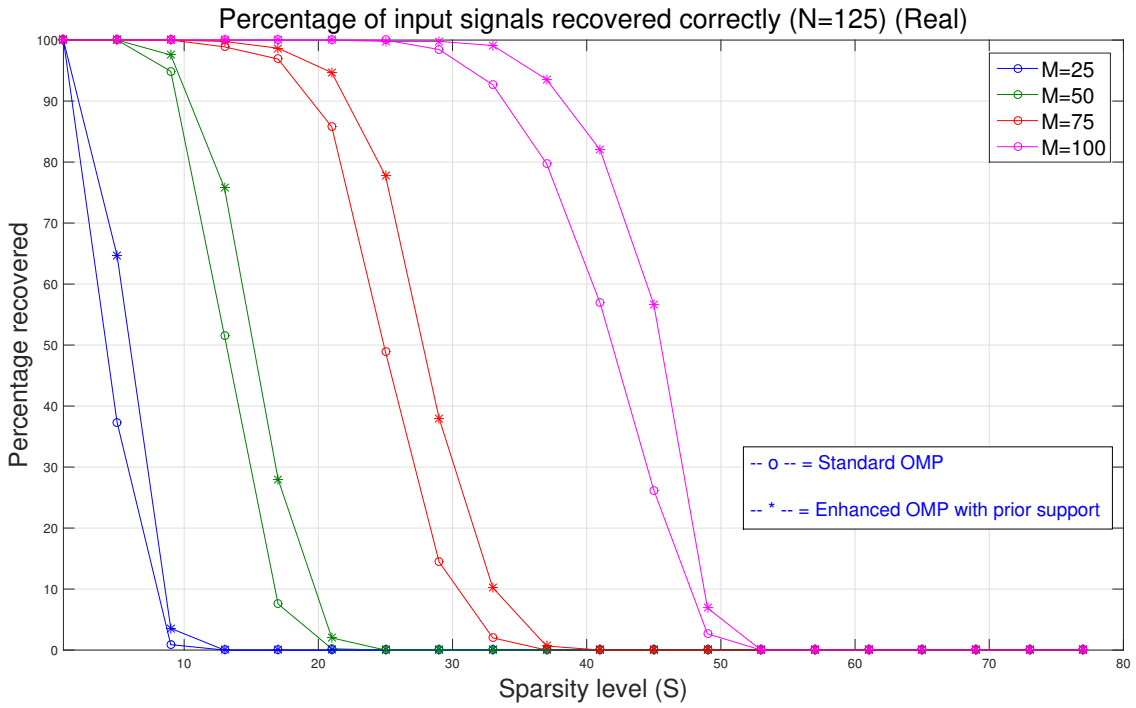

Figure 5.2: The percentage of 1000 input signals correctly recovered as a function of the sparsity level S for different number of measurements M in dimension N=125.

From the experimental results shown in Figure 5.2, given a number of nonzero terms in the vibration signal (sparsity level), the recovery probability increases using the proposed E-OMP algorithm in comparison to standard OMP. Or from another perspective, given a recovery probability, a reduced number of measurements are required to recover an $S-$sparse vibration signal using the enhanced OMP (with prior support) respect to standard OMP as exemplified in Table 5.1. Using less measurements without adding additional instructions or iterations to the selected signal recovery algorithm means faster processing time to recover the signal. More importantly, less measurements to recover a vibration signal means fewer transmissions from the wireless sensor nodes to the receiver which results in energy savings for the wireless vibration sensing system.

Table 5.2: The number of nonzero terms that can be recovered using M measurements (pieces of data) with >95% recovery probability in dimension $N = 125$ using standard OMP and the proposed E-OMP.

Standard OMP		Enhanced OMP	
Measurements (M)	Nonzero terms (S)	Measurements (M)	Nonzero terms (S)
25	3	25	5
50	10	50	12
75	20	75	23
100	33	100	38

The situation shown in Table 5.2 (based on Figure 5.2) highlights the importance of the enhanced OMP algorithm. For instance, in a given application the number of measurements to process at the receiver may be fixed to update a monitoring system at a fixed rate due to application requirements or constraints in memory, time or processing power. Table 5.2 shows that to recover a vibration signal with high probability (>95%) given a fixed number of measurements, the number of nonzero terms that can be recovered in that vibration signal is higher using the proposed algorithm than the standard OMP. In other words, more information about the signal (a greater number of frequency components) can be recovered using the enhanced OMP algorithm compared to standard OMP using the same number of measurements.

Power Savings

Energy efficiency is fundamental in this application. The power consumption is optimised when the signal is recovered using a reduced number of data packets. This occurs when the signal sparsity level of X_S increases at the sensor node at the expense of incrementing distortion followed by Compressed Sensing (CS). The sparsity level is induced at the wireless sensor nodes through a proposed adaptive thresholding algorithm described in Section 3.5 in Chapter 3. For instance, Table 5.3 shows the impact on power savings using thresholding (TH) and CS at the sensor node. TH=0% means that CS and TH are not used which implies that all data packets are

required at the receiver to recover the vibration signal. The results show a trade-off enabled by CS and TH. When the number of samples M are increased, more data packets need to be sent. Hence, frequency components of smaller magnitude may be recovered but power savings are reduced. However, this approach is robust to random packet loss during wireless transmission, providing the minimum number of data packets (column 4 in Table 5.3) are received at the base station.

Table 5.3: Power consumption savings using compressed sensing and adaptive signal thresholding.

TH (%)	Sinusoids (S)	Samples (M)	Data Packets	Power (mW)	Distortion (mg)	Power Savings (%)
0	125	125	10	28.8	0	0
13	29	116	9	25.92	29.02	10
14	23	92	7	20.16	31.25	30
15	19	76	6	17.28	33.49	40
18	9	36	3	8.64	40.18	70
20	6	24	2	5.76	44.65	80

The situation presented in Table 5.3 essentially gives an insight of the power savings that are obtained from using compressed sensing and adaptive thresholding (Algorithm 3.1 proposed and shown in Chapter 3). This is achieved by reducing the dimensionality of the frequency domain vibration signal. In other words, the vibration signal is thresholded to maintain the main spectral components while the components of low magnitude are discarded.

Also, Table 5.3 exhibits a point that is important in applications. For instance, assume that a wireless health monitoring system requires to perform vibration sensing and the wireless sensors are deployed in a noisy environment such as in a Gas Turbine Engine where random packet loss during wireless transmission is likely to occur. Consider the dimension of the original vibration signal for this scenario is $N = 125$. Therefore, assuming that the payload for each data packet contains between 12-13 samples, a total of 10 wireless data packet transmissions would be required to cover

the complete frequency spectrum for each FFT-based vibration signal. Assume that the selected wireless sensor node is autonomous and the energy generated through an energy harvester is only enough to allow 10 wireless transmissions. Or consider that the condition monitoring application requires to update the system at fixed intervals and there is only time available to process the data from 10 wireless transmissions. This scenario would require a 100% rate of success (0% packet loss) for transmission and reception of all wireless data packets to recover the vibration signal sent by the wireless sensor node. However, this situation is uncommon in most applications as random packet loss is likely to occur especially if the wireless communication occurs in an environment subject to interference, obstacles, electrical noise and so on. To mitigate this effect, the vibration signal is thresholded and encoded in compressive sensing samples. Suppose that the wireless transmission occurs in a harsh environment and there is about 40% random packet loss. For instance, from 10 wireless transmissions, only 6 are successful. The vibration signal can be thresholded in the wireless sensor node to contain the main 19 spectral components (sparsity level $S = 19$, as shown in row 4 in Table 5.3) and the vibration signal would still be recovered at the base station even if 4 packets out of 10 are lost randomly. Depending on the expected/detected packet loss percentage or the number of frequencies of interest for the application, the vibration signal can be conditioned and encoded accordingly to mitigate random packet loss effect or increase energy savings. The next section presents the reconstruction results of vibration signals from compressive sensing measurements using signal recovery methods after wireless data packet transmission.

Signal recovery from CS measurements

In Section 5.2, it was shown experimentally that the E-OMP requires less number of measurements for signal recovery than the standard OMP. In [124], Troop et. al demonstrate theoretically and empirically that OMP is an effective alternative to basis pursuit to recover signals from random measurements and conclude that OMP may be faster and easier to implement [124]. As shown in Figure 5.1, given a fixed sparsity level in a vibration signal, the recovery probability increases as more CS measurements are used for signal recovery.

The fundamental empirical question is to define the number of measurements M required to recover an S-sparse signal in $\mathbb{R}^N$ with high probability. It has been shown empirically [107] that a number of measurements M of about $4\times S$ (sparsity level) are sufficient for signal reconstruction. This four-to-one practical rule says that signal recovery can be exact if four incoherent measurements are taken per unknown non-zero term (S) [107]. However, in a real application, the number of measurements may vary. An example of signal reconstruction with/without consideration of this rule is shown in Figure 5.3.

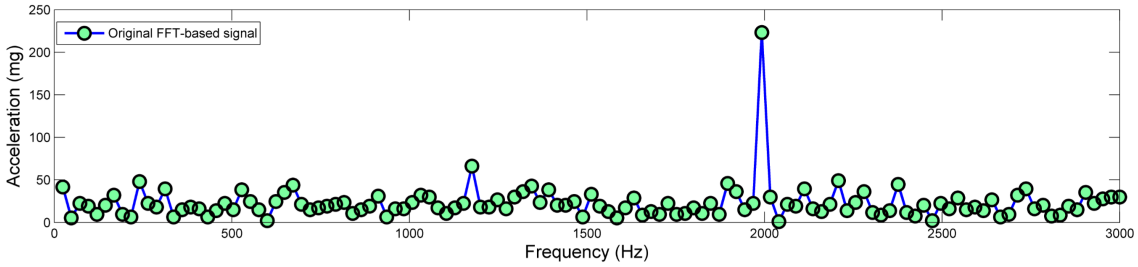

(a)

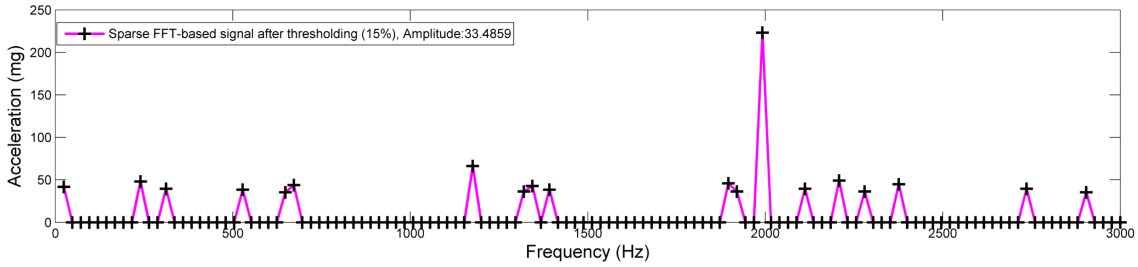

(b)

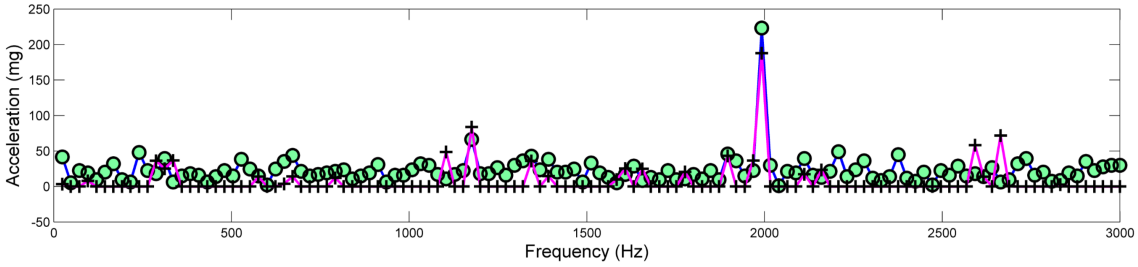

(c)

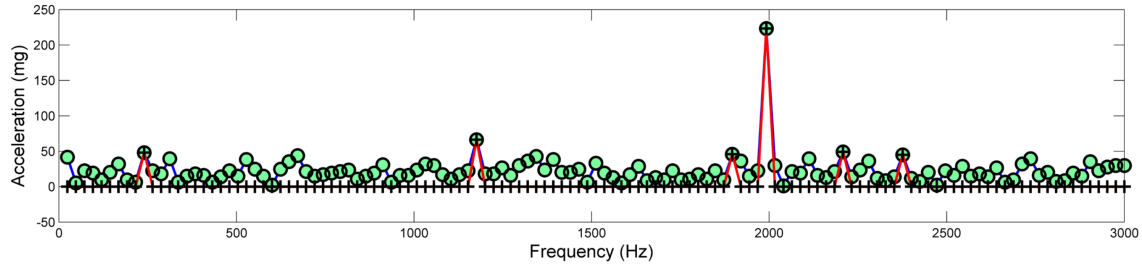

(d)

Figure 5.3: Signal recovery of an $S-$sparse signal with different sparsity levels. Showing a) Original FFT-based signal X from the vibration sensor, b) Thresholded FFT-based signal X_S with $S = 19$, c) Inaccurate signal reconstruction with $M = 24$ and $S = 19$. d) Accurate signal reconstruction with $M = 24$ and $S = 6$.

Under this scenario, the original vibration signal shown in Figure 5.3a (output from the vibration sensor) is sparsified initially to a level $S = 19$ to be used for CS (using the algorithm proposed and presented in Section 3.5). Assume that only about 25 measurements are used for signal recovery (after wireless vibration data transmission). It can be seen in Figure 5.3c, that the signal reconstruction is not accurate (circles and crosses do not match), this is because 25 measurements are not enough to recover an S-sparse signal $X_s$with 19 non-zero elements. In Figure 5.3d, the same number of measurements are used for signal recovery. However, the signal is perfectly recovered because the mentioned practical rule $M \sim 4S$ was used. Hence, the signal sparsity S was adjusted accordingly to produce an S-sparse signal X_s with 6 non-zero elements, resulting in accurate signal recovery.

5.3 Chapter Summary

This chapter presented the experimental setup to evaluate the wireless vibration sensing system. The hardware, vibration signals and experimental conditions used for signal recovery were described. Then, the performance of the standard OMP and the proposed E-OMP was evaluated and compared. Graphs showing the number of measurements required to recover a sparse signal with high probability for both algorithms were presented for performance comparison. It was shown that the proposed E-OMP uses less number of measurements compared to the standard OMP for a given rate of success. This was achieved by including prior information from the application as frequency support in the recovery algorithm. On the other hand, the power savings derived from performing local signal processing at the wireless sensor nodes were presented. This was achieved through frequency domain analysis, sparsity induction and compressed sensing at the sensor nodes prior to wireless transmission. Finally, examples of vibration signal recovery using a different number of measurements are shown to highlight the importance of using the required number of compressed sensing measurements to recover a sparse vibration signal with high accuracy.

Chapter 6

Conclusions and Future Work

6.1 Conclusions

The use of wireless vibration sensing systems allows to remotely monitor equipment health, perform preventive maintenance and improve system performance. Opposed to wired sensors, wireless functionality enables to monitor equipment remotely. Wireless sensor nodes can be installed into existing machinery infrastructure in the industrial sector or gas turbine engines to enable continuous wireless condition monitoring to evaluate equipment performance and conduct predictive maintenance. However, electrically noisy environments such as those found in gas turbine engines, affect wireless communication from the sensor nodes. Factors such as interference, obstacles, multipath propagation, noise from nearby machinery, and so on, contribute to random packet loss during wireless data transfer. This situation directly impacts system performance and power consumption in the sensor nodes as wireless retransmissions are derived from this effect. Moreover, energy conservation is vital in autonomous wireless sensor nodes as they are battery-powered or an energy harvester is used as the power source.

It was demonstrated that the proposed wireless sensor network meets specific requirements defined by Rolls-Royce for the wireless sensor infrastructure. More importantly, self-powered wireless vibration sensors were successfully demonstrated on a running Trent-1000 aeroengine running on a testbed to collect vibration data.

During this test, the wireless communication was affected by random packet loss causing multiple data packet retransmissions, unexpected time delays and affected data integrity. This problem is common on wireless networks, and packet loss is commonly minimised by boosting the signal, changing the communication channel or by removing interference. Hence, the features from the transceiver in the sensor nodes were used during the running aeroengine test in order to try to mitigate this problem. For instance, the output power was automatically increased in case of poor signal conditions to improve signal quality and frequency hopping was used to migrate among different channels to evade channels subject to interference or noise. However, the use of these techniques was not enough to deal with the packet loss problem.

A second issue was noted during the active gas turbine engine test, the signal recovery problem. This happened because the FFT-based vibration signal computed at the sensor node was distributed in several data packets and transmitted via wireless. Each data packet contained information about a portion of the frequency spectrum. At the receiver, it was required to receive all data packets for each independent vibration signal in order to recover it. Even if a single data packet was lost for a given vibration signal, it was not possible to determine the magnitude of the lost frequencies covered by that lost data packet. As a result, all incomplete FFTs were discarded during this test. These circumstances are not desirable as the resources of the wireless sensor nodes for vibration signal acquisition, conditioning, encoding, transmission, reception and decoding at the base station for all the received data packets are wasted, not counting any failed wireless retransmissions.

As mentioned throughout this thesis, in wireless vibration sensing applications it is critical to conserve energy and maintain a consistent system performance. That was the main reason for considering local signal processing at the sensor node. The spectral representation of the vibration signal through the Fast Fourier transform was used as the basis for signal compression using compressive sensing. Subsequently, the vibration signal dimension was reduced via a proposed adaptive thresholding algorithm presented in Chapter 3, that induced sparsity while maintaining the main spectral components. This approach resulted in signal compression and mitigation of the random packet loss problem.

For the signal recovery problem, the collected vibration data from the aeroengine

was used to generate prior information which was then used as frequency support for the novel E-OMP recovery algorithm presented in Chapter 4 and implemented at the receiver side for signal decoding. The characteristics of the collected data from the application were captured by estimating the probability density function using a proposed algorithm presented in Chapter 4. This prior was used as an additional input for the signal recovery algorithm which enhanced the performance of the standard OMP algorithm by using less number of measurements to recover the vibration signal sent by the wireless sensor nodes. This resulted in a reduction of data packet transmissions which maximises the useful life of sensor nodes, power efficiency and data integrity in the wireless vibration sensing system. Overall, the proposed framework encoded the data in a way that reduced the effect of random packet loss during wireless data transmission. Moreover, by including frequency support as prior information, allowed to reduce the number of measurements required for signal recovery. This resulted in increased energy savings while improving the performance of the wireless vibration sensing system for machine health monitoring.

6.2 Future Work

The framework suggested in this thesis allows handling the packet loss and signal recovery problem by exploiting the characteristics of the application. The idea proposed in this thesis about including an estimated probability density function from the application during signal recovery could be investigated and implemented in other signal recovery methods. Other avenues of future work identified in this thesis are presented as follows:

Minimisation of wireless retransmissions.- Decision making at the sensor node may include a cost function that considers power consumption per bit transmitted, power available (or generated power if an energy harvester is used), packet loss percentage, sparsity in the signal, signal dimension, desired recovery probability and the number of measurements required. This would encode the signal in the best possible way to increase the probabilities of successful recovery. As part of the communication protocol, every wireless data packet sent from a sensor node is acknowledged by the receiver. A notification is sent to the sensor node to confirm successful message reception. In many applications, the data packets are numbered so that if packet loss

occurs, then the lost packet can be requested by the receiver. By using compressive sensing, the order of the data packets is irrelevant. This approach is tolerant to random packet loss, the only requirement to recover an S-sparse signal from compressed sensing measurements is to have received the minimum number of measurements described in Chapter 3.7.2 regardless of the reception order. Therefore, it may not be required to acknowledge the reception of each data packet but to send a single notification from the receiver to the sensor node when enough measurements have been received to recover the sparse vibration signal. This could potentially increase power savings in the sensor nodes as they are active after each wireless transmission. When the sensor nodes transmit a message, they enter into listen mode waiting for a notification (acknowledgement) from the receiver that the packet was received. For instance, if an S-sparse vibration signal is to be sent from the wireless sensor node and an estimate of the number of M measurements needed to recover that signal is known, then the required transmissions T for that number of measurements M may be defined. This means that the acknowledgement mode may be deactivated for $T-1$ transmissions to save valuable energy. The impact on power conservation from this idea can be analysed and reported as future work.

Sensor Node Design.- The proposed framework in this research work did not alter the current hardware design of the sensor nodes and the vibration sensor selected by the Rolls-Royce sponsored University Technology Centre. The available features of the sensor node, the vibration sensor and the application were exploited to increase the wireless vibration sensing system performance without physical modifications to existing hardware. However, the speed of the vibration sensing system could be increased and the cost of the sensor nodes reduced by using a simpler vibration sensor. For instance, by selecting an accelerometer without embedded FFT analysis and perform compressed sensing directly without acquiring the complete signal, which means taking measurements directly over the signal in the time domain. However, a thorough evaluation of the new scenario would be required to determine if the existing hardware can be maintained. Moreover, benefits from local signal processing would not be exploited. Under this scenario, the sensor would not be able to take samples of a frequency bandwidth of interest as it would not include spectral analysis. Also, when a vibration signal is available in the frequency domain at the sensor node, event detection can be incorporated. For example, sending data only when the vibration signal exceeds a given magnitude. This allows data compression and reduction of

wireless transmissions, which would not be possible using a simple sensor without signal processing. These trade-offs are to be considered depending on the application.

Further improvement of the E-OMP recovery algorithm.- Preliminary experimentation suggests that the number of measurements may be further reduced if the choice of the optimal column in the measurement matrix at each iteration is not only based in the selection of the maximum correlated column to the residual in step 2. The suggested additional step involves increasing the search space among most correlated columns. The signal recovery performance is likely to improve when the search space is augmented. For instance, in the standard OMP, it is expected to recover an $S-$sparse signal after S iterations with the final residual close to zero. The objective of this greedy algorithm is to find the right set of S columns of the measurement matrix Φ that participated in the measurement vector y. When the residual or error is not close to zero after S iterations, it means that one or more columns were incorrectly chosen during the execution of the algorithm. It was noted that in most cases even if the algorithm fails (error between original and recovered signal exceed a given value), the recovered signal matches most of the active frequency components in the original sparse vibration signal, this is because the majority of the columns were correctly identified. This motivated to increase the search space, it was observed that this led to an accurate signal recovery in the majority of the cases. However, this needs to be further explored to define the implications, the cost added from modifying the recovery algorithm, theoretical proof of optimal search space and so on. After solving this issue, the performance of that algorithm may be compared to other signal recovery methods such as $L1$-minimisation algorithms based on $L1$ norm. Although these algorithms require a smaller number of measurements than standard OMP, the computation is intensive as it is based on convex optimisation. As reported in the literature, OMP is an effective alternative to basis pursuit for signal recovery of sparse signals and may be faster and easier to implement. Moreover, the OMP structure is clear and allowed to include prior information from the application in the form of an estimated PDF as an additional input. It may worth exploring if a PDF can be included in other signal recovery algorithms. Then, a study comparing different signal recovery methods in terms of required processing power, the number of measurements, speed and performance would be valuable as the most suitable can be selected depending on the requirements of the application.

Bibliography

[1] B. Lu, T. G. Habetler, and R. G. Harley, "A survey of efficiency estimation methods of in-service induction motors with considerations of condition monitoring," *in Proc. 2005 International Electric Machine and Drive Conference (IEMDC'05)*, May 2005, pp.1365-1372.

[2] S. K. Korkua and W.-J. Lee, "Wireless sensor network for performance monitoring of electrical machine," *in Proc. North Amer. Power Symp.*, Starkville, MS, USA, Oct. 2009, pp. 1–5.

[3] A. Willig, K. Matheus, and A. Wolisz, "Wireless technology in industrial networks," *Proc. IEEE*, vol. 93, no. 6, pp. 1130–1151, Jun. 2005.

[4] A. Willig, "Recent and Emerging Topics in Wireless Industrial Communications: A Selection," *IEEE Trans. Industrial Informatics*, vol. 4, no. 2, pp. 102-124, May 2008.

[5] S. Kim, R. Fonseca, D. Culler, "Reliable transfer on wireless sensor networks", *Proc. IEEE SECON*, pp. 449-459, 2004-Oct.-47.

[6] W. Chen and I. Wassell, "Energy-efficient signal acquisition in wireless sensor networks: A compressive sensing framework," *IET Wireless Sensor Syst.*, vol. 2, no. 1, pp. 1–8, Mar. 2012.

[7] V. Jeli, M. Magno, D. Brunelli, V. Bilas, and L. Benini, "An Energy Efficient Multimodal Wireless Video Sensor Network with eZ430-RF2500 modules," *in Proc. 5th Int. Conf. Pervasive Comput. Appl. (IPCA)*, pp. 161–166, 2010.

[8] S. Lacey, "An overview of bearing vibration analysis," *Maintenance & Asset Management*, vol. 23, no. 6, pp. 32-42, 2008.

[9] Patidar, S. and P.K. Soni, "An Overview on Vibration Analysis Techniques for the Diagnosis of Rolling Element Bearing Faults," *in International Journal of Engineering Trends and Technology (IJETT)*, vol. 4, no. 5, 2013.

[10] H. Yang, J. Mathew, and L. Ma, "Intelligent diagnosis of rotating machinery faults - A review," *Conference on Systems Integrity and Maintenance*, ACSIM 2002, Cairns, Australia, 2002.

[11] N. A. Othman, N. S. Damanhuri, and V. Kadirkamanathan, "The Study of Fault Diagnosis in Rotating Machinery," *Cspa: 2009 5th International Colloquium on Signal Processing and Its Applications*, Proceedings, pp. 69-74, 2009.

[12] A. K. S. Jardine, D. Lin, and D. Banjevic, "A review on machinery diagnostics and prognostics implementing condition-based maintenance," *Mechanical Systems and Signal Processing*, vol. 20, pp. 1483-1510, 2006.

[13] R. K. Mobley, *An Introduction to Predictive Maintenance*, MA, Burlington:Elsevier Butterworth-Heinemann, 2002.

[14] Gridhar, P. and C. Scheffer, *Practical machinery vibration analysis and predictive maintenance*, Elsevier, 2004.

[15] A. Heng, S. Zhang, A. C. C. Tan, and J. Mathew, "Rotating machinery prognostics: State of the art, challenges and opportunities," *Mechanical Systems and Signal Processing*, vol. 23, pp. 724-739, Apr 2009.

[16] J. S. Mitchell, *Introduction to Machinery Analysis and Monitoring*, Tulsa:Pennwell, 1993.

[17] J. M. Robichaud, "Reference standards for vibration monitoring and analysis," *Bretech Engineering Ltd.*, Saint John, NB Canada, 2004.

[18] Q. Liu and H. Wang, "A case study on multisensor data fusion for imbalance diagnosis of rotating machinery," *Artificial Intelligence For Engineering Design Analysis and Manufacturing*, vol. 15, pp. 203-210, 2001.

[19] H.-C. Lee, Y.-C. Chang, Y.-S. Huang, "A reliable wireless sensor system for monitoring mechanical wear-out of parts", *IEEE Trans. Instrum. Meas.*, vol. 63, no. 10, pp. 2488-2497, Oct. 2014.

[20] A. Villanueva-Marcocchio and D. G. Holtby, "Wireless Sensor Network Proof of Concept Report SILOETII/Shef/R/14401," *Rolls-Royce*, Sheffield UTC, 2014.

[21] A. Villanueva-Marcocchio, B. Ll. Jones, "A Low-Power Wireless Vibration Sensing Framework for Machine Health Monitoring using a Packet Loss Tolerant Approach", in *ISCM 1st World Congress on Condition Monitoring*, London UK, 13th -16th June 2017.

[22] R. B. Randall, *Vibration-Based Condition Monitoring: Industrial Aerospace and Automotive Applications*, Chichester, U.K.:Wiley, 2011.

[23] K. Islam, W. Shen, S. Member, and X. Wang, "Wireless Sensor Network Reliability and Security in Factory Automation : A Survey," *IEEE Trans. Syst. Man, Cybern. - Part C Appl. Rev.*, vol. 42, no. 6, pp. 1243-1256, 2012.

[24] K. S. Low, W. Nu, N. Win, and M. J. Er, "Wireless Sensor Networks for Industrial Environments," *Proc. 2005 Int. Conf. Comput. Intell. Model. Control Autom.*, 2005.

[25] I. F. Akyildiz, W. Su, Y. Sankarasubramaniam, and E. Cayirci, "Wireless sensor networks : a survey," *Comput. Networks*, vol. 38, no. 4, pp. 393-422, 2002.

[26] Advanced Manufacturing Office, "Industrial wireless technology for the 21st century," *Tech. report, U.S. Dep. Energy*, 2002.

[27] J. E. Mitchell, X. Dai, P. Dutta, I. Glover, Y. Yang, W. Schiffers, R. Atkinson, J. Strong, K. Sasloglou, and I. Panella, "Development and

validation of a simulator for wireless data acquisition in gas turbine engine testing," *IET Wirel. Sens. Syst.*, vol. 3, no. 3, pp. 183–192, Sep. 2013.

[28] Z. Wang, F. Bouwens, R. Vullers, F. Petre, and S. Devos, "Energy-Autonomous Wireless Vibration Sensor for Condition-based Maintenance of Machinery," *IEEE Sensors*, pp. 11-14, 2011.

[29] V. Raja, A. Sanchez, B. Van der Zwaag, N. Meratnia, and P. Havinga, "Energy-Efficient On-node Signal Processing for Vibration Monitoring," in *Intelligent Sensors, Sensor Networks and Information Processing (ISSNIP)*, 2014, no. April, pp. 21–24.

[30] K. Sasloglou, I. A. Glover, P. Dutta, and R. Atkinson, "A Channel Model for Wireless Sensor Networks in Gas Turbine Engines," in *Loughborough Antennas & Propagation*, 2009, vol. 2, pp. 15–18.

[31] P. D. Mcfadden and J. D. Smith, "Vibration monitoring of rolling element bearings by the high- frequency resonance technique- a review," *Vib. Monit. Roll. Bear.*, vol. 17, no. 1, pp. 3–10, 1984.

[32] J. C. Chan and P. W. Tse, "A Novel , Fast , Reliable Data Transmission Algorithm for Wireless Machine Health Monitoring," *IEEE Trans. Reliab.*, vol. 58, no. 2, pp. 295–304, 2009.

[33] Jun Zheng and Abbas Jamalipour, "Introduction to Wireless Sensor Networks", *Wireless Sensor Networks: A Networking Perspective*, Wiley-IEEE Press, 2009.

[34] C. Y. Chong, S. Kumar, "Sensor networks: Evolution opportunities and challenges", *Proc. IEEE*, vol. 91, no. 8, pp. 1247-1256, Aug. 2003.

[35] I. Akyildiz, W. Su, Y. Sankarasubramniam, E. Cayirci, "A survey on sensor networks", *IEEE Commun. Mag.*, no. 8, pp. 102-114, Aug. 2002.

[36] D. Estrin, D. Culler, K. Pister, G. Sukhatme, "Connecting the physical world with pervasive networks", *IEEE Pervasive Comput.*, vol. 1, no. 1, pp. 59-69, 2002.

[37] ABB, "Condition Monitoring WiMon 100 Wireless Vibration Sensor," 2010.

[38] Inertia Technology, "V-Mon 4000 series product datasheet," 2013.

[39] Prftechnik, "Vibconnect RF Wireless Condition Monitoring," 2013.

[40] ICON Research, "WiVib Wireless Monitoring - Operating Manual," 2009.

[41] I. Cisco Systems, "Integrating an Industrial Wireless Sensor Network with Your Plant's Switched Ethernet and IP Network," pp. 1–18, 2009.

[42] T. Kevan, "Upgrading a steel mill wirelessly," in *Wireless Sens. Mag.*, 2005.

[43] T. Kevan, "Shipboard machine monitoring for predictive maintenance," in *Wireless Sens. Mag.*, 2006.

[44] L. Krishnamurthy, R. Adler, P. Buonadona, J. Chhabra, M. Flanigan, N. Kushalnagar, L. Nachman, and M. Yarvis, "Design and deployment of industrial sensor networks: Experiences from a semiconductor plant and the north sea," *3rd Int. Conf. Embed. Netw. Sens. Syst*, pp. 64–75, 2005.

[45] G. Gbur, W. Wier, T. Bark, and B. Baldwin, "Wireless vibration monitoring in a US coal-fired plant," *Insight*, vol. 48, no. 8, 2006.

[46] V. Jagannath and B. Raman, "WiBeaM : Wireless Bearing Monitoring System," *Proc. 2nd Int. Conf. Commun. Syst. Softw. Middlew.*, pp. 1–8, 2007.

[47] B. Lu, T. G. Habetler, R. G. Harley, J. A. Gutierrez, and D. B. Durocher, "Energy Evaluation Goes Wireless," *IEEE Industry Applications Magazine*, pp. 17–23, 2007.

[48] V. Sundararajan, A. Redfern, and P. Wright, "Distributed monitoring of steady-state system performance using wireless sensor networks," in *ASME Int. Mech. Eng. Congr.*, 2004.

[49] A. K. S. Jardine, D. Lin, and D. Banjevic, "A review on machinery diagnostics and prognostics implementing condition-based maintenance," *Mech. Syst. Signal Process.*, vol. 20, no. 7, pp. 1483–1510, Oct. 2006.

[50] P. Wright, D. Dornfeld, R. Hillaire, and N. Ota, "A Wireless Sensor for Tool Temperature Measurement and its Integration within a Manufacturing System," *Trans. North Am. Manuf. Res. Inst.*, vol. 34, 2006.

[51] K. Kunert, M. Jonsson, and E. Uhlemann, "Exploiting Time and Frequency Diversity in IEEE 802.15.4 Industrial Networks for Enhanced Reliability and Throughput," in *IEEE Conf. Emerging Technologies and Factory Automation (ETFA)*, 2010, pp. 1–9.

[52] M. Mickiewicz and D. Koscielnik, "Modeling End-to-End Reliability in Best-Effort Networked Embedded Systems," in *IEEE Conf. Emerging Technologies and Factory Automation (ETFA)*, 2010, pp. 1–4.

[53] P. Park, C. Fischione, A. Bonivento, K. H. Johansson, and A. L. Sangiovanni-vincentelli, "Breath : An Adaptive Protocol for Industrial Control Applications Using Wireless Sensor Networks," *IEEE Trans. Mob. Comput.*, vol. 10, no. 6, pp. 821-838, 2011.

[54] J. Jasperneite and P. Neumann, "Measurement, analysis and modeling of real-time source data traffic in factory communication systems," in *Factory Communication Systems*, 2000, pp. 327-333.

[55] J. R. Moyne and D. M. Tilbury, "The Emergence of Industrial Control Networks for Manufacturing Control , Diagnostics , and Safety Data," *Proc. IEEE*, vol. 95, no. 1, pp. 29-47, 2007.

[56] J. Thomesse, "Fieldbus Technology in Industrial Automation," *Proc. IEEE*, vol. 93, no. 6, pp. 1073-1101, 2005.

[57] D. Siegel, C. Ly, J. Lee, "Methodology and framework for predicting helicopter rolling element bearing failure", *IEEE Trans. Rel.*, vol. 61, no. 4, pp. 846-857, Dec. 2012.

[58] S. Khan, S. Atamturktur, M. Chowdhury, M. Rahman, "Integration of Structural Health Monitoring and Intelligent Transportation Systems for Bridge Condition Assessment: Current Status and Future Direction", *IEEE Transactions on Intelligent Transportation Systems*, no. 99, pp. 1-16, 2016.

[59] Manum, H.; Schmid, M. "Monitoring in a harsh environment" *Control &Automation*, vol. 18, no. 5, pp. 22-27, 2007.

[60] M. Cerullo, G. Fazio, M. Fabbri, F. Muzi, G. Sacerdoti, "Acoustic signal processing to diagnose transiting electric trains", *IEEE Trans. Intell. Transp. Syst.*, vol. 6, no. 2, pp. 238-243, Jun. 2005.

[61] Y. Dai, Y. Xue, J. Zhang, "Vibration-based milling condition monitoring in robot-assisted spine surgery", *IEEE/ASME Trans. Mechatronics*, vol. 20, no. 6, pp. 3028-3039, Dec. 2015.

[62] F. Tauro, C. Pagano, P. Phamduy, S. Grimaldi, M. Porfiri, "Large-scale particle image velocimetry from an unmanned aerial vehicle", *IEEE/ASME Trans. Mechatronics*, vol. 20, no. 6, pp. 3269-3275, Dec. 2015.

[63] T. Oepomo, "Line replaceable unit (LRU) analysis in the space shuttle orbiter electrical power system", *IEEE Trans. Power App. Syst.*, vol. PAS-104, no. 12, pp. 3501-3509, Dec. 1985.

[64] P. Sloetjes and A. de Boer, "Vibration reduction and power generation with piezoceramic sheets mounted to a flexible shaft," *Journal of Intelligent Material Systems and Structures*, vol. 19, pp. 25-34, Jan 2008.

[65] D. Xiang, L. Ran, P. J. Tavner, S. Yang, "Control of a doubly-fed induction generator in a wind turbine during grid fault ride-through", *IEEE Trans. Energy Convers.*, vol. 21, no. 3, pp. 652-662, Sep. 2006.

[66] D. Ludois, J. Reed, K. Hanson, "Capacitive power transfer for rotor field current in synchronous machines", *IEEE Trans. Power Electron.*, vol. 27, no. 11, pp. 4638-4645, Nov. 2012.

[67] F. A. Bejarano, Y. Jia, and F. Just, "Crack Identification of A Rotating Shaft with Integrated Wireless Sensor," *International Journal On Smart Sensing and Intelligent Systems*, vol. 2, pp. 564-578, 2009.

[68] L. Baghli, J. F. Pautex, and S. Mezani, "Wireless Instantaneous Torque measurement, Application to Induction Motors," in *XIX International Conference on Electrical Machines - ICEM*, Rome, 2010.

[69] J. C. Chan, P. W. Tse, "A novel fast reliable data transmission algorithm for wireless machine health monitoring", *IEEE Trans. Rel.*, vol. 58, no. 2, pp. 295-304, Jun 2009.

[70] N. Bachschmid, P. Pennacchi, E. Tanzi, and A. Vania, "Accuracy of Modelling and Identification of Malfunctions in Rotor Systems: Experimental Results," *Journal of the Brazilian Society of Mechanical Sciences*, vol. 22, 2000.

[71] A. Sekhar, "Model-based identification of two cracks in a rotor system," *Mechanical Systems and Signal Processing*, vol. 18, pp. 977-983, Jul 2004.

[72] J. K. Sinha, M. I. Friswell, and S. Edwards, "Simplified models for the location of cracks in beam structures using measured vibration data," *Journal of Sound and Vibration*, vol. 251, pp. 13-38, 2002.

[73] K. R. Mobley, *An introduction to predictive maintenance*, Butterworth-Heinemann., 2002.

[74] C. Scheffer, P*ractical machinery vibration analysis and predictive maintenance:* Newnes, 2004.

[75] J. Stephens, "Advances in signal processing technology for electronic warfare", *IEEE Aerospace and Electronic Systems Magazine*, pp. 31-38, Nov. 1996.

[76] S. Haykin, "Signal processing: Where physics and mathematics meet", *IEEE Signal Processing Mag.*, vol. 18, no. 4, pp. 6-7, July 2001.

[77] F.-L. Luo, W. Williams, R. M. Rao, R. Narasimha, M. Montpetit, "Trends in signal processing applications and industry technology," *IEEE Signal Process. Mag.*, vol. 29, no. 1, pp. 172-174 and 184, Jan. 2012.

[78] L. Tan, *Digital Signal Processing - Fundamentals and Applications*, Elsevier, 2008.

[79] J. D. Broesch, *Digital Signal Processing*, Newnes, 2009.

[80] D. Donoho, "Compressed sensing," *IEEE Trans. Inf. Theory*, vol. 52, no. 4, pp. 1289–1306, Apr. 2006.

[81] C. W. Tan, S. Park, "Design of accelerometer-based inertial navigation systems", *IEEE Trans. Instrum. Meas.*, vol. 54, no. 6, pp. 2520-2530, Dec. 2005.

[82] D. Chwa, J. Y. Choi, "Observer-based control for tail-controlled skid-to-turn missiles using a parametric affine model", *IEEE Transactions on Control Systems Technology*, vol. 12, no. 1, pp. 335-347, Jan. 2004.

[83] A. Sabato, C. Niezrecki, G. Fortino, "Wireless MEMS-based accelerometer sensor boards for structural vibration monitoring: A review", *IEEE Sensors J.*, vol. 17, no. 2, pp. 226-235, Jan. 2017.

[84] P. Gupta, T. Dallas, "Feature selection and activity recognition system using a single triaxial accelerometer", *IEEE Trans. Biomed. Eng.*, vol. 61, no. 6, pp. 1780-1786, Jun. 2014.

[85] J. P. Barton, S. J. Watson, "Analysis of electrical power data for condition monitoring of a small wind turbine", *IET Renew. Power Gener.*, vol. 7, no. 4, pp. 341-349, Jul. 2013.

[86] M. Tanaka, "An industrial and applied review of new MEMS devices features," *Microelectronic Engineering*, vol. 84, pp. 1341-1344, Aug 2007.

[87] R. Kok and C. Furlong, "Development and characterization of a wireless mems inertial system for health monitoring of structures part 2:

Applications of the developed system," *Experimental Techniques*, vol. 29, pp. 50-53, Nov-Dec 2005.

[88] R. Kok and C. Furlong, "Development and characterization of a wireless MEMS inertial system for health monitoring of structures, part 1: description of sensor and data acquisition system," *Experimental Techniques*, vol. 29, p. 4, 2005.

[89] C. Ratcliffe, D. Heider, R. Crane, C. Krauthauser, M. K. Yoon, and J. W. Gillespie, "Investigation into the use of low cost MEMS accelerometers for vibration based damage detection," *Composite Structures*, vol. 82, pp. 61-70, Jan 2008.

[90] S. Thanagasundram and F. S. Schlindwein, "Comparison of integrated micro-electrical-mechanical system and piezoelectric accelerometers for machine condition monitoring," *Proceedings of the Institution of Mechanical Engineers Part C-Journal of Mechanical Engineering Science*, vol. 220, pp. 1135-1146, Aug 2006.

[91] A. E. Badri and J. K. Sinha, "Dynamics of MEMS accelerometer," presented at the 17th International Congress on Sound and Vibration, Cairo, 2010.

[92] N. Chaimanonart and D. Young, "Remote RF powering system for wireless MEMS strain sensors," *IEEE Sensors Journal*, vol. 6, pp. 484-489, Apr 2006.

[93] V. Varadan, V. Varadan, and H. Subramanian, "Fabrication, characterization and testing of wireless MEMS-IDT based microaccelerometers," *Sensors and Actuators a-Physical*, vol. 90, pp. 7-19, May 2001.

[94] S. Sharma, D. Kumar, and K. Kishore, "A Review on Topologies and Node Architecture," vol. 1, no. 2, pp. 19-25, 2013.

[95] B. Pannetier, J. Dezert, and G. Sella, "Multiple target tracking with wireless sensor network for ground battlefield surveillance," in *Proceedings of the 17th International Conference on Information Fusion*, pp. 1-8, July 2014.

[96] M. Navarro, Y. Li, and Y. Liang, "Energy Profile for Environmental Monitoring Wireless Sensor Networks," in *Proceedings of the IEEE Colombian Conference on Communications and Computing (COLCOM)*, pp. 1-6, 2014.

[97] P. Jiang, H. Ren, L. Zhang, Z. Wang, and A. Xue, "Reliable Application of Wireless Sensor Networks in Industrial Process Control," *Proc. 6th World Congr. Intell. Control Autom.*, pp. 99-103, 2006.

[98] S. Babu and S. Raju, "Routing Protocols in Wireless Sensor Networks A Survey," Int. J. Innov. Technol. Explor. Eng., vol. 3, no. 12, pp. 3-5, 2014.

[99] J. A. Stankovic, Q. Cao, T. Doan, L. Fang, Z. He, R. Kiran, S. Lin, S. Son, R. Stoleru, and A. Wood, "Wireless Sensor Networks for In-Home Healthcare : Potential and Challenges," *Proc. of the Workshop on High Confidence Medical Devices Software and Systems*, June 2005.

[100] E. Stattner, N. Vidot, P. Hunel, and M. Collard, "Wireless Sensor Network for Habitat Monitoring : A Counting Heuristic," in *12th IEEE International Workshop on Wireless Local Networks*, pp. 753-760, 2012.

[101] M. Spadacini, S. Savazzi, and M. Nicoli, "Wireless home automation networks for indoor surveillance: technologies and experiments," *EURASIP J. Wirel. Commun. Netw.*, vol. 2014, no. 1, p. 6, 2014.

[102] H. Bai, M. Atiquzzaman, and D. Lilja, "Wireless Sensor Network for Aircraft Health Monitoring," *Proc. First Int. Conf. Broadband Networks*, 2004.

[103] M. Chu, H. Haussecker, and F. Zhao, "Scalable Information-Driven Sensor Querying and Routing for ad hoc Heterogeneous Sensor Networks," *Xerox Palo Alto Res. Cent. Tech. Rep.*, 2001.

[104] A. Manjeshwar, D.P. Agrawal, " TEEN: A Routing Protocol for Enhanced Efficiency in Wireless Sensor Networks", *Proc. Int Parallel and Distributed Processing Symp. (IPDPS)*, Apr. 2001.

[105] A.M.Abdulghani and E.R.Villegas. "Compressive sensing: From compressing while sampling to compressing and securing while sampling," In *Annual International Conference of the IEEE EMBS Buenos Aires*, volume 32, pages 1127-1130, 2010.

[106] M. S. Asif, F. Fernandes, J. Romberg, "Low-complexity video compression and compressive sensing", *Proc. ACSSC*, pp. 579-583, Nov. 2013.

[107] E.J.Candes and M.B.Wakin, "An introduction to compressive sampling," *IEEE Signal Processing Magazine*, pages 21-30, March 2008.

[108] F. Esqueda, S. Bilbao, V. Valimaki, "Aliasing reduction in clipped signals", *IEEE Trans. Signal Process.*, vol. 60, no. 20, pp. 5255-5267, Oct. 2016.

[109] J. Romberg, "Imaging via compressive sampling," *IEEE Signal Process. Mag.*, vol. 25, no. 2, pp. 14-20, Mar. 2008.

[110] E.J.Candes. "Compressive sampling," In *Proc. of the International Congress of Mathematicians*, 2006.

[111] J.Romberg and M.B.Wakin, "Compressed sensing: A tutorial IEEE statistical signal processing workshop madison," *IEEE Statistical Signal Processing Work-shop, Georgia Tech University of Michigan*, 2007.

[112] C. Karakus, A. C. Gurbuz, and B. Tavli, "Analysis of energy efficiency of compressive sensing in wireless sensor networks," *IEEE Sensors J.*, vol. 13, no. 5, pp. 1999-2008, May 2013.

[113] D. Donoho, "Compressed sensing", *IEEE Trans. Inform. Theory*, vol. 52, no. 4, pp. 1289-1306, Apr. 2006.

[114] T. Chernyakoba, Y. C. Eldar, "Fourier-domain beamforming: The path to compressed ultrasound imaging", *IEEE Trans. Ultrason. Ferroelect. Freq. Control*, vol. 61, no. 8, pp. 1252-1267, May 2014.

[115] A. N. O'Donnell, J. L. Wilson, D. M. Koltenuk, R. J. Burkholder, "Compressed sensing for radar signature analysis", *IEEE Trans. Aerosp. Electron. Syst.*, vol. 49, no. 4, pp. 2631-2939, Oct. 2013.

[116] M. Lustig, D.L. Donoho, J. M. Santos, J. M. Pauly, "Compressed sensing MRI", *IEEE Signal Process. Mag.*, vol. 25, no. 2, pp. 72-82, Mar. 2008.

[117] R. Baraniuk, "Compressed sensing", *IEEE Signal Process. Mag.*, vol. 24, no. 4, pp. 14-20, Jul. 2007.

[118] A. S. Bandeira, E. Dobriban, D. G. Mixon, W. F. Sawin, "Certifying the restricted isometry property is hard", *IEEE Trans. Inf. Theory*, vol. 59, no. 6, pp. 3448-3450, Jun. 2013.

[119] M. F. Duarte, M. A. Davenport, D. Takhar, J. N. Laska, T. Sun, K. F. Kelly, R. G. Baraniuk, "Single-pixel imaging via compressive sampling", *IEEE Signal Processing Mag.*, vol. 25, no. 2, pp. 83-91, 2008.

[120] J.-L. Starck, F. Murtagh, J. Fadili, Sparse Image and Signal Processing: Wavelets and Related Geometric Multiscale Analysis, Cambridge, U.K.:Cambridge Univ. Press, 2015.

[121] E. J. Candes and T. Tao, "Decoding by linear programming," *IEEE Trans. Inf. Theory*, vol. 51, no. 12, pp. 4203-4215, Dec. 2005.

[122] X. Chen, E. Sobhy and B. Sadler, "A sub-Nyquist rate compressive sensing data acquisition front-end," *IEEE J. Emerg. Sel. Topics Circuits Syst.*, vol. 2, no. 3, pp. 542-551, Sep. 2012.

[123] S. Chen, D. Donoho, and M. Saunders, "Atomic decomposition by basis pursuit," *SIAM J. on Sci. Comp.*, vol. 20, no. 1, pp. 33-61, 1998.

[124] J. A. Tropp and A. C. Gilbert, "Signal recovery from random measurements via orthogonal matching pursuit," *IEEE Trans. Inf. Theory*, vol. 53, no. 12, pp. 4655–4666, Dec. 2007.

[125] E.J. Candes and T. Tao, "Near-optimal signal recovery from random projections: Universal encoding strategies", *IEEE Trans. Inf. Theory*, vol. 52, no. 12, pp. 5406-5425, Dec. 2006.

[126] S. Tarannum, "Energy conservation challenges in wireless sensor networks: A comprehensive study", *Wireless Sens. Netw.*, vol. 2, no. 6, pp. 483-491, Jun. 2010.

[127] W. K. G. Seah, Z. A. Eu, H.-P. Tan, "Wireless sensor networks powered by ambient energy harvesting (WSN-HEAP)—Survey and challenges", *Proc. 1st Int. Conf. Wireless VITAE*, pp. 1-5, 2009-May.

[128] M. Banitalebi-Dehkordi, J. Abouei, K. N. Plataniotis, "Compressive-sampling-based positioning in wireless body area networks", *IEEE J. Biomedical and Health Informatics*, vol. 18, no. 1, pp. 335-344, 2014.

[129] Z. Zou, Y. Bao, H. Li, B. F. Spencer, J. Ou, "Embedding compressive sensing-based data loss recovery algorithm into wireless smart sensors for structural health monitoring", *IEEE Sens. J.*, vol. 15, no. 2, pp. 797-808, Feb. 2015.

[130] E. E. Egbogah, A. O. Fapojuwo, "Achieving Energy Efficient Transmission in Wireless Body Area Networks for the Physiological Monitoring of Military Soldiers", *Military Communications Conference IEEE MILCOM 2013*, pp. 1371-1376, 2013.

[131] A. Gamage, "System Requirement Document for SILOET II Advanced Measurement Technique - Wireless Sensor Infrastructure, DNS190661," *Rolls-Royce*, 2013.

[132] Texas Instruments, "EZ430-RF2500 Development Tool Users Guide," 2009. [Online]. Available: www.ti.com/lit/ug/slau227f/slau227f.pdf.

[133] Texas Instruments, "MSP430 Ultra-Low-Power Microcontrollers," 2014.

[134] Texas Instruments, "CC2500 Low Cost Low Power 2.4 GHz RF Transceiver," 2014.

[135] Würth Elektronik, "Chip Antenna Specification," 2004.

[136] Analog Devices, "ADIS16227 Datasheet- Digital Triaxial Vibration Sensor with FFT Analysis and Storage," 2010. [Online]. Available: http://www.analog.com/media/en/technical-documentation/data-sheets/ADIS16227.pdf.

[137] A. M. R. Dixon, E. G. Allstot, D. Gangopadhyay, D. J. Allstot, "Compressed sensing system considerations for ECG and EMG wireless

bio-sensors", *IEEE Trans. Biomed. Circuits Syst.*, vol. 6, no. 2, pp. 156-166, May 2012.

[138] D.S. Taubman and M.W. Marcellin, *JPEG 2000: Image Compression Fundamentals, Standards and Practice*. Norwell, MA: Kluwer, 2001.

[139] M. Davenport, M. Duarte, Y. Eldar, and G. Kutyniok, "Introduction to compressed sensing," in *Compressed Sensing: Theory and Applications*. Cambridge, U.K.: Cambridge Univ. Press, pp. 1-68, 2011.

[140] Zaixing HE, and Takahiro Ogawa, "The Simplest Measurement Matrix for Compressed Sensing of Natural Images,", *IEEE 17th International Conference on Image Processing*. pp. 4301-4304, 2010.

[141] J. Pant, W. Lu, and A. Antoniou, "Recovery of sparse signals from noisy measurements using a regularized least-squares algorithm," *PacRim 2011*, pp. 48-53, Aug. 2011.

[142] E. Uysal-Biyikoglu, B. Prabhakar, and A.E. Gamal, "Energy-Efficient Packet Transmission over a Wireless Link," *IEEE/ACM Trans. Networking*, vol. 10, no. 4, pp. 487-499, 2002.

[143] B. W. Silverman, *Density Estimation for Statistics and Data Analysis*. Chapman and Hall, 1986, vol. 26.

[144] Fan Yang, Shengquian Wanf, Chengzhi deng, "Compressive Sensing of Image Reconstruction using Multi-wavelet Transforms," *IEEE International Conference*, pp. 702-705, 2010.

[145] S. Kunis, h. Rauhat, "Random sampling of sparse trigonometric polynomials II: Orthogonal matching pursuit versus basis pursuit," *Applied and Computational Harmonic Journal*, vol. 22, 2007.

[146] J. J. Saucedo-Dorantes and A.G. Garcia-Dorantes, "Reliable methodology for gearbox wear monitoring based on vibration analysis," *in Proc. 40th Conf. IEEE Ind. Electron.* Soc., 2014.

[147] A. W. Bowman and A. Azzalini. *Applied Smoothing Techniques for Data Analysis: The Kernel Approach with S-Plus Illustrations*. New York:Oxford University Press, 1997.

[148] X. Li, X. Lan, M. Yang, J. Xue, and N. Zheng, "Efficient lossy compression for compressive sensing acquisition of images in compressive sensing imaging systems," *Sensors*, vol. 14, no. 12, pp. 23398–23418, 2014.

[149] Arias-Castro, E.; Eldar, Y. "Noise folding in compressed sensing". *IEEE Signal Process. Lett.*, vol. 18, pp. 478–481, 2011.

[150] J. Laska and R. Baraniuk, Regime change: Bit-depth versus measurement-rate in compressive sensing [Online]. Available: http://arxiv.org/ abs/1110.3450.

[151] Yifu Zhang, Shunliang Mei, Quqing Chen, Zhibo Chen, " A novel image/video coding method based on compressed sensing theory," in *Proc. IEEE Int. Conf. Acoust., Speech and Signal Processing*, pp. 1361-1364 , 2008.

[152] H. Mansour and O. Yilmaz, "Adaptive compressed sensing for video acquisition," in *Proc. IEEE Int. Conf. Acoust., Speech, Signal Process., Mar. 2012, pp. 3465–3468.*

[153] C. Luo, F. Wu, J. Sun, and C. W. Chen, "Compressive data gathering for large-scale wireless sensor networks," in *Proc. 15th Annu. Int. Conf. Mobile Comput. Netw.*, 2009, pp. 145-146.

[154] J. Haupt, W. U. Bajwa, M. Rabbat, and R. Nowak, "Compressed sensing for networked data," *IEEE Signal Process. Mag.*, vol. 25, no. 2, pp. 92–101, Mar. 2008.

[155] S. Voronin and R. Chartrand, "A new generalized thresholding algorithm for inverse problems with sparsity constraints," in *Proc. IEEE Int. Conf. Acoust., Speech Signal Process. (ICASSP)*, 2013.

[156] W. Chen and I. J. Wassell, "Energy efficient signal acquisition via compressive sensing in wireless sensor networks," in *Proc. Int. Symp. Wireless Pervasive Comput.*, Feb. 2011, pp. 1–6.

[157] G. Cao, F. Yu, and B. Zhang, "Improving network lifetime for wireless sensor network using compressive sensing," in *Proc. IEEE Int. Conf. High Perform. Comput. Commun. (HPCC)*, Sep. 2011, pp. 448–454.

[158] M. Duarte, S. Sarvotham, D. Baron, M. Wakin, and R. Baraniuk, "Distributed compressed sensing of jointly sparse signals," in *Conference Record of the Thirty-Ninth Asilomar Conference on Signals, Systems and Computers*, 2005, pp. 1537–1541.

[159] M. Duarte, M. Wakin, D. Baron, and R. Baraniuk, "Universal distributed sensing via random projections," in *The Fifth International Conference on Information Processing in Sensor Networks (ISPN)*, 2006, pp. 177–185.

[160] M. A. Razzaque and S. Dobson, "Energy-Efficient Sensing in Wireless Sensor Networks Using Compressed Sensing," *Sensors*, vol. 14, no. 2, 2014, pp. 2822–59.

[161] L. Guo, R. Beyah, and Y. Li, "SMITE: A stochastic compressive data collection protocol for mobile wireless sensor networks," in *Proc. IEEE Conf. Comput. Commun.*, 2011, pp. 1611–1619.

[162] S. G. Mallat and Z. Zhang, "Matching Pursuits with Time-Frequency Dictionaries," *IEEE Transactions on Signal Processing*, vol. 41, no. 12, pp. 3397–3415, Dec, 1993.

Appendix A

System Level Requirements

A set of experiments were conducted to address the system requirements defined by Rolls-Royce for the WSN infrastructure [131]. A summary of the most relevant to this research work is shown in Figure A.1. The objective was to demonstrate the capabilities of the proposed WSN within a Gas Turbine Engine to support Equipment Health Management. The implementation of WSN in a GTE is of significant interest to RR because currently it is not possible to carry out measurements on rotating machinery without making modifications to the actual hardware.

Requirement	Description
1	The WSN shall support multiple nodes
1.1	Each sensor node shall have a local, self-powered sensor transmitting to a receiver attached to either the EMU or the EEC via an Ethernet or CAN link
1.2	The WSN should be modifiable and should facilitate rapid deployment of sensor nodes
1.3	The WSN shall be self-initialising
1.4	The network shall deploy a transmission technique to mitigate multipath propagation
1.5	Channel sharing should not deteriorate the communications efficiency below design expectations
1.6	The WSN should be capable of frequency diversity and intelligent RF power management
1.7	The network shall deploy a communication protocol which allows operation of many sensor nodes in a concentrated area on the engine
1.8	The WSN shall consist of multiple sensor nodes and a gateway node acting as the data concentrator
1.8.1	The gateway node shall be able to recognise signal failure from individual nodes
1.8.2	The WSN topology for SILOET II demonstration shall be 'star' topology
2	The WSN should include the option to retransmit data in the event that it is corrupted or lost during transmission

Figure A.1: List of relevant system level requirements.

Requirement	Description
3	The transmission range of the wireless network shall be large enough to sensibly facilitate wireless transmission around a standard civil aerospace fan case
4	The network shall deploy a communication protocol which is capable of automatically switching to lower data rates, if encountered poor signal conditions
5	The system should have the option to provide flexibility to improve communications between the sensor nodes and the transmitter
6	For local communication around the engine smaller data packets should be used
7	The gateway node shall be connected to the EMU via a physical cable link
8	Potential signal leakage to the external environment during active in-engine wireless communication should be minimised
9	Measures of the performance of the wireless links established such as Link quality indicator should be used to achieve optimal performance
10	Application of a signal and data encryption scheme should be considered to ensure data security

Figure A.1: List of relevant system level requirements.

Appendix B

Communication with Vibration Sensor

As described in Section 3.2, the sensor node includes a CC2500 2.4 GHz Radio Frequency transceiver chip to handle data packets sent and received. This radio and the ADIS16227 vibration sensor described in Section 3.4, both act as slaves and communicate via Serial Peripheral Interface (SPI) with the microcontroller which acts as the master. However, the SPI settings for each of the slaves is different in terms of the maximum allowed SPI clock speed, SPI mode clock phase and/or clock polarity. Therefore the SPI configuration varies for each one of them.

The combinations of clock polarity (CPOL) and clock phases (CPHA) are often referred to as modes which are commonly numbered according to the following convention (see Table B.1). The TI target boards from the sensor node were programmed as SPI mode 3 for the vibration sensor and SPI mode 0 for the CC2500 radio as shown in Table B.2.

Table B.1: SPI modes in relation to combinations of clock polarity and phase.

SPI Mode	CPOL / UCCKPL	CPHA/UCCKPH
0	0	0
1	0	1
2	1	0
3	1	1

Table B.2: Radio and vibration sensor SPI modes considered for programming the TI boards.

Device	SPI mode	Max. SPI clock rate	CPOL	CPHA
ADIS16227	3	2.5 MHz	1	1
CC2500	0	10 MHz	0	0

A set of functions (listed in Table B.3) were programmed in the microcontroller to interface with the vibration sensor through SPI.

Table B.3: Functions programmed to interface with the vibration sensor via SPI.

SPI programmed functions			
1	void spiConfig (void)	9	void spiTX(char value)
2	void radioEnable (void)	10	char spiRX(void)
3	void radioDisable (void)	11	void shutDownSens (void)
4	void sensEnable (void)	12	void delay1ms (void)
5	void sensDisable (void)	13	void spiconfig_srx_acc (void)
6	void clearKPL_KPH (void)	14	void spiconfig_avg_bufpntr (void)
7	void spiVibSensConfig (void)	15	void spitrigger (void)
8	void spiRadioConfig (void)	16	void reset_bufpntr (void)

1. Initial SPI configuration: Function used to configure the ports, clock speed and

SPI parameters such as clock polarity and clock phase.

2,3. Enable / Disable Radio (CC2500): The pin assigned as CS (chip select) / SS (slave select) is set low to enable communication or set high to disable communication from the microcontroller (master) to the radio (slave). Note: The master communicates only with one slave at a time, therefore when communicating with one slave all the other slaves must be disabled.

4,5. Enable / Disable Vibration Sensor (ADIS16227): The digital triaxial vibration sensor is activated or deactivated by changing the state of the assigned CS pin (P4.5).

6. Clear polarity/phase settings on SPI clock signal: Resets UCCKPL (Clock Polarity) and UCCKPH (Clock Phase) so that the radio can be reconfigured.

7. Configure the digital tri-axial vibration sensor SPI mode: This function allows the ADIS16227 vibration sensor to be configured as the datasheet indicates.

8. Configure the 2.4 GHz RF Transceiver CC2500: The following function configure the radio in SPI mode 0 and sets the SPI clock speed rate. Although SPI mode 0 requires CPOL/UCCKPL=0 and CPHA/UCCKPH=0 since the UCCKPH flag is inverted, UCCKPH is set as a consequence.

9. Write value in TX buffer: After the bus master (microcontroller) configures the SPI settings required by the slave. The master enables communication with the desired slave by transmitting a logic 0 to the chip select/ slave select line. Since the chip select line is active low, hence a logic 0 is transmitted. User control registers govern several internal operations. The Data In (DIN) bit sequence shown in Figure 1 allows writing to these registers, one byte at a time. Some functions and configuration changes need only one write cycle. For example, writing DIN= 0xBF08 (Data sent from the microcontroller to the tri-axial vibration sensor) starts a manual capture sequence (SPI trigger), for a more detailed description refer to function 16. The size of the input parameter of the following function is one byte long, as a result, it may be required to call this function twice for functions that require two write cycles. It is important to remember that SPI communication is a synchronous protocol that operates in full duplex mode, hence when a value is written into the TX FIFO buffer, a value is received simultaneously in the RX FIFO buffer.

10. Read value in RX buffer: A single register read requires two 16-bit SPI cycles, the bit assignments are shown in the previous figure 1. The first sequence communicates the target address (Bits[A6:A0]). Bits [D7:D0] are bits that don't care for a read Data In sequence. Data Out (DOUT) clocks out the contents of the requested register during the second sequence.

11. Shut-down sensor: To power down the tri-axial vibration sensor after performing data acquisition and processing, it is necessary to set GLOB_CMD[1] = 1 which is done by writing Data In (DIN) = 0xBE02. The GLOB_CMD register (Address: 0x3E) is a global command register that provides an array of single-write commands for convenience. To activate each function the assigned bit should be set to 1 (refer to table A5). The bit restores itself to 0 when the function is completed.

12. Delay 1 millisecond: Delays are required during the program execution. For example, a small delay after performing functions such as SPI writing ensures that the data is available to save it or for posterior use in different sections of the program code. The CPU is a finite state machine whose transitions are triggered by a circuit and oscillator that periodically generates clock pulses. One pulse duration is commonly known as a "clock cycle". To determine the exact amount of time generated by delaying 'n' clock cycles, it is important to know the CPU clock frequency, in this case, the Master Clock (MCLK) allows the program to run at 8 MHz. Since time = 1 / frequency, 1 second = 8' 000,000 clock cycles.

13. Sample rate configuration and Acceleration settings (signal range)

Sample Rate Selection: The ADC samples each accelerometer sensor at a rate of 100.2 kSPS. Four different sample rate options are provided for FFT analysis, SR0 (fs), SR1 (fs/8), SR2 (fs/64), and SR3 (fs/512). The reduced rates are due to a decimation filter, which reduces the bandwidth and bin widths. See table A6 for the performance trade-offs associated with each sample rate setting.

Acceleration/range selection: The record control register is REC_CTRL, that register provides controls for the recording mode, record storage, dynamic range, sample rate and power management.

14. Set buffer pointer: After the completion of an FFT event and updating the data buffer, the vibration sensor loads the first data samples from the data buffer into the

buffer registers (X_BUF, Y_BUF and Z_BUF). The index buffer pointer increments with ever buffer read command (for any of the axis), it causes the next set of capture data to be loaded automatically into each capture buffer register. This enables a process-efficient method for reading all 256 samples in a record, using sequential reads commands, without having to manipulate the buffer pointer register (BUF_PNTR). Example: After a record acquisition, if the buffer of the x-axis acceleration data (X_BUF) wants to be recorded/read, then it is just necessary to sequentially read the same X_BUF address (0x14), the index pointer is automatically incremented each time. The index pointer determines which data samples load into the Buffer registers, in this case, data in X_BUF register.

15. SPI trigger: By setting GLOB_CMD [11] =1 (DIN=0xBF08) results in the initialisation of a manual capture sequence. The manual capture starts immediately after the last DIN bit received (16th SCLK rising edge).

16. Reset buffer pointer: As mentioned previously in function 15, the index buffer pointer increments with ever buffer read command, given an application where essential data is only in the bandwidth of 3 KHz, it is possible to select SR1 as the sample rate setting (bandwidth: 6.262 KHz, see table A6) and use the index buffer pointer to read only the first half of the total bandwidth for that sample rate selection. Since the index buffer pointer moves automatically, it resets when it reaches 256 since the stored FFT spectral records are 256 (from index pointer 0 to 255). Therefore if we are manipulating the index pointer it is important to reset the buffer pointer to 0x0000 after recording/handling FFT data so that the index pointer is in the right place on the start of the next FFT record.

Table B.4: Set of instructions for 'spiConfig' function.

Configure Ports	
Code	Comments
WDTCTL=WDTPW + WDTHOLD;	// Stop watchdog timer (WDT) to prevent interrupting program execution.
P3SEL | = 0x0E;	// Port/pins active: P3.1=MOSI, P3.2=MISO, P3.3=CLK.
P4SEL = 0x00;	// P4 pins used as general I/O.
P3DIR | = 0x0B;	// Port 3 direction: 0000 1011 P3.3 = Output (CLK), P3.2 = Input (MISO), P3.1=Output (MOSI), P3.0=Output (CS).
P4DIR | = 0xFF;	// P4.3 Output direction (P8 -> CS).
Initialise and configure SPI interface	
Code	Comments
UCB0CTL0 |= UCSWRST;	// UCB0CTL0 can be modified only when UCSWRST=1 UCSWRST =0 (USCI released).
UCB0CTL1 |= UCSWRST;	// Allows to modify/configure UCB0CTL1.
UCB0CTL0 |= UCMSB + UCMST + UCSYNC;	// 3-pin, 8-bit SPI master, MSB first.
UCB0CTL1 |= UCSSEL_2;	// Use SMCLK as clock source = 8 Mhz.
UCB0BR0 = 0x04;	// Low byte division factor for baud rate (/4) = 8/4 = 2 Mhz.
UCB0BR1 = 0x00;	// High byte division factor.
UCB0CTL0 &= ~UCSWRST;	// Released (UCSWRST =0) UCB0 CTL0 configures clock phase, clock polarity.
UCB0CTL1 &= ~UCSWRST;	// Start SPI hardware (UCSWRST =0) UCB0 CTL1 configures USCI clock source select.

Table B.5: Bit value changes to enable/disable the radio and vibration sensor

Enable/Disable radio/vibration sensor	
Code	Comments
P3OUT &= ~0x01;	// P3.1 (Low), enables radio
P3OUT |= 0x01;	// P3.1 (High), disables radio
P4OUT &= ~BIT5;	// P4.5 (Low), enables vibration sensor
P4OUT |= BIT5;	// P4.5 (High), disables vibration sensor

Table B.6: Set of instructions for 'clearKPL_KPH' function.

Clear polarity/phase settings on SPI clock signal	
Code	Comments
UCB0CTL0 |= UCSWRST;	// USCI in reset state (To allow modifications)
UCB0CTL0 &= ~UCCKPL;	// Reset Clock polarity - UCCKPL (off)
UCB0CTL0 &= ~UCCKPH;	// Reset Clock phase - UCCKPH (off)
UCB0CTL0 &= ~UCSWRST;	// Release USCI

Table B.7: Set of instructions for 'spiVibSensConfig' function.

Configure the digital vibration sensor SPI mode	
Code	Comments
UCB0CTL0 |= UCSWRST;	// UCB0CTL0 can be modified only when UCSWRST=1. (This allows to modify/set: Clock polarity, clock phase) UCSWRST=1, USCI holds in reset. UCSWRST=0, USCI released.
UCB0CTL1 |= UCSWRST;	// UCB0CTL1=1 -> Software reset enable
UCB0CTL0 |= UCMSB + UCMST + UCSYNC + UCCKPL;	// 3-pin, 8-bit SPI master, MSB 1st, clock polarity (UCCKPL=CPOL=1). // UCCKPL =1 -> Data clocks in the falling edge (ADIS16227 inactive state is high). // UCCKPL =0 -> Data clocks in the rising edge.
UCB0CTL1 |= UCSSEL_2;	//UCSSEL_2 -> Uses sub master clock (SMCLK) as clock source = 8 Mhz
UCB0BR0 = 0x04;	//Low byte division factor for baud rate (/4) SMCLK = 8 MHz/ 4 = 2 Mhz. Note: SCLK Rate in ADIS16227 <= 2.25 Mhz.
UCB0BR1 = 0x00;	//High byte division factor
UCB0CTL0 &= ~UCSWRST;	//Released (UCSWRST =0)
UCB0CTL1 &= ~UCSWRST;	//Start SPI hardware (UCSWRST =0)

Table B.8: Set of instructions for 'spiTX' function.

SPI Transmit, input parameter: 'value'	
Code	Comments
while (!(IFG2 & UCB0TXIFG));	// USCI_B0 TX buffer ready?
UCB0TXBUF = value;	// Write value in TX buffer
while (!(UCB0STAT & UCBUSY));	// Transmission done
return;	// Return statement, function call end

Table B.9: Set of instructions for 'spiRX' function.

SPI Receive, output parameter: 'UCB0RXBUF'	
Code	Comments
while (!(IFG2 & UCB0RXIFG));	// Wait for RX buffer
return UCB0RXBUF;	// Output parameter, the function returns the contents of the requested register, now stored in the RX Buffer.

Table B.10: Set of instructions for 'spiconfig_srx_acc' function.

Sample rate configuration	
Code	Comments
spiTX(0x9D);	// Value to be written to configure sample rate (Upper byte)
dummyRX = spiRX();	// Receive 1st dummy byte
spiTX(0x02);	//0x01 = SR0 Selection, 0x02=SR1 Selection, 0x04=SR2 Selection. (Sample rate configuration and windowing)
dummyRX = spiRX();	// Receive 2nd dummy byte
delay1ms();	// 1 millisecond delay
spiTX(0x9C);	// Value written to configure acceleration range (Upper byte)
dummyRX = spiRX();	// Receive 1st dummy byte
spiTX(0x30);	//0x30 = 70 g , 0x20= 20 g, 0x01= 5g, 0x00=1g (Manual FFT and Signal Range configuration)
dummyRX = spiRX();	// Receive 2nd dummy byte

Table B.11: Set of instructions for 'shutDownSens' function.

Shutdown sensor	
Code	Comments
spiTX(0xBE);	// Command to power down the ADIS16227 (Upper byte)
dummyRX = spiRX();	// Receive 1st dummy byte
spiTX(0x02);	// Command to power down the ADIS16227 (Lower byte)
dummyRX = spiRX();	// Receive 2nd dummy byte
delay1ms();	// 1 millisecond delay
sensDisable();	// Set high the CS pin assigned to the sensor to disable communication with the microcontroller
return;	

Table B.12: Set of instructions for 'spiconfig_bufpntr' function.

Set buffer pointer (BUF_PNTR) to 0x0000	
Code	Comments
spiTX(0xBF);	// Command to set buffer pointer = 0x0000. Register: GLOB_CMD (Address: 0x3E) Upper byte
dummyRX = spiRX();	// Receive 1st dummy byte
spiTX(0x04);	// Command to set GLOB_CMD=0x0000. Lower byte
dummyRX = spiRX();	// Receive 2nd dummy byte

Table B.13: Set of instructions for 'spitrigger' function.

Start FFT capture	
Code	Comments
spiTX(0xBF);	// Command to start a capture sequence. Upper byte
dummyRX = spiRX();	// Receive 1st dummy byte
spiTX(0x08);	// Command to start a capture sequence. Lower byte
dummyRX = spiRX();	// Receive 2nd dummy byte
___delay_cycles(3240000);	// Wait for data to be ready, delay= 405 msec

Table B.14: Set of instructions for 'reset_bufpntr' function.

Reset buffer pointer	
Code	Comments
spiTX(0xBF);	// Command to set buffer pointer = 0x0000. Register: GLOB_CMD (Address: 0x3E) Upper byte
dummyRX = spiRX();	// Receive 1st dummy byte
spiTX(0x04);	// Command to set GLOB_CMD=0x0000. Lower byte
dummyRX = spiRX();	// Receive 2nd dummy byte

The following Figure C.1 shows the physical Serial Peripheral Interface (SPI) connection diagram between the microcontroller which acts as the bus master and two slaves which are the radio transceiver and the vibration sensor. SPI bus uses separated lines for data (Master Output Slave Input or MOSI, Master Input Slave Output or MISO) and SPI clock (SCLK) generated by the master which is used to synchronise full-duplex communication with the slaves. The SPI clock pin and the data lines (MOSI and MISO) are shared between all existing slaves in SPI communication. The microcontroller communicates with one single slave at a time via an independent slave select (SS) line.

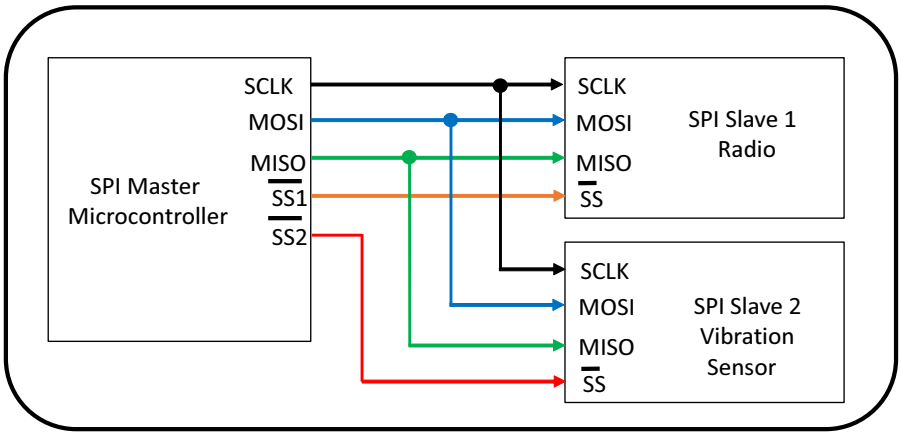

Figure B.1: Vibration sensor and microcontroller SPI connection diagram.